

SOLUTIONS AND GENERALIZATIONS OF PARTIAL DIFFERENTIAL
EQUATIONS OCCURRING IN PETROLEUM ENGINEERING

A Thesis

by

JEFFREY J. DACUNHA

Submitted to the Office of Graduate and Professional Studies of
Texas A&M University
in partial fulfillment of the requirements for the degree of
MASTER OF SCIENCE

Chair of Committee, Thomas A. Blasingame
Committee Members, Peter P. Valkó
Maria A. Barrufet
Head of Department, A. Daniel Hill

August 2014

Major Subject: Petroleum Engineering

Copyright 2014 Jeffrey J. DaCunha

ABSTRACT

Partial differential equations are ubiquitous in petroleum engineering. In this thesis, we begin by introducing a generalization to Darcy's law which includes the effects of fluid inertia. We continue by using the generalization of Darcy's law to derive the hyperbolic diffusion equation (a generalization of the parabolic diffusion equation) which takes into account a finite propagation speed for pressure propagation in the fluid. We develop the mathematical theory used to solve the diffusion equations with various boundary conditions, which include the theory of Sturm-Liouville problems, eigenfunction expansions, and Laplace transformations. Further, we introduce the application of a nonsingular Hankel transform method for finding the solution to the diffusion equations with nonzero and nonconstant initial and boundary conditions. It will be shown that the Hankel transform method developed herein proves to be a more straightforward and less time consuming computation than those found in the literature.

To show the application of the parabolic diffusion equation in the industry, we proceed to derive the solution to the pressure pulse decay method as well as the well-known GRI crushed core permeability method. After derivation of the solutions, we show that the results obtained have excellent agreement with the data that can be found from sources for the pressure pulse decay method and the actual crushed core experiments from the GRI. To provide further insight, we investigate the pressure behavior inside the crushed core sample and core samples as the pressure response moves from transient to steady-state. This type of analysis has not been discussed in existing literature.

DEDICATION

To my wife Brandi and our children Croix, Mattix, and Gabriella. Thank you for your patience and support during my graduate studies. I love you so, so much.

ACKNOWLEDGMENTS

I would like to thank God for his uncountably many blessings that he has bestowed upon my family and me. Only through His grace have I realized opportunities, been successful in my endeavors, and accomplished my goals.

Thank you Dr. Thomas A. Blasingame for his support and permission in allowing me to pursue topics of my choice for this thesis. It is my hope that this work serves as a useful reference to those in academia and in the industry that enjoy working with partial differential equations and their applications to petroleum engineering.

To my two committee members, Dr. Peter P. Valkó and Dr. Maria A. Barrufet, thank you very much for your support, input to the thesis, and wishes for success.

To the management at Pioneer Natural Resources USA, Inc., thank you very much for your permission and support of my pursuit of this advanced degree. I am very grateful to have had this opportunity from my employer.

Once again, ten years later, thank you Dr. John M. Davis for conversations and problem solving sessions over the phone and at Baylor University.

A very, very special thank you to Ken B. Nolen and Dr. Sam G. Gibbs. For the past eight and a half years you Aggie gentlemen have been instrumental in shaping my personal, spiritual, and professional life. I owe so much of my success to your mentoring. Thank you both so very much for all your guidance and mentoring.

TABLE OF CONTENTS

	Page
ABSTRACT	ii
DEDICATION	iii
ACKNOWLEDGMENTS	iv
TABLE OF CONTENTS	v
LIST OF FIGURES	viii
LIST OF TABLES	xi
1. INTRODUCTION	1
1.1 Mathematics in Petroleum Engineering	1
1.2 Research Objectives	4
1.3 Statement of the Problem	5
1.4 Literature Review	7
1.5 Strategy and Outline of the Thesis	10
2. HYDRODYNAMIC EQUATIONS DESCRIBING THE FLOW OF FLUIDS IN POROUS MEDIA	12
2.1 Introduction	12
2.2 Hydrodynamic Relationships	12
2.3 Classical Hydrodynamics	15
2.4 Generalized Darcy's Law	17
2.5 Generalized Darcy Equations and the Navier-Stokes Equations	18
2.6 Equations of Motion	19
2.6.1 Implementation of the generalized Darcy equations	20
2.6.2 Implementation of the generalized Darcy and Navier-Stokes equations	22
3. METHODS OF SOLUTION	27
3.1 Introduction	27
3.2 Sturm-Liouville Theory	28
3.2.1 Regular Sturm-Liouville theory	30
3.2.2 Singular Sturm-Liouville theory	33
3.3 The Method of Separation of Variables	35
3.4 Laplace Transform Theory	39

3.4.1	The Laplace transformation	40
3.4.2	The inversion integral for the Laplace transformation	44
4.	PARABOLIC DIFFUSION	49
4.1	Introduction	49
4.2	Solutions for Radial Flow Defined at Both Boundaries	50
4.3	Solutions for Pressure Defined at the Inner Boundary and Radial Flow Defined at the Outer Boundary	58
4.4	Solutions for Pressure Defined at Both Boundaries	63
5.	HYPERBOLIC DIFFUSION	68
5.1	Introduction	68
5.2	Solutions for Radial Flow Defined at Both Boundaries	69
5.3	Solutions for Pressure Defined at the Inner Boundary and Radial Flow Defined at the Outer Boundary	75
5.4	Solutions for Pressure Defined at Both Boundaries	78
5.5	Comparison of the Solutions to the Hyperbolic and Parabolic Diffusion Equations	80
5.5.1	Solution to the dimensionless hyperbolic diffusion initial bound- ary value problem	81
5.5.2	Analytic comparison of solutions	87
5.5.3	Graphical comparison of the solutions	88
6.	PRESSURE PULSE DECAY METHOD	95
6.1	Introduction	95
6.2	Mathematical Model in the Cartesian Coordinate System	96
6.2.1	Derivation of the continuity equation in the Cartesian coordi- nate system	96
6.2.2	Derivation of the diffusion equation in the Cartesian coordinate system	98
6.3	Description of the experimental system set-up and development of the initial conditions and boundary conditions for the pressure pulse decay method	101
6.4	Solution to the Mathematical Model	104
6.5	Comparison of Results	108
7.	GRI CRUSHED CORE PERMEABILITY METHOD	111
7.1	Introduction	111
7.2	Mathematical Model in the Spherical Coordinate System	111
7.2.1	Derivation of the continuity equation in the spherical coordi- nate system	112
7.2.2	Derivation of the diffusion equation in the spherical coordinate system	114

7.3	Description of the experimental system set-up and development of the initial conditions and boundary conditions for the crushed core permeability method	117
7.4	Solution to the Mathematical Model	120
7.5	Comparison of Results	125
8.	SUMMARY AND CONCLUSIONS	137
8.1	Summary	137
8.2	Conclusions	138
8.3	Recommendations for Future Work	139
8.3.1	Hyperbolic diffusion equation to model the pressure pulse decay method and the GRI method	139
8.3.2	Solution of the Hyperbolic Diffusion Equation with Boundary Conditions Specified at the Wellbore	140
	REFERENCES	144

LIST OF FIGURES

FIGURE	Page
1.1 Plot of the surface and pump dynagraph cards.	4
3.1 The parties responsible for the development of the Sturm-Liouville theory.	28
3.2 Oliver Heaviside (1850–1925).	40
3.3 Pierre-Simon Laplace (1749–1827).	41
5.1 Plot of dimensionless pressure vs. dimensionless time with different values for the parameter τ	89
5.2 Plot of dimensionless logarithmic pressure derivative vs. dimensionless time with different values for the parameter τ	90
5.3 Plot of dimensionless pressure and dimensionless logarithmic derivative vs. dimensionless time with $\tau = 100$	91
5.4 Plot of dimensionless pressure and dimensionless logarithmic derivative vs. dimensionless time with $\tau = 10$	91
5.5 Plot of dimensionless pressure and dimensionless logarithmic derivative vs. dimensionless time with $\tau = 1$	92
5.6 Plot of dimensionless pressure and dimensionless logarithmic derivative vs. dimensionless time with $\tau = 0.1$	92
5.7 Plot of dimensionless pressure and dimensionless logarithmic derivative vs. dimensionless time with $\tau = 0.01$	93
5.8 Plot of dimensionless pressure and dimensionless logarithmic derivative vs. dimensionless time with $\tau = 0.001$	93
5.9 Plot of dimensionless pressure and dimensionless logarithmic derivative vs. dimensionless time with $\tau = 0.0001$	94

5.10	Plot of dimensionless pressure and dimensionless logarithmic derivative vs. dimensionless time with $\tau = 0$ (diffusion).	94
6.1	Fixed control volume ΔV for the experiment.	97
6.2	Experimental set-up of the pressure pulse permeability method on crushed cores.	101
6.3	Example solution showing gas pressure in the upstream and downstream volumes as well as the pressure at different points in the sample throughout the experiment where $\beta = 1$ and $\gamma = \frac{1}{10}$	109
6.4	Example solution showing gas pressure in the upstream and downstream volumes as well as the pressure at different points in the sample throughout the experiment where $\beta = \frac{1}{10}$ and $\gamma = 1$	109
6.5	Example solution showing gas pressure in the upstream and downstream volumes as well as the pressure at different points in the sample throughout the experiment where $\beta = \gamma = 1$	110
6.6	Example solution showing gas pressure in the upstream and downstream volumes as well as the pressure at different points in the sample throughout the experiment where $\beta = 1$ and $\gamma = 10$	110
7.1	Model of spherical crushed core sample showing the spatially fixed control volume ΔV	113
7.2	Experimental set-up of the pressure pulse permeability method on crushed cores [41].	117
7.3	Comparison of digitized GRI Model [29] and digitized GRI data [29], and the dimensional solution (7.27).	126
7.4	Comparison of digitized data [41] and the dimensional solution (7.27).	127
7.5	Interesting pressure v. time behavior at multiple radii using the dimensionless solution (7.26).	127
7.6	GRI method type curve for the dimensionless volume ratio $C_D = \frac{1}{256}$	128
7.7	GRI method type curve for the dimensionless volume ratio $C_D = \frac{1}{128}$	128
7.8	GRI method type curve for the dimensionless volume ratio $C_D = \frac{1}{64}$	129
7.9	GRI method type curve for the dimensionless volume ratio $C_D = \frac{1}{32}$	129

7.10	GRI method type curve for the dimensionless volume ratio $C_D = \frac{1}{16}$.	130
7.11	GRI method type curve for the dimensionless volume ratio $C_D = \frac{1}{8}$.	130
7.12	GRI method type curve for the dimensionless volume ratio $C_D = \frac{1}{4}$.	131
7.13	GRI method type curve for the dimensionless volume ratio $C_D = \frac{1}{2}$.	131
7.14	GRI method type curve for the dimensionless volume ratio $C_D = 1$.	132
7.15	GRI method type curve for the dimensionless volume ratio $C_D = 2$.	132
7.16	GRI method type curve using $\frac{p_D}{p_\infty}$ for the dimensionless volume ratio $C_D = \frac{1}{256}$.	133
7.17	GRI method type curve using $\frac{p_D}{p_\infty}$ for the dimensionless volume ratio $C_D = \frac{1}{128}$.	133
7.18	GRI method type curve using $\frac{p_D}{p_\infty}$ for the dimensionless volume ratio $C_D = \frac{1}{64}$.	134
7.19	GRI method type curve using $\frac{p_D}{p_\infty}$ for the dimensionless volume ratio $C_D = \frac{1}{32}$.	134
7.20	GRI method type curve using $\frac{p_D}{p_\infty}$ for the dimensionless volume ratio $C_D = \frac{1}{16}$.	135
7.21	GRI method type curve using $\frac{p_D}{p_\infty}$ for the dimensionless volume ratio $C_D = \frac{1}{8}$.	135
7.22	GRI method type curve using $\frac{p_D}{p_\infty}$ for the dimensionless volume ratio $C_D = \frac{1}{4}$.	136
7.23	GRI method type curve using $\frac{p_D}{p_\infty}$ for the dimensionless volume ratio $C_D = \frac{1}{2}$.	136

LIST OF TABLES

TABLE	Page
7.1 Parameters used to model the pressure decay in the GRI Topical Report 93/0297 [29].	124
7.2 Parameters used to model the pressure decay in Profice [41].	125

1. INTRODUCTION

All science requires mathematics. The knowledge of mathematical things is almost innate in us. This is the easiest of sciences, a fact which is obvious in that no one's brain rejects it; for laymen and people who are utterly illiterate know how to count and reckon.

Roger Bacon (1214–1294)

1.1 Mathematics in Petroleum Engineering

All disciplines of the arts and sciences are rooted in mathematics. In particular, partial differential equations are used to model the phenomena that is observed in the physical world. In the study of petroleum engineering, this fact is very evident. Within petroleum engineering, partial differential equations are derived from first principles to model many behaviors.

For example, predicting the movement of acid and permeability fronts in sandstone can be modeled by a system of two partial differential equations. Summarizing [32], as acid progresses in the axial direction through a sandstone core, the mixture reacts with and dissolves some of the solids on the surface of the pore space. By disregarding any axial dispersion in the sandstone, a differential mole balance on a solute i in the liquid phase gives

$$\frac{\partial(\phi C_i)}{\partial t} + \frac{\partial(V C_i)}{\partial x} = (R_s + R_h)_i, \quad (1.1)$$

where ϕ is the porosity, C_i is the concentration of the solute i in moles/cm³ of fluid, V is the superficial velocity in cm/min, t is the time in min, x is the distance in the axial direction in cm, and R_s and R_h are the heterogeneous and homogeneous reaction rates respectively of solute i in moles/cm³ of bed volume/min. In a similar

fashion, a differential mole balance in the solid phase on a mineral species j in the sandstone, that is in this case dissolvable, gives

$$\frac{\partial ((1 - \phi)W_j)}{\partial t} = r_j, \quad (1.2)$$

where W_j is the concentration of mineral species j in mole/cm³ of solids and r_j is the rate of reaction of mineral j in mole/cm³ of bed volume/min.

Another example can be found in modeling the behavior of a rod string in a sucker rod pumping system. In deriving the force balance of a segment of a sucker rod string, the resulting partial differential equation is the one dimensional damped wave equation, with the rare instance of both boundary conditions prescribed at one end of the rod string, in particular at the surface. Application of the damped wave equation to modeling the sucker rod string yields

$$\frac{\partial^2 y}{\partial t^2} = a^2 \frac{\partial^2 y}{\partial x^2} - c \frac{\partial y}{\partial t} + g, \quad (1.3)$$

where y is the total displacement (dynamic plus static) in ft, x is the distance from the surface in ft, t is time in sec, a is speed of sound in the rod material in ft/sec, c is a damping coefficient in sec⁻¹ and g is the acceleration of gravity in ft/sec². In essence, to determine the behavior of the rod string at any depth x , the two boundary conditions of position and load are measured at the surface. From this information and the assumption is that for each stroke of the pumping unit the rod string is in a steady-state, where the initial conditions have damped out, we see that the solution

to (1.3) is uniquely dependent upon the boundary conditions

$$y(0, t) = P_{\text{pr}}(t), \quad (1.4)$$

$$EA \frac{\partial y(0, t)}{\partial x} = L_{\text{pr}}(t), \quad (1.5)$$

where P_{pr} is the position of the polished rod (at the surface) in in, E is the Young's modulus of the rod material in psi, A is the cross sectional area of the rod in in², and L_{pr} is the load at the polished rod in lbs. Figure 1.1 shows the parametric plots of load and position of the polished rod and the downhole pump. These parametric plots are known as surface and downhole (pump) dynagraph cards. The downhole pump card is computed using (1.3)–(1.5).

As a final example, we can also consider the partial differential equation that is currently used to model the flow of fluids through porous media. Upon derivation from first principles, we obtain

$$\kappa \nabla^2 p = \frac{\partial p}{\partial t}, \quad (1.6)$$

where p is the pressure in psi, r is the distance into the porous medium from the wellbore in ft, t is the time in seconds, κ is the diffusivity coefficient in ft²/sec, and $\nabla^2 := \frac{1}{r^k} \frac{\partial}{\partial r} \left(r^k \frac{\partial}{\partial r} \right)$ is the Laplacian in the cases of linear (dimension $k = 1$) flow and radial (dimension $k = 2, 3$) flow, respectively. The partial differential equation (1.6) and a generalization of it will make up the bulk of the subject matter of this thesis.

While the aforementioned examples barely scratch the surface of the utility of mathematically modeling the physical world, they do clearly show that PDEs are at the heart of diagnosing and predicting the behavior of the phenomena that can be found in petroleum engineering. And that is part of the elegance and power of mathematics... it gives man the ability to determine the outcome and the behavior

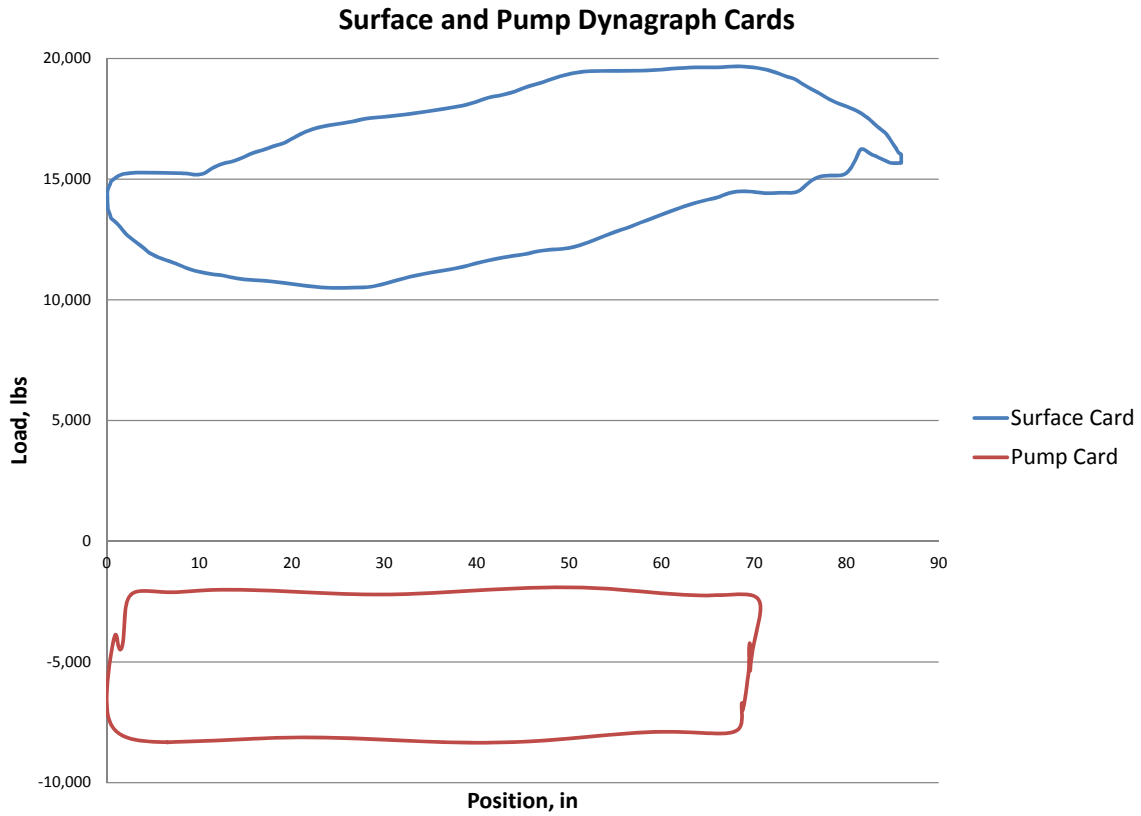


Figure 1.1: Plot of the surface and pump dynagraph cards.

of a system before it occurs, to predict, to tell the future. No greater power exists.

1.2 Research Objectives

The objectives of this thesis are

- To *provide* a self-contained account of the mathematical theory needed to derive and solve the parabolic diffusion equation and hyperbolic diffusion equation as applied to modeling the flow of fluids in porous media.
- To *demonstrate* the utility of the mathematical theory developed herein by solving the different diffusion equations with different boundary conditions in different coordinate systems.

- To *investigate* a generalization of Darcy’s law which incorporates the inertia of the fluid, thus eliminating the assumption of an infinite pressure propagation speed.
- To *provide* the mathematical rigor and detail for the some of the solutions to the diffusion equation that are missing in known literature.
- To *demonstrate* a generalization of the parabolic diffusion equation by implementation of the hyperbolic wave equation, which tends to the usual parabolic diffusion equation as the pressure propagation speed tends to infinity.
- To *propose* and *demonstrate* a new application of the Hankel transform for solving the parabolic and hyperbolic diffusion equations with nonconstant initial and boundary conditions via an eigenfunction expansion technique.
- To *provide* from first principles a complete derivation of, and solution to, the parabolic diffusion equation which models the pressure pulse decay method for determining rock properties from core samples.
- To *provide* from first principles a complete derivation of, and solution to, the parabolic diffusion equation which models the Gas Research Institute’s (GRI) crushed core method for determining rock properties from crushed core samples.
- To *investigate* a novel formulation of modeling the flow of fluids in porous media by enforcing the two required boundary conditions at the interior boundary.

1.3 Statement of the Problem

This work focuses on the parabolic diffusion equation and the hyperbolic diffusion equation with different initial and boundary conditions. In particular, a complete

derivation of these equations we be provided, beginning with appropriate continuity equations, equations of state, and equations of motion for the fluid in the porous media.

Once these equations are derived, we demonstrate a new method of solution via Hankel transformations. The solutions obtained by the Hankel transforms developed in this thesis are for general initial and boundary conditions. As special cases of these solutions, the solutions in the literature [35,36,51] where initial and boundary conditions are assumed to be constants are easily verified. It is believed by the author that the solution method derived in this thesis is a new contribution to the literature.

We then modify the equation of motion used to derive the parabolic diffusion and include the effects of the fluid density and inertia. The resulting partial differential equation is a hyperbolic diffusion equation. This is a generalization of the usual parabolic diffusion equation in that it takes into account the fact that pressure propagates at a finite speed in a compressible fluid. It will be shown that if one lets this propagation speed in the hyperbolic diffusion equation go to infinity, then, as expected, the parabolic diffusion equation will result. The Hankel transform method developed for the parabolic diffusion equation is also developed herein to solve the hyperbolic diffusion equation. We will also investigate specific cases with constant boundary conditions to compare and contrast the behaviors of the two diffusion equations.

Once the parabolic diffusion equation and the hyperbolic diffusion equation and their respective solutions are developed, we continue by providing a detailed derivations and solutions to two popular methods used in determining the properties of reservoir rock. The methods that are investigated are the pressure pulse decay method [3,8,13,15,23,24,37] and the GRI crushed core method [13,15,17,18,22,24,25,29–31,33,37,41,44,46]. After developing these solutions, new insight is provided

regarding the behavior of the pressure within the reservoir rock as the pressure moves from transient to steady-state.

To conclude, we consider the problem of prescribing the two required boundary conditions for the hyperbolic diffusion equation at the interior boundary. This is an interesting problem to consider since there seems to be no evidence of any investigation of this problem prior to this thesis. Further development of the solution obtained in this work is recommended for future research.

1.4 Literature Review

There is a tremendous amount of literature regarding the use of the parabolic diffusion equation to model the flow of fluids through porous media [4, 6, 10, 13, 15, 17, 18, 23–25, 27, 29, 30, 33–37, 41, 42, 51]. The equation of motion that is used to derive the parabolic diffusion equation is Darcy’s law. This law omits any possible inertia effects of the fluid by assuming that the flow is sufficiently slow so that this omission is acceptable. The solution method that seems to be the most popular the use of the method of Laplace transform [51]. The author conjectures that one of the reasons that this method is most popular is because as the solution develops, the pseudo-steady state portion of the entire solution is evident and readily identified. Regarding the use of separation of variables and the Hankel transform, the latter of which is developed in this thesis, identifying the form of the pseudo-steady state portion of the complete solution is not as straightforward.

The generalization of the parabolic diffusion equation to the hyperbolic diffusion equation in this thesis is derived by including the potential effects of including a term the fluid inertia in the equation of motion. The resulting model for the flow of fluid in porous media is the hyperbolic diffusion equation. There is a significant amount of literature devoted to this idea [5, 11, 16, 19, 20, 28, 34, 38–40, 52]. However, the author

did not find anything which attempts to solve the hyperbolic diffusion equation on a similar domain or with the implementation of a Hankel transform using eigenfunction expansions. The resulting equation of motion is both Newton-like and Darcy-like. It is similar to Newton in that it relates the differences in forces on the fluid to the mass of the fluid times its acceleration. It is similar to Darcy's law because as the density of the fluid approaches zero (disregarded), the equation of motion tends to the popular Darcy's law.

Once the mathematics are completed and the solutions have been given for the two different diffusion equations, we turn our attention to applying this theory to solving two modeling problems in the petroleum industry. The GRI began a program in 1991 to research and develop new methods to determine the reservoir and rock properties of the Devonian shale in the Application Basin which involved special coring, logging, and testing of the rock samples. The GRI topical report [29] and related papers [30,31] provide descriptions for the three experimental methods that were developed in order to determine the properties of the shale rock from two wells in Pike County, Kentucky. The methods of determining the matrix gas permeability that were developed are pressure pulse permeability of shale core plugs, pressure pulse permeability of crushed core samples, and permeability from degassibility of core plugs. The two topics we investigate in this thesis are the pressure pulse decay method and the GRI crushed core permeability method.

Knowledge of the porosity and permeability characteristics of a formation is of paramount importance. These rock properties can be measured by using constant-flow equipment, which can be quite time consuming and inaccurate on samples from tight ($k < 1$ mD) reservoirs [15]. A method developed to mitigate these issues is the pressure pulse decay method. This method offers is completed in a shorter amount of time and offers more accurate estimates of rock properties. This type of test was

pioneered by Brace [8], who suggested a nonsteady-state technique called a pressure-pulse technique, to determine the permeability of tight rock samples [23]. Many other sources in the literature model the pressure pulse decay method using a model for slightly compressible fluid [3, 15, 24, 37] and/or a pseudopressure approach [13, 15, 23]. The experimental set-up for the pressure pulse decay method will be discussed in Chapter 6.

There is a considerable amount of discussion in the literature regarding the determination of matrix gas permeability from crushed core samples [13, 15, 17, 18, 22, 24, 25, 31, 33, 37, 41, 44, 46]. According to [29], the crushed core method takes core samples (or drill cuttings), crushes them, then sorts the particles by size using a sieve. A known mass of the crushed sample of similar size are taken and loaded into a sample cell of known volume. Helium is then expanded from a reference cell, also of known volume, at a higher pressure, into the sample cell, which causes the ambient pressure surrounding the crushed core samples to increase virtually instantaneously. Then, as time progresses, the pressure in the sample cell decays further as the higher pressure gas surrounding the crushed core samples seeps into the pores of the particles. The matrix permeability as well as the gas-filled porosity can now be computed from the pressure decay data. The experimental set-up for the pressure pulse decay method will be discussed further in Chapter 7.

The test data used for determining the validity of our solution comes from two sources. The first source is from [29] which uses core sample #36, taken from the well Ford Motor Company No. 69, with a particle size of 20/35 mesh. The other details of the experimental set-up, including important parameters such as sample cell and reference cell volume as well as initial reference cell pressures and sample mass, had to be estimated since these values were absent from all sources that the author could find. The second source is from [41], which provides a much more

detailed description of a specific data set where all parameter values are provided. The solution developed in this paper matches both pressure decay data sets with excellent agreement.

A specific difference between the model that is developed in this thesis and the model that is discussed very, very briefly in [29] is that the shape assumed in our model is a sphere, while the shape assumed in [29] is a cylinder with height equal to half the diameter. A direction toward further development of our model would be to investigate any material differences in the solution that is found in this paper assuming a spherical particle shape versus a the solution that would be derived assuming a cylindrical particle shape.

1.5 Strategy and Outline of the Thesis

The idea of this work being a self-contained account of the required mathematical theory needed to develop and solve the aforementioned parabolic and hyperbolic diffusion equations, along with applications to existing methods which implement these equations to determine properties of reservoir rock lends itself to the following format.

Chapter 2 discusses and develops the continuity equation, equations of state, and equations of motion resulting in a complete hydrodynamical system for the flow of fluids in porous media. Depending on the equation of motion that is used, the parabolic diffusion equation or the hyperbolic diffusion equation results. In Chapter 3, the Sturm-Liouville theory, the Laplace transform, and the method of separation of variables are developed in detail. These theories are at the heart of solving the boundary value problems posed in this thesis. As such, it is critical that the reader has a full understanding of these methods.

Following this development, Chapters 4 and 5 waste no time in immediately diving

into solving the parabolic diffusion equation and the hyperbolic diffusion equation, respectively, on limited reservoirs, which were fully derived and explained in Chapter 2. By limited reservoirs we mean that the spatial domain on which the initial value problems are solved is $0 < r_1 < r < r_2$, where r_1 represents the nonzero interior radius of the reservoir (the wellbore) and r_2 represents the exterior radius of the reservoir.

Once the derivation, mathematical theory, solution methodologies, and the solutions themselves are determined for the two different diffusion equations, in Chapters 6 and 7 we apply the solution methods discussed to show the detail involved in obtaining models to accurately describe the pressure pulse decay method and the GRI crushed core permeability method, respectively. In addition to providing the details, we also provide respective graphical representations of the pressure traverses that occur within the core sample and crushed core particles.

To conclude the thesis, in Chapter 8, we summarize the topics that were covered in thesis and provide two new ideas for future research. The first recommendation for future work is to model the transient pressure response methods in Chapters 6 and 7 using the hyperbolic diffusion equation. The second recommendation is to consider a new type of boundary value problem for the hyperbolic diffusion equation on a semi-infinite domain. In this boundary value problem, we propose considering the fact that we can only really measure the conditions at the interior boundary $r = r_1$. Because of this, we wish to define our two required boundary conditions at the interior boundary. A solution is obtained, but the author believes that there exists a more tractable form than that what is provided. This semi-infinite boundary value problem has proven to be an interesting problem which has tremendous potential for further study.

2. HYDRODYNAMIC EQUATIONS DESCRIBING THE FLOW OF FLUIDS IN POROUS MEDIA

No amount of experimentation can ever prove me right; a single experiment can prove me wrong.

Albert Einstein (1879–1955)

2.1 Introduction

We begin this chapter by introducing the hydrodynamic principles of a general flow system. We then become more specific and concentrate on the flow of fluids through porous media. The most fundamental law that we must consider in this development is the conservation of mass which states that in a closed system the mass (in this case, of the fluid) can neither be created nor destroyed.

2.2 Hydrodynamic Relationships

In our case, we are referring to a system of fluid in motion, so it behooves us to restate the law in terms that are more representative of the system being investigated. “The net excess of mass flux, per unit time, into or out of any infinitesimal volume element in the fluid system is exactly equal to the change per unit of time of the fluid density in that element multiplied by the free volume of the element [35].” We may represent this statement, mathematically by

$$\nabla \cdot (\rho \vec{v}) = \frac{\partial}{\partial x}(\rho v_x) + \frac{\partial}{\partial y}(\rho v_y) + \frac{\partial}{\partial z}(\rho v_z) = -\frac{\partial(\phi \rho)}{\partial t}, \quad (2.1)$$

where ϕ is the porosity of the element, $\nabla := \langle \frac{\partial}{\partial x}, \frac{\partial}{\partial y}, \frac{\partial}{\partial z} \rangle$, $\vec{v} := \langle v_x, v_y, v_z \rangle$ represents the velocity vector of the fluid in the element, and ρ is the density of the element, both at an arbitrary point (x, y, z) in the element. The law of the conservation of

mass in (2.1) is the continuity equation that will be used in our development.

Next we must describe the fluid that is to be modeled by defining an equation of state which will describe the relationship between the density, pressure, and temperature. This relationship can be expressed in general by

$$\chi(\rho, p, T) = 0 \tag{2.2}$$

where p is the pressure and T is the temperature for a given point in the element. For example, when the fluid is a completely incompressible liquid (zero compressibility), (2.2) would become

$$\rho \equiv \text{const.} \tag{2.3}$$

If the fluid under consideration is a real gas, then

$$\chi(\rho, p, T) = p - \frac{z\rho RT}{M} = 0, \tag{2.4}$$

where z is the z -factor, R is the universal gas constant and M is the molecular weight of the gas.

To round out the discussion of the description of the fluid under investigation, we must also describe its thermodynamic qualities. The pay-off is in developing an equation of the thermodynamic character will allow the elimination of one of the variables p , ρ , or T so that a unified relationship of the flow and thermodynamic qualities can be obtained. An example is density as a function of pressure, $\rho = \rho(p)$. Suppose the fluid is a real gas in isothermal flow, where (2.4) is the equation of state. The relationship for the thermodynamic character would be

$$T \equiv \text{const}, \tag{2.5}$$

and thus substituting (2.5) into (2.4) would yield

$$\rho(p) = \frac{M}{zRT}p. \quad (2.6)$$

The impact on hydrodynamical problems from the equation of state is now becoming clear. Substituting in (2.3) into the continuity equation (2.1) along with the assumption that the matrix is incompressible ($\partial\phi/\partial p = 0$) we have

$$\nabla \cdot \vec{v} = \frac{\partial v_x}{\partial x} + \frac{\partial v_y}{\partial y} + \frac{\partial v_z}{\partial z} = 0. \quad (2.7)$$

Inspection of (2.7) shows that it represents a relationship that must be upheld in describing the velocity distribution in a system where the fluid is incompressible. However, from this relationship, the individual components of velocity cannot be determined nor does it differentiate between different incompressible liquids. Further, it does not allow us to tell apart fluid systems that are under the influence of external forces or if the flow is only dependent upon differences in pressure. Finally, from (2.7), whether the fluid is flowing through an unobstructed path or a porous medium is indistinguishable.

In addition to describing the fluid thermodynamically, a description of the dynamics of the fluid must also be provided as well as an explanation of how the fluid acts under external forces and pressure differentials. In particular, what is sought is a hydrodynamical equivalent to Newton's law which states that the product of the mass of a body and its acceleration is equal to and opposite the force acting on the body. To develop this equivalent, the equation of state of the fluid as well as the flowing conditions must be known [35].

2.3 Classical Hydrodynamics

To have a complete hydrodynamic system, a dynamic classification of the character of the flow system must be developed in addition to the equation of continuity and the equation of state. A unit volume element of the fluid will be acted on by three outside forces [35]:

1. Forces opposing the motion of the fluid that are a result of friction or internal resistance of the fluid.
2. Body forces acting on the elemental volume of fluid from the force vector $\vec{F} := \langle F_x, F_y, F_z \rangle$.
3. Pressure gradients of each of the components $\frac{\partial p}{\partial x}$, $\frac{\partial p}{\partial y}$, and $\frac{\partial p}{\partial z}$.

The forces for viscous flow described in item 1 in Cartesian components are given by

$$\mu \left(\nabla^2 v_\eta + \frac{1}{3} \frac{\partial \Theta}{\partial \eta} \right), \quad \eta = x, y, z,$$

where ∇^2 is the Laplacian operator defined by

$$\nabla^2 := \nabla \cdot \nabla = \frac{\partial^2}{\partial x^2} + \frac{\partial^2}{\partial y^2} + \frac{\partial^2}{\partial z^2}$$

and Θ is defined by

$$\Theta := \nabla \cdot \vec{v}.$$

The physical interpretation of Θ is that it represents the rate of volume dilatation of the fluid [35].

The dynamic classification of the character of the flow system will be determined by equating the forces listed in items 1–3 with the product of the mass and accel-

eration of the elemental volume of fluid. In correctly representing the acceleration of this volume, it must be noted that the velocity of the element will change during an interval of time at the position it once occupied originally, but it will also as an element moves its position in the fluid. As a result, the acceleration is represented by the total (material) derivative of the velocity, which is given by [35]

$$\begin{aligned}\frac{D}{Dt} &= \frac{\partial}{\partial t} + \frac{dx}{dt} \frac{\partial}{\partial x} + \frac{dy}{dt} \frac{\partial}{\partial y} + \frac{dz}{dt} \frac{\partial}{\partial z} \\ &= \frac{\partial}{\partial t} + v_x \frac{\partial}{\partial x} + v_y \frac{\partial}{\partial y} + v_z \frac{\partial}{\partial z}.\end{aligned}$$

Thus, we now have the dynamic equations of motion, known as the Navier-Stokes equations, given by

$$\rho \frac{Dv_x}{Dt} = -\frac{\partial p}{\partial x} + F_x + \mu \nabla^2 v_x + \frac{\mu}{3} \frac{\partial \Theta}{\partial x} \quad (2.8)$$

$$\rho \frac{Dv_y}{Dt} = -\frac{\partial p}{\partial y} + F_y + \mu \nabla^2 v_y + \frac{\mu}{3} \frac{\partial \Theta}{\partial y} \quad (2.9)$$

$$\rho \frac{Dv_z}{Dt} = -\frac{\partial p}{\partial z} + F_z + \mu \nabla^2 v_z + \frac{\mu}{3} \frac{\partial \Theta}{\partial z}. \quad (2.10)$$

We can represent (2.8)–(2.10) in compact vector form by

$$\rho \frac{D\vec{v}}{Dt} = \rho \left(\frac{d\vec{v}}{dt} + (\vec{v} \cdot \nabla) \vec{v} \right) = -\nabla p + \vec{F} + \mu \nabla^2 \vec{v} + \frac{\mu}{3} \nabla \Theta. \quad (2.11)$$

The development of the required equations for a complete hydrodynamic system which includes a continuity equation (2.1), an equation of state (2.2), and a set of dynamic equations of motion (2.8)–(2.10), and in vector form (2.11), is complete. We may use these five linearly independent equations to solve for the five unknown quantities ρ , p , v_x , v_y , and v_z . With these equations the characteristics of a viscous fluid flowing through any medium can be completely described [35].

2.4 Generalized Darcy's Law

In the development of a hydrodynamic system, it is clear that the law of conservation of mass and the thermodynamic equation for a fluid must be kept constant. The theory that was outlined in Section 2.3 developed the set of dynamic equations of motion in (2.8)–(2.10). The essential difference in the dynamic equations developed in this section are that the macroscopic viewpoint of fluids flowing in a porous medium can be substantially different from the microscopic viewpoint that is provided in (2.8)–(2.10). Darcy's law states that macroscopically, in a porous medium the fluid flow is directly proportional to the pressure gradient of the fluid [35]. It is a method that can be considered similar to averaging the characteristics of the pores and flow channels in the medium.

In general, for any body forces \vec{F} having potential V (which implies $\vec{F} = -\nabla V$), along with the pressure gradients that are acting on the fluid, the generalized Darcy's law can be represented mathematically by

$$\vec{v} = -\nabla\Phi, \tag{2.12}$$

where

$$\Phi := \frac{k}{\mu}(p + V). \tag{2.13}$$

The relationships in (2.12) and (2.13) can be considered as the dynamical foundation of viscous fluid flow through porous media for any type of homogeneous fluid. These equations will be the macroscopic equivalent of and substitute for the Navier-Stokes equations developed in (2.8)–(2.10) [35].

2.5 Generalized Darcy Equations and the Navier-Stokes Equations

We now discuss one of the main ideas of this thesis. At this point we have followed the classical development of the general hydrodynamic equations of fluid flow in porous media. The natural progression is to replace the Navier-Stokes equations (2.8)–(2.10) with the generalized Darcy equations (2.12) and (2.13). There is a compelling argument given by Muskat [35] which provides excellent reasoning to make this replacement, which we will now outline.

The generalized Darcy equations (2.12) and (2.13) are different in both form from the Navier-Stokes equations (2.8)–(2.10) as well as in omitting the density ρ . In the Navier-Stokes equations, the density is multiplied by the total derivative which gives a representation of the acceleration forces (inertia) in the fluid. Since density is omitted from the generalized Darcy equations, so too are the inertia forces in the fluid. The reason that this omission is valid is due to the belief that the viscous resistance greatly exceeds the inertia forces in the fluid; that is unless turbulent conditions arise. In other words, the predominate forces on the fluid are due to viscous resistance on the fluid. The difference in the form of the generalized Darcy equations from that of the Navier-Stokes equations are due to the “statistical averaging” of the classical equations over the individual pores and flow channels in order to yield a simplified macroscopic representation [35].

However, along with the author, there is considerable interest in the literature [11, 16, 19, 20, 28, 34, 38, 40, 52] on the maximum velocity of heat transmission and the effects of fluid inertia on the flow of fluids in porous media. In particular, by including the effects of inertia, the assumption of an infinite propagation speed of the pressure disturbances is removed. This assumption is inherent in the generalized Darcy’s law, which is an analog of Fourier’s law of heat transfer in the theory of heat conduction.

The assumption of an infinite propagation speed is actually discussed briefly in [35]. It is mentioned that the velocity of propagation does in fact have an upper bound, but the claim is that “*physically* it is not the absolute magnitude of the velocity of propagation which is of primary importance, but rather its magnitude *relative* to the fluid velocity in the medium [35].”

In [34] an argument is made showing that the assumption of an infinite propagation speed in the transmission of heat in the usual diffusion equation is that it predicts an increase in temperature at all points in a given body if there is an increase in heat at some point in the body. Since this is physically impossible, it must be assumed that the diffusion equation is correct after a sufficiently long period of time has passed.

In the remaining sections and chapters of this thesis, we will develop the equations of motion for fluid flow in porous media considering the two separate cases of an infinite propagation speed and a finite propagation speed. In the development of the case of infinite propagation speed, the usual parabolic diffusion equation will result. This is the familiar form that serves as the foundation throughout the petroleum engineering discipline to model fluid flow in porous media. In the development of the case of finite propagation speed, a hyperbolic diffusion equation results. This hyperbolic diffusion equation is nothing more than a special form of the telegrapher’s equation, which in essence is a damped wave equation.

2.6 Equations of Motion

At this point, the dynamic laws of qualifying the fluid flow in porous media have been developed. The procedure to complete the development of the fluid flow system is to combine the dynamical equations with the equation of continuity. We make the assumption that the viscosity μ is independent of pressure, the porous medium is

isotropic, and that the compressibility of the formation is negligible.

2.6.1 Implementation of the generalized Darcy equations

To implement the generalized Darcy equations, we substitute in (2.12) into (2.1) obtaining

$$\nabla \cdot (\rho \nabla \Phi) = \frac{\partial(\phi \rho)}{\partial t}, \quad (2.14)$$

which upon implementing the chain rule in (2.14) results in

$$(\nabla \cdot \rho) \nabla (p + V) + \rho \nabla^2 (p + V) = \frac{\mu}{k} \frac{\partial(\phi \rho)}{\partial p} \frac{\partial p}{\partial t}. \quad (2.15)$$

Neglecting gravity and assuming no other body forces, we have that $V = 0$, which transforms the left hand side of (2.15) into

$$\begin{aligned} (\nabla \cdot \rho) \nabla p + \rho \nabla^2 p &= \frac{\partial \rho}{\partial p} \nabla p \nabla p + \rho \nabla^2 p \\ &= \frac{\partial \rho}{\partial p} (\nabla p)^2 + \rho \nabla^2 p \end{aligned} \quad (2.16)$$

Applying the product rule to the right hand side of (2.15), we have

$$\begin{aligned} \frac{\mu}{k} \frac{\partial(\phi \rho)}{\partial p} \frac{\partial p}{\partial t} &= \frac{\mu}{k} \left(\phi \frac{\partial \rho}{\partial p} + \rho \frac{\partial \phi}{\partial p} \right) \frac{\partial p}{\partial t} \\ &= \frac{\mu}{k} \rho \phi \left(\frac{1}{\rho} \frac{\partial \rho}{\partial p} + \frac{1}{\phi} \frac{\partial \phi}{\partial p} \right) \frac{\partial p}{\partial t}. \end{aligned} \quad (2.17)$$

Using the equation of state for a slightly compressible liquid [6]

$$\rho = \rho_0 e^{c(p-p_0)}, \quad (2.18)$$

and defining fluid compressibility and formation compressibility, respectively, by

$$c := \frac{1}{\rho} \frac{\partial \rho}{\partial p} \quad \text{and} \quad c_f := \frac{1}{\phi} \frac{\partial \phi}{\partial p}, \quad (2.19)$$

we can define the total compressibility by

$$c_t := c + c_f. \quad (2.20)$$

Combining (2.16)–(2.20) we obtain

$$\frac{\partial \rho}{\partial p} (\nabla p)^2 + \rho \nabla^2 p = \frac{\mu \rho \phi c_t}{k} \frac{\partial p}{\partial t} \quad (2.21)$$

Dividing (2.21) by ρ and recalling the definition of c in (2.19) yields

$$c (\nabla p)^2 + \nabla^2 p = \frac{\mu \phi c_t}{k} \frac{\partial p}{\partial t}. \quad (2.22)$$

The term $c (\nabla p)^2$ in (2.22) is the product of the fluid compressibility, which is typically a weak function of pressure for liquid that is above the bubblepoint pressure, and the square of the gradient of the pressure, which is nonlinear. If an assumption of small and constant compressibility is made, then this term can be neglected [6]. The end result is the parabolic diffusion equation

$$\nabla^2 p = \frac{1}{\kappa} \frac{\partial p}{\partial t}, \quad (2.23)$$

where the diffusion constant κ is defined by

$$\kappa := \frac{k}{\mu \phi c_t}. \quad (2.24)$$

2.6.2 Implementation of the generalized Darcy and Navier-Stokes equations

Recall that in Section 2 we sought a hydrodynamical equivalent to Newton's law which states that the product of the mass of a body and its acceleration is equal to and opposite the force acting on the body. To accomplish this task, we assume horizontal flow and merge the ideas of the Navier-Stokes equations (2.8)–(2.10) with the generalized Darcy equation (2.12). The thought is to create a new set of dynamic equations of motion which includes the effect of the fluid density (inertia) and also tends to the generalized Darcy equation when the inertia tends to zero. Neglecting external body forces and the effects of gravity, the set of dynamic equations that realizes these two requirements is [38, 40]

$$\frac{\rho}{\phi} \frac{dv_x}{dt} = -\frac{\partial p}{\partial x} - \frac{\mu}{k} v_x \quad (2.25)$$

$$\frac{\rho}{\phi} \frac{dv_y}{dt} = -\frac{\partial p}{\partial y} - \frac{\mu}{k} v_y \quad (2.26)$$

$$\frac{\rho}{\phi} \frac{dv_z}{dt} = -\frac{\partial p}{\partial z} - \frac{\mu}{k} v_z. \quad (2.27)$$

We represent (2.25)–(2.27) in compact vector form by

$$\frac{\rho}{\phi} \frac{d\vec{v}}{dt} = -\nabla p - \frac{\mu}{k} \vec{v}, \quad (2.28)$$

Recalling the equation of state (2.18) for a slightly compressible fluid, we have

$$\frac{\partial \rho}{\partial p} = c\rho$$

which implies

$$\frac{\partial \rho}{\partial x} \frac{\partial x}{\partial p} = c\rho.$$

Thus, we have

$$\frac{\partial p}{\partial x} = \frac{1}{c\rho} \frac{\partial \rho}{\partial x}. \quad (2.29)$$

Now substituting (2.29) into (2.25) we have

$$\frac{\rho}{\phi} \frac{dv_x}{dt} = -\frac{1}{\rho} \left(\frac{1}{c} \frac{\partial \rho}{\partial x} + \frac{\mu}{k} \rho v_x \right), \quad (2.30)$$

and similarly for (2.26)–(2.27) we have

$$\frac{\rho}{\phi} \frac{dv_y}{dt} = -\frac{1}{\rho} \left(\frac{1}{c} \frac{\partial \rho}{\partial y} + \frac{\mu}{k} \rho v_y \right) \quad (2.31)$$

$$\frac{\rho}{\phi} \frac{dv_z}{dt} = -\frac{1}{\rho} \left(\frac{1}{c} \frac{\partial \rho}{\partial z} + \frac{\mu}{k} \rho v_z \right). \quad (2.32)$$

Along the same lines as (2.29) we also have

$$\frac{\partial \rho}{\partial t} = c\rho \frac{\partial p}{\partial t}. \quad (2.33)$$

Using the assumption that c is sufficiently small and using the relationship (2.33), we can make the approximation

$$\frac{\partial(\rho v_x)}{\partial t} = v_x \frac{\partial \rho}{\partial t} + \rho \frac{\partial v_x}{\partial t} = v_x c\rho \frac{\partial p}{\partial t} + \rho \frac{\partial v_x}{\partial t} \approx \rho \frac{\partial v_x}{\partial t}. \quad (2.34)$$

Similarly we have

$$\frac{\partial(\rho v_y)}{\partial t} \approx \rho \frac{\partial v_y}{\partial t} \quad (2.35)$$

$$\frac{\partial(\rho v_z)}{\partial t} \approx \rho \frac{\partial v_z}{\partial t}. \quad (2.36)$$

Now differentiating the continuity equation (2.1) with respect to time and com-

binning (2.30)–(2.32) with (2.34)–(2.36) we obtain

$$\begin{aligned}
-\frac{\partial^2(\phi\rho)}{\partial t^2} &= \frac{\partial^2(\rho v_x)}{\partial x\partial t} + \frac{\partial^2(\rho v_y)}{\partial y\partial t} + \frac{\partial^2(\rho v_z)}{\partial z\partial t} \\
&\approx \frac{\partial}{\partial x} \left(\rho \frac{\partial v_x}{\partial t} \right) + \frac{\partial}{\partial y} \left(\rho \frac{\partial v_y}{\partial t} \right) + \frac{\partial}{\partial z} \left(\rho \frac{\partial v_z}{\partial t} \right) \\
&= -\frac{\partial}{\partial x} \left(\frac{\phi}{\rho} \left(\frac{1}{c} \frac{\partial \rho}{\partial x} + \frac{\mu}{k} \rho v_x \right) \right) - \frac{\partial}{\partial y} \left(\frac{\phi}{\rho} \left(\frac{1}{c} \frac{\partial \rho}{\partial y} + \frac{\mu}{k} \rho v_y \right) \right) \\
&\quad - \frac{\partial}{\partial z} \left(\frac{\phi}{\rho} \left(\frac{1}{c} \frac{\partial \rho}{\partial z} + \frac{\mu}{k} \rho v_z \right) \right) \\
&= -\phi \left(\frac{\partial^2 p}{\partial x^2} + \frac{\mu}{k} \frac{\partial v_x}{\partial x} + \frac{\partial^2 p}{\partial y^2} + \frac{\mu}{k} \frac{\partial v_y}{\partial y} + \frac{\partial^2 p}{\partial z^2} + \frac{\mu}{k} \frac{\partial v_z}{\partial z} \right) \\
&= -\phi \left[\frac{\partial^2 p}{\partial x^2} + \frac{\partial^2 p}{\partial y^2} + \frac{\partial^2 p}{\partial z^2} \right] - \frac{\phi\mu}{k} \left[\frac{\partial v_x}{\partial x} + \frac{\partial v_y}{\partial y} + \frac{\partial v_z}{\partial z} \right] \\
&= -\phi \left[\frac{\partial^2 p}{\partial x^2} + \frac{\partial^2 p}{\partial y^2} + \frac{\partial^2 p}{\partial z^2} \right] - \frac{\phi\mu}{\rho k} \left[\frac{\partial(\rho v_x)}{\partial x} + \frac{\partial(\rho v_y)}{\partial y} + \frac{\partial(\rho v_z)}{\partial z} \right] \\
&= -\phi \left[\frac{\partial^2 p}{\partial x^2} + \frac{\partial^2 p}{\partial y^2} + \frac{\partial^2 p}{\partial z^2} \right] + \frac{\phi\mu}{\rho k} \frac{\partial(\phi\rho)}{\partial t}. \tag{2.37}
\end{aligned}$$

Applying the relationships obtained from (2.17)–(2.20) to the left hand side of (2.37) yields

$$\begin{aligned}
\frac{\partial^2(\phi\rho)}{\partial t^2} &= \frac{\partial}{\partial t} \left(\frac{\partial(\phi\rho)}{\partial t} \right) \\
&= \frac{\partial}{\partial t} \left(\rho\phi c_t \frac{\partial p}{\partial t} \right) \\
&= \phi c_t \frac{\partial}{\partial t} \left(\rho \frac{\partial p}{\partial t} \right) \\
&= \phi c_t \left(\frac{\partial \rho}{\partial t} \frac{\partial p}{\partial t} + \rho \frac{\partial^2 p}{\partial t^2} \right) \\
&= \mu\phi c_t \left(\frac{\partial \rho}{\partial p} \left(\frac{\partial p}{\partial t} \right)^2 + \rho \frac{\partial^2 p}{\partial t^2} \right) \\
&\approx \rho\phi c_t \frac{\partial^2 p}{\partial t^2}. \tag{2.38}
\end{aligned}$$

Similarly applying the relationships obtained from (2.17)–(2.20) to the right hand

side of (2.37) yields

$$-\phi \left[\frac{\partial^2 p}{\partial x^2} - \frac{\partial^2 p}{\partial y^2} + \frac{\partial^2 p}{\partial z^2} \right] + \frac{\mu\phi}{\rho k} \frac{\partial(\phi\rho)}{\partial t} = -\phi \left[\frac{\partial^2 p}{\partial x^2} - \frac{\partial^2 p}{\partial y^2} - \frac{\partial^2 p}{\partial z^2} \right] + \frac{\mu\phi^2 c_t}{k} \frac{\partial p}{\partial t}. \quad (2.39)$$

Combining (2.38) and (2.39), using (2.24), and assuming that $\rho \approx \rho_0$, we see that (2.37) becomes

$$\frac{\partial^2 p}{\partial x^2} + \frac{\partial^2 p}{\partial y^2} + \frac{\partial^2 p}{\partial z^2} = \rho_0 c_t \frac{\partial^2 p}{\partial t^2} + \frac{1}{\kappa} \frac{\partial p}{\partial t}. \quad (2.40)$$

Assuming that c_t is constant and c_f is negligible, we have

$$c_t = \frac{1}{\rho} \frac{\partial \rho}{\partial p} \approx \frac{1}{\rho_0} \frac{\partial \rho}{\partial p} =: \frac{1}{\rho_0 a^2},$$

where a is the speed of sound in the fluid.

Thus, substituting in (2.24), we can rewrite (2.40) in a more general form as

$$\nabla^2 p = \frac{1}{a^2} \frac{\partial^2 p}{\partial t^2} + \frac{1}{\kappa} \frac{\partial p}{\partial t}. \quad (2.41)$$

In Cartesian coordinates (2.41) is given by

$$\frac{\partial^2 p}{\partial x^2} + \frac{\partial^2 p}{\partial y^2} + \frac{\partial^2 p}{\partial z^2} = \frac{1}{a^2} \frac{\partial^2 p}{\partial t^2} + \frac{1}{\kappa} \frac{\partial p}{\partial t}. \quad (2.42)$$

In cylindrical coordinates (2.41) is given by

$$\frac{1}{r} \frac{\partial p}{\partial r} \left(r \frac{\partial p}{\partial r} \right) + \frac{1}{r^2} \frac{\partial^2 p}{\partial \varphi^2} + \frac{\partial^2 p}{\partial z^2} = \frac{1}{a^2} \frac{\partial^2 p}{\partial t^2} + \frac{1}{\kappa} \frac{\partial p}{\partial t}, \quad (2.43)$$

which reduces to

$$\frac{1}{r} \frac{\partial p}{\partial r} \left(r \frac{\partial p}{\partial r} \right) = \frac{1}{a^2} \frac{\partial^2 p}{\partial t^2} + \frac{1}{\kappa} \frac{\partial p}{\partial t} \quad (2.44)$$

for purely radial flow.

In spherical coordinates (2.41) is given by

$$\frac{1}{r^2} \frac{\partial}{\partial r} \left(r^2 \frac{\partial p}{\partial r} \right) + \frac{1}{r^2 \sin(\theta)} \frac{\partial}{\partial \theta} \left(\sin(\theta) \frac{\partial p}{\partial \theta} \right) + \frac{1}{r^2 \sin^2(\theta)} \frac{\partial^2 p}{\partial \varphi^2} = \frac{1}{a^2} \frac{\partial^2 p}{\partial t^2} + \frac{1}{\kappa} \frac{\partial p}{\partial t}, \quad (2.45)$$

which reduces to

$$\frac{1}{r^2} \frac{\partial}{\partial r} \left(r^2 \frac{\partial p}{\partial r} \right) = \frac{1}{a^2} \frac{\partial^2 p}{\partial t^2} + \frac{1}{\kappa} \frac{\partial p}{\partial t} \quad (2.46)$$

for purely radial flow.

Solutions of (2.23) for purely radial flow in cylindrical coordinates will be developed in Chapter 4, while the more general solutions of (2.44) for purely radial flow in cylindrical coordinates will be developed in Chapter 5.

Note that as the speed of sound $a \rightarrow \infty$, the hyperbolic diffusion equations (2.42)–(2.46) all tend to their parabolic diffusion equation counter parts since the coefficient $1/a^2 \rightarrow 0$. Thus it is expected (and will be confirmed) that the solutions obtained in Chapter 5 should tend to the corresponding solutions in Chapter 4 as $a \rightarrow \infty$.

3. METHODS OF SOLUTION

God used beautiful mathematics in creating the world.

Paul Dirac (1902–1984)

3.1 Introduction

Many of the models that are derived in petroleum engineering turn out to be nonlinear partial differential equations and, in many cases, can be impossible to solve analytically. To circumvent this impasse, assumptions are made about the system and the relative magnitude of certain terms in the differential equation which allow their omission, thus making the resulting simplified partial differential equation linear and at the same time accurate enough for engineering purposes. In addition, the newly obtained differential equation is solvable and from the solution the general behavior of the entire system can still be determined.

Different methods exist for solving the linear partial differential equations that are found in the study of fluid flow in porous media. One method of solution is using a transform method. The methods that will be used in this thesis are the transforms of Laplace and Hankel. The most popular of these transform methods is the Laplace transform and the theory of this method will be discussed below. The Hankel transform will be implemented in subsequent chapters and it will be constructed for specific solutions to given problems. Separation of variables is another method that will be introduced in this chapter as a means to solve the problems found in this thesis.

Implementation of the Hankel transform and separation of variables produce regular or singular (to be defined later) Sturm-Liouville problems, depending on the spatial domain. Thus, in order to implement these solution methods, we must be



(a) Charles Sturm (1803–1855).



(b) Joseph Liouville (1809–1882).

Figure 3.1: The parties responsible for the development of the Sturm-Liouville theory.

able to solve Sturm-Liouville problems. Due to this requirement, we will begin this chapter with the necessary development of Sturm-Liouville theory. We follow with a discussion of the method of separation of variables and Laplace transform theory .

3.2 Sturm-Liouville Theory

In this section a detailed introduction to Sturm-Liouville theory and orthogonal series expansions will be provided following the development in [14].

We take as our foundation the generalized second order eigenvalue problem of the form

$$a_2(x)y'' + a_1(x)y' + a_0(x)y + \lambda y = 0, \quad a < x < b, \quad (3.1a)$$

$$\alpha_1 y(a) + \alpha_2 y'(a) = 0, \quad (3.1b)$$

$$\beta_1 y(b) + \beta_2 y'(b) = 0, \quad (3.1c)$$

where it is assumed that the coefficient functions a_i are continuous and $a_2(x)$ is positive for all $a < x < b$. Central to the solution methodology for (3.1) is Sturm-Liouville

theory, named after Charles François Sturm and Joseph Liouville (see Figure 3.1).

We first define the operator L by

$$Ly := a_2(x)y'' + a_1(x)y' + a_0(x)y \quad (3.2)$$

and then convert this into Sturm-Liouville form. The resulting Sturm-Liouville operator is

$$\begin{aligned} Sy &:= \frac{1}{w(x)} [(p(x)y')' + q(x)y] \\ &= \frac{1}{w(x)} [p(x)y'' + p'(x)y' + q(x)y] \\ &= a_2(x)y'' + a_1(x)y' + a_0(x)y, \end{aligned} \quad (3.3)$$

where the operator S is also defined for all $a < x < b$. We solve (3.3) for p , q , and w obtaining

$$p(x) = a_2(x)w(x), \quad p'(x) = a_1(x)w(x), \quad q(x) = a_0(x)w(x). \quad (3.4)$$

By differentiating the first equation in (3.4) and combining it with the second equation in (3.4) we obtain

$$w'(x) = \frac{a_1(x) - a_2'(x)}{a_2(x)} w(x)$$

which has the solution

$$w(x) = \exp \left[\int \left(\frac{a_1(x) - a_2'(x)}{a_2(x)} \right) dx \right]. \quad (3.5)$$

Since $w(x)$ is now known, we can find all three functions in (3.4). It should be noted that since $a_2(x)$ is assumed to be positive for all $a < x < b$, we now also have that

$p(x)$ and $w(x)$ are also positive for all $a < x < b$ as well.

3.2.1 Regular Sturm-Liouville theory

We are now in a position to develop the regular Sturm-Liouville theory. Given the Sturm-Liouville problem

$$\frac{1}{w(x)} [(p(x)y')' + q(x)y] + \lambda y = 0, \quad a < x < b, \quad (3.6a)$$

$$\alpha_1 y(a) + \alpha_2 y'(a) = 0, \quad (3.6b)$$

$$\beta_1 y(b) + \beta_2 y'(b) = 0, \quad (3.6c)$$

we say that λ is an *eigenvalue* of (3.6) if there exists a nonzero solution $y(x)$ associated with the value of λ . If so, then the function $y(x)$ is an *eigenfunction* corresponding to λ . Furthermore, (3.6) is a *regular Sturm-Liouville problem* and S is a *regular Sturm-Liouville operator* if we have

1. $\alpha_1^2 + \alpha_2^2 \neq 0$ and $\beta_1^2 + \beta_2^2 \neq 0$,
2. p, q, w, p' are continuous on $a < x < b$,
3. $p(x), w(x) > 0$ on $a < x < b$.

We now state three necessary theorems for the development of the regular Sturm-Liouville theory, all of which can be found in [14]. This theory will be used in subsequent sections and chapters to develop different transforms and solutions. Theorem 3.1 defines Lagrange's Identity and Green's Identity, both of which are used in the proof of Theorem 3.2.

Theorem 3.1 (Lagrange's Identity and Green's Identity). *Let S be a Sturm-Liouville*

operator with $p \in C^1[a, b]$ and $u, v \in C^2[a, b]$. Then

$$uSv - vSu = \frac{1}{w} \frac{d}{dx} [p(uv' - u'v)] \quad (3.7)$$

is called Lagrange's Identity. The weighted integration of (3.7) is

$$\int_a^b [u(x)Sv(x) - v(x)Su(x)]w(x) dx = p(x)[u(x)v'(x) - u'(x)v(x)] \Big|_a^b, \quad (3.8)$$

which can be written as

$$\langle u, Sv \rangle_w - \langle Su, v \rangle_w = p(x)[u(x)v'(x) - u'(x)v(x)] \Big|_a^b. \quad (3.9)$$

Both (3.8) and (3.9) are called Green's Identity.

It is straightforward to see that Green's Identity is determined by multiplying (3.7) by the weight function $w(x)$ and then integrating over the finite interval $[a, b]$. The results of Theorem 3.1 are used in the proof (which is omitted here) of Theorem 3.2 below.

Theorem 3.2 (Regular Sturm-Liouville Operators are Symmetric). *Let S be a regular Sturm-Liouville operator and $u, v \in C^2[a, b]$ satisfy the boundary conditions in (3.6b) and (3.6c). Then*

$$\langle u, Sv \rangle_w = \langle Su, v \rangle_w, \quad (3.10)$$

which indicates that S is symmetric with respect to the weighted inner product.

The result of Theorem 3.2 is essential in the development of the theory for general Sturm-Liouville problems. The third theorem that we state identifies properties of regular Sturm-Liouville problems. The most important of the properties listed in

Theorem 3.3 is the completeness of the eigenfunctions. The series solution methods that we employ in this thesis depend upon this fact, as we will soon see that in computing the coefficients in the series solutions, we rely on the fact that the eigenfunctions are orthogonal.

Theorem 3.3 (Properties of Regular Sturm-Liouville Problems). *Consider the regular Sturm-Liouville problem (3.6).*

(a) *The eigenvalues are real and can be arranged into an increasing sequence*

$$\lambda_1 < \lambda_2 < \cdots < \lambda_n < \lambda_{n+1} < \cdots ,$$

such that $\lambda_n \rightarrow \infty$ as $n \rightarrow \infty$.

(b) *The sequence of eigenfunctions $\{y_n(x)\}_{n=1}^{\infty}$ forms a complete orthogonal family on $a < x < b$ with respect to the weight function $w(x)$; that is, if λ_n and λ_m are distinct with corresponding eigenfunctions $y_n(x)$ and $y_m(x)$, then*

$$\langle y_n, y_m \rangle_w := \int_a^b y_n(x)y_m(x)w(x) dx = 0, \quad n \neq m.$$

(c) *The eigenfunction $y_n(x)$ corresponding to the eigenvalue λ_n is unique up to a constant multiple.*

(d) *The eigenfunction $y_n(x)$ corresponding to the eigenvalue λ_n has $(n-1)$ interior zeroes in the interval (a, b) .*

(e) *If $f \in L_w^2[a, b]$ is expanded in an infinite series of these eigenfunctions,*

$$f(x) = \sum_{n=1}^{\infty} c_n y_n(x), \quad a < x < b, \tag{3.11}$$

then the coefficients in (3.11) are given by

$$c_n = \frac{\langle f, y_n \rangle_w}{\langle y_n, y_n \rangle_w} = \frac{\int_a^b f(x) y_n(x) w(x) dx}{\int_a^b y_n^2(x) w(x) dx}. \quad (3.12)$$

Here, equality is meant in the sense of L^2 convergence weighted by $w(x)$. We denote the weighted L^2_w space by $L^2_w[a, b]$, where

$$L^2_w[a, b] := \left\{ f : [a, b] \rightarrow \mathbb{R} \mid \int_a^b |f(x)|^2 w(x) dx < \infty \right\}.$$

We note that if zero is an eigenvalue of a Sturm-Liouville problem, we will set $\lambda_0 = 0$. In this case, we will begin the infinite series in (3.11) with $n = 0$ instead of $n = 1$ and part (d) in Theorem 3.3 will of course now read y_n has n interior zeroes.

3.2.2 Singular Sturm-Liouville theory

When employing the method of separation of variables and the Hankel transforms found in this thesis, it may be that the resulting Sturm-Liouville problem does not meet the criteria to be considered regular. However, it is still desirable to have an monotone sequence of eigenvalues that are real with corresponding eigenfunctions that make up a complete orthogonal family in an apposite weighted L^2 space. In what follows, we will make the necessary modifications to the regular Sturm-Liouville theory that was developed in Subsection 3.2.1 in order to maintain these properties.

We again consider (3.6). Suppose that both properties

1. p, q, w, p' are continuous on $a < x < b$ and
2. $p(x), w(x) > 0$ on $a < x < b$

are true. Also, suppose that at least one of the following properties

- (a) $p(x)$ or $w(x)$ is zero at an endpoint,

(b) p , q , or w becomes infinite at an endpoint, or

(c) $a = -\infty$ or $b = \infty$,

is also true. Then we say that (3.6) is a *singular Sturm-Liouville problem* and the operator S is called a *singular Sturm-Liouville operator*. The endpoint where at least one of (a)–(c) are true is called *singular*.

Considering the singular Sturm-Liouville problem (3.6), our goal is to have an analogous theorem to Theorem 3.3. However, in order to do so, we must establish a result that states that the singular Sturm-Liouville operator is also symmetric. In order to do so, we must show that the right hand side of Green's Identity (3.9) is zero. In order to do so, we must make sure that we modify the endpoint(s) where the problem is singular and enforce conditions such that Green's Identity is zero, which in turn causes the singular Sturm-Liouville operator to be symmetric. We now state a theorem that is a singular version of Theorem 3.3.

Theorem 3.4 (Singular Sturm-Liouville Operators are Symmetric). *Let S be a singular Sturm-Liouville operator and $u, v \in C^2[a, b]$. If we have*

$$\lim_{x \rightarrow a^+} p(x)[u(x)v'(x) - u'(x)v(x)] = \lim_{x \rightarrow b^-} p(x)[u(x)v'(x) - u'(x)v(x)] \quad (3.13)$$

for all u, v that satisfy the properly modified boundary conditions of (3.6b) and (3.6c), then

$$\langle u, Sv \rangle_w = \langle Su, v \rangle_w,$$

which indicates that S is symmetric with respect to the weighted inner product.

We remark that for a regular endpoint, the condition (3.13) is equivalent to (3.9). The use of limits in (3.13) is due to the fact that some of the functions p , u , v may not be defined at the endpoints, or may even be infinite.

Proving that the eigenvalues of a singular Sturm-Liouville problem are real and that the corresponding eigenfunctions are orthogonal with respect to the weight function $w(x)$ can be accomplished by showing that the singular Sturm-Liouville operator S is symmetric. This is why the importance of Theorem 3.4 cannot be overstated.

3.3 The Method of Separation of Variables

In order to introduce the method of separation of variables, we will outline the solution method to the IBVP

$$\frac{1}{r} \frac{\partial}{\partial r} \left(r \frac{\partial y}{\partial r} \right) = \frac{1}{\kappa} \frac{\partial y}{\partial t}, \quad a < r < b \quad (3.14a)$$

$$y(r, 0) = 0, \quad a < r < b, \quad (3.14b)$$

$$y(a, t) = 1, \quad t > 0, \quad (3.14c)$$

$$y(b, t) = 0, \quad t > 0. \quad (3.14d)$$

It is important to realize that in order to use the separation of variables method, we must have homogeneous boundary conditions. To do so, we introduce a solution $y_{ss}(r)$ that solves

$$\frac{1}{r} \frac{\partial}{\partial r} \left(r \frac{\partial y}{\partial r} \right) = 0 \quad (3.15a)$$

$$y(a) = 1, \quad (3.15b)$$

$$y(b) = 0. \quad (3.15c)$$

It is easy to see that the general solution to (3.15) is

$$y_{ss}(r) = A + B \ln(r). \quad (3.16)$$

Enforcing the boundary conditions (3.15b) and (3.15c) on (3.16), we find that the particular solution to (3.15) is

$$y_{ss}(r) = \frac{\ln\left(\frac{r}{b}\right)}{\ln\left(\frac{a}{b}\right)}. \quad (3.17)$$

We now modify the original problem to

$$\frac{1}{r} \frac{\partial}{\partial r} \left(r \frac{\partial y}{\partial r} \right) = \frac{\partial y}{\partial t}, \quad a < r < b \quad (3.18a)$$

$$y(r, 0) = -y_{ss}(r) = -\frac{\ln\left(\frac{r}{b}\right)}{\ln\left(\frac{a}{b}\right)}, \quad a < r < b, \quad (3.18b)$$

$$y(a, t) = 0, \quad t > 0, \quad (3.18c)$$

$$y(b, t) = 0, \quad t > 0. \quad (3.18d)$$

We now find the solution y_{tr} to the above. Note that the full solution to the original IBVP (3.14) that was posed at the beginning of this section will be the sum of the solution to (3.18) and (3.17) given by

$$y(r, t) := y_{tr}(r, t) + y_{ss}(r).$$

To use the method of separation of variables, we seek a solution to (3.18) of the form

$$y_{tr}(r, t) = R(r)T(t).$$

We substitute this into (3.18a) and obtain

$$\begin{aligned} \frac{1}{r} \frac{\partial}{\partial r} \left(r \frac{\partial R(r)T(t)}{\partial r} \right) &= \frac{\partial R(r)T(t)}{\partial t} \\ \frac{R''(r)}{R(r)} + \frac{1}{r} \frac{R'(r)}{R(r)} &= \frac{T'(t)}{T(t)}. \end{aligned}$$

Since the left hand side is made up only of functions of the independent variable r and the right hand side is made up only of functions of the independent variable t , it must be that both sides are constant in order for equality to hold. Thus, we set both sides equal to a *separation constant* λ by

$$\frac{R''(r)}{R(r)} + \frac{1}{r} \frac{R'(r)}{R(r)} = \frac{T'(t)}{T(t)} = -\lambda,$$

where λ is yet to be determined and only has a minus sign for convenience.

We now have two ordinary differential equations to solve. In fact, we will use the boundary values as the initial values for the differential equation for the variable r . The first differential equation one that we consider is

$$T'(t) = -\lambda T(t),$$

which has as a general solution $T(t) = Ce^{-\lambda t}$, where C is an arbitrary constant.

The second differential equation can be cast in Sturm-Liouville form as

$$\frac{1}{r} \frac{\partial}{\partial r} \left(r \frac{\partial R(r)}{\partial r} \right) + \lambda R(r) = 0 \tag{3.19}$$

$$R(a) = 0 \quad R(b) = 0. \tag{3.20}$$

We first check to see if $\lambda = 0$ is an eigenvalue. Observe,

$$\frac{1}{r} \frac{\partial}{\partial r} \left(r \frac{\partial R}{\partial r}(r) \right) = 0$$

has the solution $R_0(r) = A + B \ln(r)$. In order to satisfy the homogeneous boundary conditions, $A = B = 0$. Thus, $\lambda = 0$ is not an eigenvalue.

We now assume $\lambda > 0$ and solve

$$\frac{1}{r} \frac{\partial}{\partial r} \left(r \frac{\partial R(r)}{\partial r} \right) + \lambda R(r) = 0 \quad (3.21)$$

$$R(a) = 0 \quad R(b) = 0. \quad (3.22)$$

Enforcing the boundary conditions (3.18c) and (3.18d), the solution is given by

$$R_n(r) = J_0(a\sqrt{\lambda_n})Y_0(r\sqrt{\lambda_n}) - Y_0(a\sqrt{\lambda_n})J_0(r\sqrt{\lambda_n}),$$

where λ_n are the countably infinitely many positive roots of $R(b) = 0$. Notice by definition we also have $R_n(a) = 0$. For each λ_n , we now denote $T_n(t) = c_n e^{-\lambda_n t}$. By the Superposition Principle [14], we have the solution $y_{tr}(r, t)$ as

$$y_{tr}(r, t) = \sum_{n=1}^{\infty} R_n(r)T_n(t) = \sum_{n=1}^{\infty} c_n \left[J_0(a\sqrt{\lambda_n})Y_0(r\sqrt{\lambda_n}) - Y_0(a\sqrt{\lambda_n})J_0(r\sqrt{\lambda_n}) \right] e^{-\lambda_n t}.$$

We must have $y_{tr}(r, 0) = -y_{ss}(r)$. Thus, using (3.11) and (3.12) in Theorem 3.2, we have

$$y_{tr}(r, 0) = -y_{ss}(r) = \sum_{n=1}^{\infty} c_n \left[J_0(a\sqrt{\lambda_n})Y_0(r\sqrt{\lambda_n}) - Y_0(a\sqrt{\lambda_n})J_0(r\sqrt{\lambda_n}) \right],$$

which implies that for each n we have

$$\begin{aligned}
c_n &= -\frac{\int_a^b y_{ss}(r)[J_0(a\sqrt{\lambda_n})Y_0(r\sqrt{\lambda_n}) - Y_0(a\sqrt{\lambda_n})J_0(r\sqrt{\lambda_n})]r \, dr}{\int_a^b [J_0(a\sqrt{\lambda_n})Y_0(r\sqrt{\lambda_n}) - Y_0(a\sqrt{\lambda_n})J_0(r\sqrt{\lambda_n})]^2 r \, dr} \\
&= \frac{\pi^2 \lambda_n J_0^2(b\sqrt{\lambda_n})}{2(J_0^2(b\sqrt{\lambda_n}) - J_0^2(a\sqrt{\lambda_n}))} \int_a^b y_{ss}(r) \left[J_0(a\sqrt{\lambda_n})Y_0(r\sqrt{\lambda_n}) \right. \\
&\quad \left. - Y_0(a\sqrt{\lambda_n})J_0(r\sqrt{\lambda_n}) \right] r \, dr.
\end{aligned}$$

Thus, the complete solution to (3.14) is

$$\begin{aligned}
y(r, t) &= y_{ss}(r) + y_{tr}(r, t) \\
&= \frac{\ln\left(\frac{r}{b}\right)}{\ln\left(\frac{a}{b}\right)} + \sum_{n=1}^{\infty} c_n \left[J_0(a\sqrt{\lambda_n})Y_0(r\sqrt{\lambda_n}) - Y_0(a\sqrt{\lambda_n})J_0(r\sqrt{\lambda_n}) \right] e^{-\lambda_n t}.
\end{aligned}$$

This solution is the same as that found in [35, 36]. Other IBVPs can be solved similarly. The methods outlined in this chapter can be used to solve any of the standard diffusion equations found in [27, 35, 36, 51].

3.4 Laplace Transform Theory

Laplace transforms can sometimes offer the engineer a simpler technique in obtaining solutions to linear partial differential equations, particularly if at least one of the boundary conditions are not constant. The theory of Laplace transforms is also sometimes referred to as operational calculus, due to the famous English electrical engineer, mathematician, and physicist Oliver Heaviside (see Figure 3.2). Originally, Heaviside used his operational calculus to solve equations in electromagnetic theory and communications.

The development of the Laplace transform was led by French mathematician and astronomer Pierre-Simon Laplace (see Figure 3.3) who worked primarily in the development of similar transforms in probability theory. He began by introducing



Figure 3.2: Oliver Heaviside (1850–1925).

various transforms which were initially used to transform difference equations. The idea was to solve the transformed difference equation in the new domain and then invert the solution back to the original domain, thus obtaining the solution to the original difference equation. The development of the Laplace transform came soon after. Laplace also made the observation that the Fourier transform for solving linear partial differential equations, in particular the diffusion equation, was only applicable to solutions which were periodic.

3.4.1 The Laplace transformation

We begin the introduction of the Laplace transformation with some necessary definitions. We assume that the reader has a basic understanding of functions of a complex variable. In this section we follow the development in [12].

We define the *Laplace transform* of a real or complex-valued function $f(t)$ of the



Figure 3.3: Pierre-Simon Laplace (1749–1827).

real variable t by

$$F(s) := \mathcal{L}\{f(t)\}(s) = \lim_{\varepsilon \rightarrow 0^+} \lim_{T \rightarrow \infty} \int_{\varepsilon}^T e^{-st} f(t) dt = \int_0^{\infty} e^{-st} f(t) dt, \quad (3.23)$$

where $s \in \mathbb{C}$ and \mathbb{C} is the set of complex numbers. In other words, $s = x + iy$, where both $x, y \in \mathbb{R}$ and $i := \sqrt{-1}$. The function f typically has the property that $f(t) = 0$ for all $t < 0$.

We remark that in the case that $f(t)$ is a function that has a jump discontinuity at $t = 0$ or is continuous at that point, then the lower limit $\varepsilon \rightarrow 0^+$ can be replaced by $\varepsilon \rightarrow 0$. However, if the function $f(t)$ is singular at $t = 0$, then the lower limit should be chosen as in (3.23). This choice of the lower limit omits the singular point at $t = 0$, thus defining the Laplace transform $F(s)$ in terms of $f(t)$ only when $t > 0$.

As with any transformation, uniqueness needs to be contemplated. By (3.23), it can be observed that there exists only one Laplace transform $F(s)$ for $f(t)$. If two functions f and g have the same Laplace transform, then it can be said that $f = g$

almost everywhere, which takes into account the possibility that there are a finite number of isolated points $\{t_k\}_{k=1}^n$ in any finite interval $[a, b]$ (with $0 \leq a < b < \infty$) such that $f(t_k) \neq g(t_k)$. If both functions have the same Laplace transform and are continuous for all $t \geq 0$, then $f = g$ for all $t \geq 0$.

According to (3.23), we can write $F(s)$ as

$$F(s) = u(x, y) + iv(x, y), \quad (3.24)$$

where

$$u(x, y) = \int_0^\infty e^{-xt} \cos(yt) f(t) dt \quad \text{and} \quad v(x, y) = - \int_0^\infty e^{-xt} \sin(yt) f(t) dt. \quad (3.25)$$

Given that the function $f(t)$ is piecewise continuous over any interval $(0, T)$ and can be bounded by an exponential function as $t \rightarrow \infty$, there exist positive constants α and M such that $|f(t)| < Me^{\alpha t}$, for all $t \geq 0$. When α and M exist, we say that f is $\mathcal{O}(e^{\alpha t})$.

Considering (3.24) and (3.25), as well as supposing that f is piecewise continuous and $\mathcal{O}(e^{\alpha t})$, we can now state the following theorem [12].

Theorem 3.5. *Let a real-valued function f be piecewise continuous over any interval $0 < t < T$ and $\mathcal{O}(e^{\alpha t})$ as $t \rightarrow \infty$. Then, for $s \in \mathbb{C}$, its transform*

$$F(s) = \mathcal{L}\{f(t)\}(s) = \int_0^\infty e^{-st} f(t) dt$$

is analytic function of s over the half plane $x > \alpha$. Its Laplace integral is absolutely and uniformly convergent over each half plane $x \geq x_0 > \alpha$, and f and its derivatives

are bounded there. Also, for $x > \alpha$,

$$F^{(n)}(s) = \mathcal{L}\{(-t)^n f(t)\}(s), \quad n = 1, 2, \dots,$$

$$\overline{F(s)} = F(\bar{s}).$$

We may expand Theorem 3.5 to the case of where f is infinite at some $t = t_0$, but $(t - t_0)^k f(t)$ remains bounded as $t \rightarrow t_0$ for some $k < 1$.

When the magnitude of the complex number s approaches ∞ in a half plane of convergence of the Laplace integral, the behavior of the transform $F(s)$ is controlled by the regularity properties of the function $f(t)$. Accordingly, we have the subsequent theorem [12].

Theorem 3.6. *Let a function f and its derivative f' be piecewise continuous on any bounded interval $(0, T)$ and let f be $\mathcal{O}(e^{\alpha t})$. Then, in any half plane where $\text{Re}(s) \geq x_0 > \alpha$, the transform F obeys*

$$\lim_{|s| \rightarrow \infty} F(s) = 0.$$

For slightly stronger conditions of continuity, piecewise continuity, and of exponential order on f and its derivatives, we can state the resulting useful theorem [12].

Theorem 3.7. *Given $n > 0$, suppose $f, f', \dots, f^{(n-1)}$ are continuous, the next two derivatives $f^{(n)}, f^{(n+1)}$ are piecewise continuous over each interval $[0, T]$ while the functions f and its first n derivatives are $\mathcal{O}(e^{\alpha t})$. Then we have that*

$$s^n F(s) - s^{n-1} f(0^+) - s^{n-2} f'(0^+) - \dots - s f^{n-2}(0^+) - f^{n-1}(0^+) \quad (3.26)$$

is bounded over any half plane $x \geq x_0 > \alpha$ and

$$\lim_{|s| \rightarrow \infty} s^n F(s) - s^{n-1} f(0^+) - s^{n-2} f'(0^+) - \dots - s f^{n-2}(0^+) = f^{n-1}(0^+). \quad (3.27)$$

Additionally, $f(0^+) = f'(0^+) = \dots = f^{(n-2)}(0^+) = 0$ is a necessary and sufficient condition for $F(s)$ to be $\mathcal{O}(s^{-n})$ over the half plane and $\lim_{|s| \rightarrow \infty} s^n F(s) = f^{(n-1)}(0^+)$ in the half plane.

If the function f or any of the $(n - 1)$ derivatives are continuous at $t = 0$, then we may use 0 instead of 0^+ . Theorem 3.7 is extremely important and its results will be used when inverting a Laplace transform. In fact, from Theorem 3.7 we have the general formula for the Laplace transform of the n th derivative of the function $f(t)$

$$\mathcal{L}\{f^{(n)}(t)\}(s) = s^n F(s) - s^{n-1} f(0^+) - s^{n-2} f'(0^+) - \dots - s f^{n-2}(0^+) - f^{n-1}(0^+), \quad (3.28)$$

for all $n \geq 0$.

3.4.2 The inversion integral for the Laplace transformation

In order to ensure the existence of the inverse Laplace transform of a function $F(s)$, the following theorem is stated which provides the requirements that are sufficient for a real or complex-valued function $f(t)$ of the real variable t [12]. The following theorem [12] is known as the *Laplace inversion formula* or the *Bromwich integral formula*.

Theorem 3.8 (Laplace inversion formula). *Let F be any function of the complex variable $s = x + iy$ that is analytic and $\mathcal{O}(s^{-k})$ for all s over a half plane $x \geq \alpha$, where $k > 1$; also let $F(x)$ be real-valued for $x \geq \alpha$. Then for all real t the inversion integral of $F(s)$ along any line $x = \gamma$, where $\gamma \geq \alpha$, converges to a real-valued*

function f that is independent of γ ,

$$f(t) = \mathcal{L}^{-1}\{F(s)\}(t) = \frac{1}{2\pi i} \int_{\gamma-i\infty}^{\gamma+i\infty} e^{zt} F(z) dz, \quad |t| < \infty, \quad (3.29)$$

whose Laplace transform is the given function $F(s)$:

$$\mathcal{L}\{f(t)\}(s) = F(s), \quad \text{Re } s > \alpha.$$

Furthermore, $f(t)$ is $\mathcal{O}(e^{\alpha t})$, it is continuous for all real t , and $F(t) = 0$ for all $t \leq 0$.

Theorem 3.8 demonstrates the conditions under which the inverse Laplace transform of $F(s)$ exists and that the resulting function is represented by $f(t)$. The last part of Theorem 3.8 can be proved by implementing an extension of Cauchy's integral theorem, and showing for any $\gamma > 0$ and $t \leq 0$, we have

$$\int_{\gamma-i\infty}^{\gamma+i\infty} e^{zt} F(z) dz = 0,$$

which implies $f(t) = 0$ for all $t \leq 0$, and in particular $f(0) = 0$.

As will be demonstrated in this thesis, solutions to boundary value problems that are found using the inverse Laplace transform of a function F can usually be verified by examining the properties of F . We state two theorems that make this possible [12].

Theorem 3.9. *Let F be an analytic function of the complex variable s and $\mathcal{O}(s^{-k-m})$, with $m \in \mathbb{Z}^+$ and $k > 1$, over a half plane $x \geq \alpha$. Also let $F(x)$ be real for $x \geq \alpha$. Then the inversion integral of F along any line $x = \gamma \geq \alpha$ converges to the inverse*

transform of F , a real-valued function f , given by

$$\mathcal{L}^{-1}\{F(s)\}(t) = f(t), \quad t \geq 0,$$

and the derivatives of f are given by

$$f^{(n)}(t) = \mathcal{L}^{-1}\{s^n F(s)\}(t), \quad n = 1, 2, \dots, m.$$

Furthermore, f and each of its derivatives are continuous when $t \geq 0$ and $\mathcal{O}(e^{\alpha t})$, and their initial values are zero:

$$f(0) = f'(0) = \dots = f^{(m)}(0) = 0.$$

The next theorem considers a function F that has two independent variables and how differentiation and continuity with respect to the second parameter are dealt with [12].

Theorem 3.10. *Let F be a continuous function of two variables r and $s = x + iy$ when $x \geq \alpha$, analytic with respect to s over that half plane for each fixed r , and such that $|F(r, s)| < M|s|^{-k}$ there, where $k > 1$, and the constants M , k , and α are independent of r . Also, let $F(r, x)$ be real when $x \geq \alpha$. Even if r has an unbounded range of values, let $F(r, \alpha + iy)$ be bounded for all r and y . Then the inverse transform of F with respect to s , which can be written as*

$$f(r, t) = \mathcal{L}^{-1}\{F(r, s)\}(t), \quad \gamma \geq \alpha, \quad t \geq 0,$$

is a continuous real-valued function of its two variables r and $t \geq 0$ for which a positive constant N independent of r exists such that $|f(r, t)| < Ne^{\alpha t}$. In particular,

f is a bounded function of r for each fixed t . If the partial derivative $f_r(r, t)$ also satisfies the conditions imposed here on F , then

$$\frac{\partial}{\partial r} f(r, t) = \mathcal{L}^{-1} \left\{ \frac{\partial}{\partial r} F(r, s) \right\} (t),$$

and $|f_r(r, t)| < Ne^{\alpha t}$.

The results of Theorem 3.10 are extremely important and will be used throughout the sequel when boundary value problems are solved using the method of Laplace transforms.

The next theorem provides a means to represent the inverse Laplace transform of a function F as the sum of the residues of $e^{zt}F(z)$.

Theorem 3.11. *Let F be analytic everywhere except for isolated singular points s_n , $n \in \mathbb{Z}^+$ in a half plane $x < \gamma$ and such that its inversion integral along the line $x = \gamma$ represents the inverse Laplace transform $f(t)$ of $F(s)$. On appropriate contours C_N , $N \in \mathbb{Z}^+$ in the left half plane $x \leq \gamma$, let F satisfy the order condition $|F(z)| < M|z|^{-k}$, where M and k are positive constants independent of N . Then when $t > 0$, the series of residues $\rho_n(t)$ of $e^{zt}F(z)$ at s_n converges to $f(t)$,*

$$f(t) = \sum_{n=1}^{\infty} \rho_n(t), \quad t > 0,$$

if its terms corresponding to points s_n within the ring between successive paths C_N and C_{N+1} are grouped as a single term of the series.

Also, if $k > 1$ and $\mathcal{L}^{-1}\{F\}$ represents $\frac{1}{2}f(0^+)$ when $t = 0$, then

$$\frac{1}{2}f(0^+) = \sum_{n=1}^{\infty} \rho_n(0).$$

The results of Theorem 3.11 are also of tremendous significance and will be employed when finding solutions via the inverse Laplace transform.

4. PARABOLIC DIFFUSION

When the solution is simple, God is answering.

Albert Einstein (1879–1955)

4.1 Introduction

In this chapter, the solution to the parabolic diffusion equation in cylindrical coordinates that was developed in (2.23) will be derived. The problem will be cast in terms of a limited reservoir in which there exists one initial condition and two boundary conditions. Of the two boundary conditions, the first will be specified at the internal boundary $r = r_1$, which is the wellbore, while the second will be specified at the external boundary, $r = r_2$, which is the edge of the reservoir. The reservoir is assumed to be of purely horizontal radial flow and the effects of gravity are neglected.

The two most popular analytical methods that are discussed in the literature are the Laplace transform [51] and the method of separation of variables [35, 36]. In the types of problems contained in this chapter, the Laplace transform is useful because it allows the engineer the ability to at once see the pseudo-steady state part of the solution. The difficult part seems to be the inversion of the Laplace transform, especially in the case when there exists a double pole. The method of separation of variables has the same advantage in that it allows the engineer to glean the pseudo-steady state solution immediately once the solution is complete. Its downfall is that in some cases one must know three elementary solutions to the parabolic diffusion equation.

In this chapter, by derivations of different Hankel transforms, which have not been found in the literature for this particular application, we will develop solutions to the radial flow parabolic diffusion equation where the pressure and/or flow rates

are arbitrary functions of time at the inner and outer radii and the initial condition is an arbitrary function of the reservoir radius. The benefit that results from using this method is that instead of computing three different solutions and then applying Duhamel's method as in [35, 36], we only need to solve one initial boundary value problem with an arbitrary function of reservoir radius for the initial condition and two arbitrary functions of time for the two boundary conditions.

To solve the following IBVPs, we will first derive an appropriate Hankel transform for each one. We then transform the IBVP via the newly developed Hankel transform and obtain an associated initial value problem. We will solve the initial value problem, which, for each case, turns out to be a nonhomogeneous first order ODE. Finally, with a clever use of the eigenfunction expansion technique from the Sturm-Liouville theory developed in Chapter 3, which will act as the inverse Hankel transform, we will invert the solution to the associated ODE, thus obtaining the solution to the original IBVP.

4.2 Solutions for Radial Flow Defined at Both Boundaries

The radial flow parabolic diffusion IBVP where the boundary conditions are flow rates represented by arbitrary functions of time at the inner and outer radii is given by

$$\frac{1}{r} \frac{\partial}{\partial r} \left(r \frac{\partial p}{\partial r} \right) = \frac{1}{\kappa} \frac{\partial p}{\partial t}, \quad (4.1a)$$

$$p(r, 0) = g(r), \quad (4.1b)$$

$$r \frac{\partial p}{\partial r} \Big|_{r=r_1} = f_1(t), \quad (4.1c)$$

$$r \frac{\partial p}{\partial r} \Big|_{r=r_2} = f_2(t). \quad (4.1d)$$

As stated in Theorem 3.3(e) and the remark following the theorem, we can repre-

sent an arbitrary function $f \in L_w^2[a, b]$ as an infinite series given by (3.11). If zero is an eigenvalue of a Sturm-Liouville problem we will begin the infinite series in (3.11) with $n = 0$ instead of $n = 1$.

With this in mind, we now begin to derive an appropriate Hankel transform for (4.1). By the Sturm-Liouville theory developed in Chapter 3, we have that the operator

$$S := \frac{1}{r} \frac{\partial}{\partial r} \left(r \frac{\partial}{\partial r} \right)$$

is a Sturm-Liouville operator with weight $w(r) = r$. By Theorem 3.1 this implies for any $u, v \in C^2[r_1, r_2]$ we have

$$\langle u, Sv \rangle_w - \langle Su, v \rangle_w = \int_{r_1}^{r_2} [u(x)Sv(x) - v(x)Su(x)]r \, dr = r[u(r)v'(r) - u'(r)v(r)] \Big|_{r_1}^{r_2},$$

Supposing that u and v both satisfy the boundary conditions $u'(r_1) = u'(r_2) = v'(r_1) = v'(r_2) = 0$, and since S is a Sturm-Liouville operator, by Theorem 3.2 we have that S is symmetric with respect to the weighted inner product. Thus, we have

$$\langle u, Sv \rangle_w = \langle Su, v \rangle_w.$$

As stated in Chapter 3, the fact that S is symmetric with respect to the weighted inner product is essential in the development of the theory for general Sturm-Liouville problems. The most important property that we glean is that there exists a complete orthogonal family of eigenfunctions on $r_1 < r < r_2$ with respect to the weight r .

Thus, we now determine the eigenvalues of S and the corresponding functions. We seek to find the eigenfunctions of

$$Su = -\lambda u$$

subject to the boundary conditions

$$u'(r_1) = u'(r_2) = 0.$$

First, we set $\lambda = 0$ to see if zero is an eigenvalue. We have

$$Su = 0,$$

which has the general solution

$$u(r) = A + B \ln(r).$$

Enforcing the homogeneous boundary conditions we see that $B = 0$, but A can be any constant value. Without loss of generality, we can define $A := 1$. Thus, $\lambda = 0$ is an eigenvalue of S with the corresponding eigenfunction

$$u_0(r) = 1. \tag{4.2}$$

We now solve

$$Su = -\lambda u,$$

where $\lambda = \alpha^2 > 0$. Thus, we now seek the solution to

$$\frac{\partial^2 u}{\partial r^2} + \frac{1}{r} \frac{\partial u}{\partial r} + \alpha^2 u = 0$$

subject to the boundary conditions

$$u'(r_1) = u'(r_2) = 0.$$

This is of course Bessel's differential equation of order zero. The general solution is given by

$$u(r) = AJ_0(\alpha r) + BY_0(\alpha r).$$

Enforcing the homogeneous boundary conditions we have the two equations

$$AJ_1(\alpha r_1) + BY_1(\alpha r_1) = 0$$

$$AJ_1(\alpha r_2) + BY_1(\alpha r_2) = 0.$$

We solve for A and obtain

$$A = -B \frac{Y_1(\alpha r_2)}{J_1(\alpha r_2)}$$

As a result we have

$$B \left(\frac{Y_1(\alpha r_1)J_1(\alpha r_2) - Y_1(\alpha r_2)J_1(\alpha r_1)}{J_1(\alpha r_2)} \right) = 0$$

To avoid a trivial solution, $B \neq 0$. Thus, we let $B = J_1(\alpha r_2)$ and define the α_n as the countably infinitely many positive roots of

$$Y_1(\alpha_n r_1)J_1(\alpha_n r_2) - Y_1(\alpha_n r_2)J_1(\alpha_n r_1) = 0.$$

From this relationship, we define the parameter ρ by

$$\rho := \frac{J_1(\alpha_n r_1)}{J_1(\alpha_n r_2)} = \frac{Y_1(\alpha_n r_1)}{Y_1(\alpha_n r_2)}. \quad (4.3)$$

The resulting solutions are

$$u_n(r) = Y_1(\alpha_n r_2)J_0(\alpha_n r) - J_1(\alpha_n r_2)Y_0(\alpha_n r). \quad (4.4)$$

Thus, the set of $\{u_n(r)\}_{n=0}^{\infty}$ form a complete orthogonal family of eigenfunctions on $r_1 < r < r_2$ with respect to the weight r with corresponding eigenvalues $\{\lambda_n\}_{n=0}^{\infty}$. As a result, by Theorem 3.3, given a function $f \in L_w^2[r_1, r_2]$, it can be expanded in an infinite series of these eigenfunctions as in (3.11) where the coefficients in (3.11) are given by (3.12).

For this particular problem, given an arbitrary $f \in L_w^2[r_1, r_2]$, we have the coefficients of the eigenfunction expansion as

$$c_0 = \frac{\langle f, u_0 \rangle_w}{\langle u_0, u_0 \rangle_w} = \frac{\int_{r_1}^{r_2} f(r) r dr}{\int_{r_1}^{r_2} r dr} = \frac{2}{r_2^2 - r_1^2} \int_{r_1}^{r_2} f(r) r dr, \quad (4.5)$$

for $n = 0$ and

$$\begin{aligned} c_n &= \frac{\langle f, u_n \rangle_w}{\langle u_n, u_n \rangle_w} = \frac{\int_{r_1}^{r_2} f(r) (Y_1(\alpha_n r_2) J_0(\alpha_n r) - J_1(\alpha_n r_2) Y_0(\alpha_n r)) r dr}{\int_{r_1}^{r_2} (Y_1(\alpha_n r_2) J_0(\alpha_n r) - J_1(\alpha_n r_2) Y_0(\alpha_n r))^2 r dr} \\ &= \frac{J_1^2(\alpha_n r_1) \pi^2 \alpha_n^2}{2(J_1^2(\alpha_n r_1) - J_1^2(\alpha_n r_2))} \int_{r_1}^{r_2} f(r) (Y_1(\alpha_n r_2) J_0(\alpha_n r) - J_1(\alpha_n r_2) Y_0(\alpha_n r)) r dr, \end{aligned} \quad (4.6)$$

for $n \geq 1$.

Given a function $f \in L_w^2[r_1, r_2]$, we now define the *Hankel transform* of f as the inner product

$$\mathcal{H}\{f\}(\alpha_n) := \langle u_n, f \rangle_w = \int_{r_1}^{r_2} u_n(r) f(r) r dr = F(\alpha_n). \quad (4.7)$$

Observe that for $n = 0$ ($\alpha_0 = 0$) we have

$$\begin{aligned}
\mathcal{H}\{Sf\}(\alpha_0) &= \langle u_0, Sf \rangle_w \\
&= \langle Su_0, f \rangle_w + r[u_0(r)f'(r) - u_0'(r)f(r)] \Big|_{r_1}^{r_2} \\
&= \int_{r_1}^{r_2} f(r)Su_0(r)r \, dr + r_2[u_0(r_2)f'(r_2) - u_0'(r_2)f(r_2)] \\
&\quad - r_1[u_0(r_1)f'(r_1) - u_0'(r_1)f(r_1)] \\
&= r_2f'(r_2) - r_1f'(r_1).
\end{aligned}$$

For $n \geq 1$ we have

$$\begin{aligned}
\mathcal{H}\{Sf\}(\alpha_n) &= \langle u_n, Sf \rangle_w \\
&= \langle Su_n, f \rangle_w + r[u_n(r)f'(r) - u_n'(r)f(r)] \Big|_{r_1}^{r_2} \\
&= \int_{r_1}^{r_2} f(r)Su_n(r)r \, dr + r_2[u_n(r_2)f'(r_2) - u_n'(r_2)f(r_2)] \\
&\quad - r_1[u_n(r_1)f'(r_1) - u_n'(r_1)f(r_1)] \\
&= -\alpha_n^2 \int_{r_1}^{r_2} f(r)u_n(r)r \, dr + r_2u_n(r_2)f'(r_2) - r_1u_n(r_1)f'(r_1) \\
&= -\alpha_n^2 \langle u_n, f \rangle_w + r_2f'(r_2)(Y_1(\alpha_nr_2)J_0(\alpha_nr_2) - J_1(\alpha_nr_2)Y_0(\alpha_nr_2)) \\
&\quad - r_1f'(r_1)(Y_1(\alpha_nr_2)J_0(\alpha_nr_1) - J_1(\alpha_nr_2)Y_0(\alpha_nr_1)) \\
&= -\alpha_n^2 \mathcal{H}\{f\}(\alpha_n) + \frac{2}{\pi\alpha_n} \left(\frac{f'(r_1)}{\rho} - f'(r_2) \right).
\end{aligned}$$

To solve the IBVP (4.1), we now apply the Hankel transform \mathcal{H} and obtain the transformed initial value problem for $n = 0$

$$\frac{1}{\kappa} \frac{dP}{dt}(\alpha_0, t) = f_2(t) - f_1(t), \quad (4.8a)$$

$$P(\alpha_0, 0) = G(\alpha_0), \quad (4.8b)$$

and for $n \geq 1$

$$\frac{1}{\kappa} \frac{dP}{dt}(\alpha_n, t) + \alpha_n^2 P(\alpha_n, t) = \frac{2}{\pi \alpha_n} \left(\frac{f_1(t)}{r_1 \rho} - \frac{f_2(t)}{r_2} \right), \quad (4.9a)$$

$$P(\alpha_n, 0) = G(\alpha_n), \quad (4.9b)$$

where

$$P = \mathcal{H}\{p\}, \quad \frac{dP}{dt} = \frac{d\mathcal{H}\{p\}}{dt} = \mathcal{H}\left\{\frac{dp}{dt}\right\}, \quad G = \mathcal{H}\{g\}.$$

It is easy to see that when $n = 0$ the solution to (4.8) is given by

$$P(\alpha_0, t) = G(\alpha_0) + \kappa \int_0^t f_2(\tau) - f_1(\tau) d\tau.$$

When $n \geq 1$ the solution to (4.9) is given by

$$P(\alpha_n, t) = G(\alpha_n) e^{-\alpha_n^2 \kappa t} + \kappa \int_0^t e^{-\alpha_n^2 \kappa (t-\tau)} \frac{2}{\pi \alpha_n} \left(\frac{f_1(\tau)}{r_1 \rho} - \frac{f_2(\tau)}{r_2} \right) d\tau.$$

Recall that, by Theorem 3.3, $p(r, t)$ can be expanded in an infinite series of the eigenfunctions $\{u_n(r)\}_{n=0}^{\infty}$ as in (3.11) where the coefficients in (3.11) are now given by (4.5) and (4.6).

Observe,

$$\begin{aligned}
p(r, t) &= \sum_{n=0}^{\infty} \frac{\langle u_n, p \rangle_w}{\langle u_n, u_n \rangle_w} u_n(r) \\
&= \sum_{n=0}^{\infty} \frac{\int_{r_1}^{r_2} p(r, t) u_n(r) r \, dr}{\int_{r_1}^{r_2} u_n^2(r) r \, dr} u_n(r) \\
&= \sum_{n=0}^{\infty} \frac{P(\alpha_n, t)}{\int_{r_1}^{r_2} u_n^2(r) r \, dr} u_n(r) \\
&= \frac{P(\alpha_0, t)}{\int_{r_1}^{r_2} u_0^2(r) r \, dr} + \sum_{n=1}^{\infty} \frac{P(\alpha_n, t)}{\int_{r_1}^{r_2} u_n^2(r) r \, dr} u_n(r) \\
&= \frac{2 \left(G(\alpha_0) + \kappa \int_0^t f_2(\tau) - f_1(\tau) \, d\tau \right)}{r_2^2 - r_1^2} \\
&\quad + \sum_{n=1}^{\infty} \left[\frac{\pi^2 \alpha_n^2 J_1^2(\alpha_n r_1)}{2(J_1^2(\alpha_n r_1) - J_1^2(\alpha_n r_2))} \right] \\
&\quad \left[G(\alpha_n) e^{-\alpha_n^2 \kappa t} + \kappa \int_0^t e^{-\alpha_n^2 \kappa(t-\tau)} \frac{2}{\pi \alpha_n} \left(\frac{f_1(\tau)}{r_1 \rho} - \frac{f_2(\tau)}{r_2} \right) \, d\tau \right] u_n(r) \\
&= \frac{2}{r_2^2 - r_1^2} \left(\int_{r_1}^{r_2} g(r) u_0(r) r \, dr + \kappa \int_0^t f_2(\tau) - f_1(\tau) \, d\tau \right) \\
&\quad + \sum_{n=1}^{\infty} \left[\frac{\pi^2 \alpha_n^2 J_1^2(\alpha_n r_1) u_n(r) e^{-\alpha_n^2 \kappa t}}{2(J_1^2(\alpha_n r_1) - J_1^2(\alpha_n r_2))} \right] \\
&\quad \left[\int_{r_1}^{r_2} g(r) u_n(r) r \, dr + \kappa \int_0^t e^{\alpha_n^2 \kappa \tau} \frac{2 J_1(\alpha_n r_2)}{J_1(\alpha_n r_1)} \frac{f_1(\tau)}{\pi \alpha_n r_1} \, d\tau - \kappa \int_0^t e^{\alpha_n^2 \kappa \tau} \frac{2}{\pi \alpha_n} \frac{f_2(\tau)}{r_2} \, d\tau \right] \\
&= \frac{2}{r_2^2 - r_1^2} \int_{r_1}^{r_2} g(r) r \, dr + \frac{2\kappa}{r_2^2 - r_1^2} \int_0^t f_2(\tau) - f_1(\tau) \, d\tau \\
&\quad + \pi \sum_{n=1}^{\infty} \left[\frac{\alpha_n^2 J_1(\alpha_n r_1) u_n(r) e^{-\alpha_n^2 \kappa t}}{J_1^2(\alpha_n r_1) - J_1^2(\alpha_n r_2)} \right] \\
&\quad \left[\frac{\pi}{2} J_1(\alpha_n r_1) \int_{r_1}^{r_2} g(r) u_n(r) r \, dr + \kappa \frac{J_1(\alpha_n r_2)}{\alpha_n r_1} \int_0^t e^{\alpha_n^2 \kappa \tau} f_1(\tau) \, d\tau \right. \\
&\quad \left. - \kappa \frac{J_1(\alpha_n r_1)}{\alpha_n r_2} \int_0^t e^{\alpha_n^2 \kappa \tau} f_2(\tau) \, d\tau \right].
\end{aligned}$$

4.3 Solutions for Pressure Defined at the Inner Boundary and Radial Flow Defined at the Outer Boundary

The radial parabolic diffusion IBVP where at the internal radius the pressure is an arbitrary function of time while at the outer radius the flow rate is an arbitrary function of time is given by

$$\frac{1}{r} \frac{\partial}{\partial r} \left(r \frac{\partial p}{\partial r} \right) = \frac{1}{\kappa} \frac{\partial p}{\partial t}, \quad (4.10a)$$

$$p(r, 0) = g(r), \quad (4.10b)$$

$$p(r_1, t) = f_1(t), \quad (4.10c)$$

$$r \frac{\partial p}{\partial r} \Big|_{r=r_2} = f_2(t). \quad (4.10d)$$

We begin by deriving an appropriate Hankel transform for (4.10). To do so, we now determine the eigenvalues of the operator S and the corresponding functions. We seek to find the eigenfunctions of

$$Su = -\lambda u$$

subject to the boundary conditions

$$u(r_1) = u'(r_2) = 0.$$

First, we set $\lambda = 0$ to see if zero is an eigenvalue. We have

$$Su = 0,$$

which has the general solution

$$u(r) = A + B \ln(r).$$

Enforcing the homogeneous boundary conditions we see that $A = B = 0$. Thus, $\lambda = 0$ is not an eigenvalue of S .

We now solve

$$Su = -\lambda u,$$

where $\lambda = \alpha^2 > 0$. Thus, we now seek the solution to

$$\frac{\partial^2 u}{\partial r^2} + \frac{1}{r} \frac{\partial u}{\partial r} + \alpha^2 u = 0$$

subject to the boundary conditions

$$u(r_1) = u'(r_2) = 0.$$

This is of course Bessel's differential equation of order zero. The general solution is given by

$$u(r) = AJ_0(\alpha r) + BY_0(\alpha r).$$

Enforcing the homogeneous boundary conditions we have the two equations

$$AJ_0(\alpha r_1) + BY_0(\alpha r_1) = 0$$

$$AJ_1(\alpha r_2) + BY_1(\alpha r_2) = 0.$$

We solve for A and obtain

$$A = -B \frac{Y_1(\alpha r_2)}{J_1(\alpha r_2)}$$

As a result we have

$$B \left(\frac{Y_0(\alpha r_1) J_1(\alpha r_2) - Y_1(\alpha r_2) J_0(\alpha r_1)}{J_1(\alpha r_2)} \right) = 0$$

To avoid a trivial solution, $B \neq 0$. Thus, we let $B = J_1(\alpha r_2)$ and define the α_n as the countably infinitely many positive roots of

$$Y_0(\alpha_n r_1) J_1(\alpha_n r_2) - Y_1(\alpha_n r_2) J_0(\alpha_n r_1) = 0$$

From this relationship, we define the parameter ρ by

$$\rho := \frac{Y_1(\alpha_n r_2)}{Y_0(\alpha_n r_1)} = \frac{J_1(\alpha_n r_2)}{J_0(\alpha_n r_1)}. \quad (4.11)$$

The resulting solutions are

$$u_n(r) = Y_1(\alpha_n r_2) J_0(\alpha_n r) - J_1(\alpha_n r_2) Y_0(\alpha_n r). \quad (4.12)$$

Thus, the set of $\{u_n(r)\}_{n=1}^{\infty}$ form a complete orthogonal family of eigenfunctions on $r_1 < r < r_2$ with respect to the weight r with corresponding eigenvalues $\{\lambda_n\}_{n=1}^{\infty}$.

For this particular problem, given an arbitrary $f \in L_w^2[r_1, r_2]$, we have the coefficients of the eigenfunction expansion as and

$$\begin{aligned} c_n &= \frac{\langle f, u_n \rangle_w}{\langle u_n, u_n \rangle_w} = \frac{\int_{r_1}^{r_2} f(r) (Y_1(\alpha_n r_2) J_0(\alpha_n r) - J_1(\alpha_n r_2) Y_0(\alpha_n r)) r dr}{\int_{r_1}^{r_2} (Y_1(\alpha_n r_2) J_0(\alpha_n r) - J_1(\alpha_n r_2) Y_0(\alpha_n r))^2 r dr} \\ &= \frac{J_0^2(\alpha_n r_1) \pi^2 \alpha_n^2 \int_{r_1}^{r_2} f(r) (Y_1(\alpha_n r_2) J_0(\alpha_n r) - J_1(\alpha_n r_2) Y_0(\alpha_n r)) r dr}{2 (J_0^2(\alpha_n r_1) - J_1^2(\alpha_n r_2))}, \end{aligned} \quad (4.13)$$

for $n \geq 1$.

Given a function $f \in L_w^2[r_1, r_2]$, we now define the *Hankel transform* of f as the

inner product

$$\mathcal{H}\{f\}(\alpha_n) := \langle u_n, f \rangle_w = \int_{r_1}^{r_2} u_n(r) f(r) r dr = F(\alpha_n). \quad (4.14)$$

Observe that for $n \geq 1$ we have

$$\begin{aligned} \langle u_n, Sf \rangle_w &= \langle Su_n, f \rangle_w + r[u_n(r)f'(r) - u_n'(r)f(r)] \Big|_{r_1}^{r_2} \\ &= \int_{r_1}^{r_2} f(r) Su_n(r) r dr + r_2[u_n(r_2)f'(r_2) - u_n'(r_2)f(r_2)] \\ &\quad - r_1[u_n(r_1)f'(r_1) - u_n'(r_1)f(r_1)] \\ &= -\alpha_n^2 \int_{r_1}^{r_2} f(r) u_n(r) r dr + r_2 u_n(r_2) f'(r_2) + r_1 u_n'(r_1) f(r_1) \\ &= -\alpha_n^2 \langle u_n, f \rangle_w + r_2 f'(r_2) (Y_1(\alpha_n r_2) J_0(\alpha_n r_2) - J_1(\alpha_n r_2) Y_0(\alpha_n r_2)) \\ &\quad - \alpha_n r_1 f(r_1) (Y_1(\alpha_n r_2) J_1(\alpha_n r_1) - J_1(\alpha_n r_2) Y_1(\alpha_n r_1)) \\ &= -\alpha_n^2 \mathcal{H}\{f\}(\alpha_n) - \frac{2}{\pi \alpha_n} (\rho \alpha_n f(r_1) + f'(r_2)) \\ &= -\alpha_n^2 F(\alpha_n) - \frac{2}{\pi \alpha_n} (\rho \alpha_n f(r_1) + f'(r_2)). \end{aligned}$$

To solve the IBVP (4.1), we now apply the Hankel transform \mathcal{H}_S and obtain the initial value problem for $n \geq 1$

$$\frac{1}{\kappa} \frac{dP}{dt}(\alpha_n, t) + \alpha_n^2 P(\alpha_n, t) = -\frac{2}{\pi} \left(\rho f_1(t) + \frac{f_2(t)}{\alpha_n r_2} \right), \quad (4.15a)$$

$$P(\alpha_n, 0) = G(\alpha_n), \quad (4.15b)$$

where $P = \mathcal{H}(p)$, $dP/dt = d\mathcal{H}(p)/dt = \mathcal{H}(dp/dt)$, and $G = \mathcal{H}(g)$. The solution to (4.15) is given by

$$P(\alpha_n, t) = G(\alpha_n) e^{-\alpha_n^2 \kappa t} - \kappa \int_0^t e^{-\alpha_n^2 \kappa (t-\tau)} \frac{2}{\pi} \left(\rho f_1(t) + \frac{f_2(t)}{\alpha_n r_2} \right) d\tau.$$

Recall that, by Theorem 3.3, $p(r, t)$ can be expanded in an infinite series of the eigenfunctions $\{u_n(r)\}_{n=1}^{\infty}$ as in (3.11) where the coefficients in (3.11) are now given by (4.13).

Observe,

$$\begin{aligned}
p(r, t) &= \sum_{n=1}^{\infty} \frac{\langle u_n, p \rangle_w}{\langle u_n, u_n \rangle_w} u_n(r) \\
&= \sum_{n=1}^{\infty} \frac{\int_{r_1}^{r_2} p(r, t) u_n(r) r \, dr}{\int_{r_1}^{r_2} u_n^2(r) r \, dr} u_n(r) \\
&= \sum_{n=1}^{\infty} \frac{P(\alpha_n, t)}{\int_{r_1}^{r_2} u_n^2(r) r \, dr} u_n(r) \\
&= \sum_{n=1}^{\infty} \frac{P(\alpha_n, t)}{\int_{r_1}^{r_2} u_n^2(r) r \, dr} u_n(r) \\
&= \sum_{n=1}^{\infty} \left[\frac{\pi^2 \alpha_n^2 J_0^2(\alpha_n r_1)}{2(J_0^2(\alpha_n r_1) - J_1^2(\alpha_n r_2))} \right] \\
&\quad \left[G(\alpha_n) e^{-\alpha_n^2 \kappa t} - \kappa \int_0^t e^{-\alpha_n^2 \kappa(t-\tau)} \frac{2}{\pi} \left(\rho f_1(t) - \frac{f_2(t)}{\alpha_n r_2} \right) d\tau \right] u_n(r) \\
&= \sum_{n=1}^{\infty} \left[\frac{\pi^2 \alpha_n^2 J_0^2(\alpha_n r_1) u_n(r) e^{-\alpha_n^2 \kappa t}}{2(J_0^2(\alpha_n r_1) - J_1^2(\alpha_n r_2))} \right] \\
&\quad \left[\int_{r_1}^{r_2} g(r) u_n(r) r \, dr - \kappa \int_0^t e^{\alpha_n^2 \kappa \tau} \frac{2}{\pi} \frac{J_1(\alpha_n r_2)}{J_0(\alpha_n r_1)} f_1(\tau) d\tau - \kappa \int_0^t e^{\alpha_n^2 \kappa \tau} \frac{2}{\pi \alpha_n} \frac{f_2(\tau)}{r_2} d\tau \right] \\
&= \pi \sum_{n=1}^{\infty} \left[\frac{\alpha_n^2 J_0(\alpha_n r_1) u_n(r) e^{-\alpha_n^2 \kappa t}}{J_0^2(\alpha_n r_1) - J_1^2(\alpha_n r_2)} \right] \\
&\quad \left[\frac{\pi}{2} J_0(\alpha_n r_1) \int_{r_1}^{r_2} g(r) u_n(r) r \, dr - \kappa J_1(\alpha_n r_2) \int_0^t e^{\alpha_n^2 \kappa \tau} f_1(\tau) d\tau \right. \\
&\quad \left. - \frac{\kappa J_0(\alpha_n r_1)}{\alpha_n r_2} \int_0^t e^{\alpha_n^2 \kappa \tau} f_2(\tau) d\tau \right].
\end{aligned}$$

4.4 Solutions for Pressure Defined at Both Boundaries

The radial parabolic diffusion IBVP where the pressures are arbitrary functions of time at the inner and outer radii is given by

$$\frac{1}{r} \frac{\partial}{\partial r} \left(r \frac{\partial p}{\partial r} \right) = \frac{1}{\kappa} \frac{\partial p}{\partial t}, \quad (4.16a)$$

$$p(r, 0) = g(r), \quad (4.16b)$$

$$p(r_1, t) = f_1(t), \quad (4.16c)$$

$$p(r_2, t) = f_2(t). \quad (4.16d)$$

We now derive an appropriate Hankel transform for (4.16). To begin, we determine the eigenvalues of S and the corresponding functions. We seek to find the eigenfunctions of

$$Su = -\lambda u$$

subject to the boundary conditions

$$u(r_1) = u(r_2) = 0.$$

First, we set $\lambda = 0$ to see if zero is an eigenvalue. We have

$$Su = 0,$$

which has the general solution

$$u(r) = A + B \ln(r).$$

Enforcing the homogeneous boundary conditions we see that $A = B = 0$. Thus, $\lambda = 0$ is not an eigenvalue of S .

We now solve

$$Su = -\lambda u,$$

where $\lambda = \alpha^2 > 0$. Thus, we now seek the solution to

$$\frac{\partial^2 u}{\partial r^2} + \frac{1}{r} \frac{\partial u}{\partial r} + \alpha^2 u = 0$$

subject to the boundary conditions

$$u(r_1) = u(r_2) = 0.$$

This is of course Bessel's differential equation of order zero. The general solution is given by

$$u(r) = AJ_0(\alpha r) + BY_0(\alpha r).$$

Enforcing the homogeneous boundary conditions we have the two equations

$$AJ_0(\alpha r_1) + BY_0(\alpha r_1) = 0$$

$$AJ_0(\alpha r_2) + BY_0(\alpha r_2) = 0.$$

We solve for A and obtain

$$A = -B \frac{Y_0(\alpha r_2)}{J_0(\alpha r_2)}$$

As a result we have

$$B \left(\frac{Y_0(\alpha r_1)J_0(\alpha r_2) - Y_0(\alpha r_2)J_0(\alpha r_1)}{J_0(\alpha r_2)} \right) = 0$$

To avoid a trivial solution, $B \neq 0$. Thus, we let $B = J_0(\alpha r_2)$ and define the α_n as the countably infinitely many positive roots of

$$Y_0(\alpha r_1)J_0(\alpha r_2) - Y_0(\alpha r_2)J_0(\alpha r_1) = 0$$

From this relationship, we define the parameter ρ by

$$\rho := \frac{Y_0(\alpha_n r_2)}{Y_0(\alpha_n r_1)} = \frac{J_0(\alpha_n r_2)}{J_0(\alpha_n r_1)}. \quad (4.17)$$

The resulting solutions are

$$u_n(r) = Y_0(\alpha_n r_2)J_0(\alpha_n r) - J_0(\alpha_n r_2)Y_0(\alpha_n r). \quad (4.18)$$

Thus, the set of $\{u_n(r)\}_{n=1}^{\infty}$ form a complete orthogonal family of eigenfunctions on $r_1 < r < r_2$ with respect to the weight r with corresponding eigenvalues $\{\lambda_n\}_{n=1}^{\infty}$.

For this particular problem, given an arbitrary $f \in L_w^2[r_1, r_2]$, we have the coefficients of the eigenfunction expansion as

$$\begin{aligned} c_n &= \frac{\langle f, u_n \rangle_w}{\langle u_n, u_n \rangle_w} = \frac{\int_{r_1}^{r_2} f(r) (Y_0(\alpha_n r_2)J_0(\alpha_n r) - J_0(\alpha_n r_2)Y_0(\alpha_n r)) r dr}{\int_{r_1}^{r_2} (Y_0(\alpha_n r_2)J_0(\alpha_n r) - J_0(\alpha_n r_2)Y_0(\alpha_n r))^2 r dr} \\ &= \frac{J_0^2(\alpha_n r_1)\pi^2\alpha_n^2}{2(J_0^2(\alpha_n r_1) - J_0^2(\alpha_n r_2))} \int_{r_1}^{r_2} f(r) (Y_0(\alpha_n r_2)J_0(\alpha_n r) - J_0(\alpha_n r_2)Y_0(\alpha_n r)) r dr, \end{aligned} \quad (4.19)$$

for $n \geq 1$.

Given a function $f \in L_w^2[r_1, r_2]$, we now define the *Hankel transform* of f as the

inner product

$$\mathcal{H}\{f\}(\alpha_n) := \langle u_n, f \rangle_w = \int_{r_1}^{r_2} u_n(r) f(r) r dr = F(\alpha_n). \quad (4.20)$$

Observe that for $n \geq 1$ we have

$$\begin{aligned} \langle u_n, Sf \rangle_w &= \langle Su_n, f \rangle_w + r[u_n(r)f'(r) - u'_n(r)f(r)] \Big|_{r_1}^{r_2} \\ &= \int_{r_1}^{r_2} f(r) Su_n(r) r dr + r_2[u_n(r_2)f'(r_2) - u'_n(r_2)f(r_2)] \\ &\quad - r_1[u_n(r_1)f'(r_1) - u'_n(r_1)f(r_1)] \\ &= \int_{r_1}^{r_2} f(r) Su_n(r) r dr - r_2 u'_n(r_2) f(r_2) + r_1 u'_n(r_1) f(r_1) \\ &= -\alpha_n^2 \int_{r_1}^{r_2} f(r) u_n(r) r dr \\ &\quad + \alpha_n r_2 f'(r_2) (Y_0(\alpha_n r_2) J_1(\alpha_n r_2) - J_0(\alpha_n r_2) Y_1(\alpha_n r_2)) \\ &\quad - \alpha_n r_1 f'(r_1) (Y_0(\alpha_n r_2) J_1(\alpha_n r_1) - J_0(\alpha_n r_2) Y_1(\alpha_n r_1)) \\ &= -\alpha_n^2 \mathcal{H}\{f\}(\alpha_n) + \alpha_n r_2 f'(r_2) \frac{2}{\pi \alpha_n r_2} - \alpha_n r_1 f'(r_1) \frac{2\rho}{\pi \alpha_n r_1} \\ &= -\alpha_n^2 F(\alpha_n) + \frac{2}{\pi} (f(r_2) - \rho f(r_1)). \end{aligned}$$

To solve the IBVP (4.16), we now apply the Hankel transform \mathcal{H} and obtain the initial value problem for $n \geq 1$

$$\frac{1}{\kappa} \frac{dP}{dt}(\alpha_n, t) + \alpha_n^2 P(\alpha_n, t) = \frac{2}{\pi} (f_2(t) - \rho f_1(t)), \quad (4.21a)$$

$$P(\alpha_n, 0) = G(\alpha_n). \quad (4.21b)$$

The solution to (4.21) is given by

$$P(\alpha_n, t) = G(\alpha_n)e^{-\alpha_n^2 \kappa t} + \kappa \int_0^t e^{-\alpha_n^2 \kappa(t-\tau)} \frac{2}{\pi} (f_2(\tau) - \rho f_1(\tau)) d\tau.$$

Recall that, by Theorem 3.3, $p(r, t)$ can be expanded in an infinite series of the eigenfunctions $\{u_n(r)\}_{n=1}^{\infty}$ as in (3.11) where the coefficients in (3.11) are now given by (4.19).

Observe,

$$\begin{aligned} p(r, t) &= \sum_{n=1}^{\infty} \frac{\langle u_n, p \rangle_w}{\langle u_n, u_n \rangle_w} u_n(r) \\ &= \sum_{n=1}^{\infty} \frac{\int_{r_1}^{r_2} p(r, t) u_n(r) r dr}{\int_{r_1}^{r_2} u_n^2(r) r dr} u_n(r) \\ &= \sum_{n=1}^{\infty} \frac{P(\alpha_n, t)}{\int_{r_1}^{r_2} u_n^2(r) r dr} u_n(r) \\ &= \sum_{n=1}^{\infty} \frac{P(\alpha_n, t)}{\int_{r_1}^{r_2} u_n^2(r) r dr} u_n(r) \\ &= \sum_{n=1}^{\infty} \left[\frac{\pi^2 \alpha_n^2 J_0^2(\alpha_n r_1)}{2(J_0^2(\alpha_n r_1) - J_0^2(\alpha_n r_2))} \right] \\ &\quad \left[G(\alpha_n) e^{-\alpha_n^2 \kappa t} + \kappa \int_0^t e^{-\alpha_n^2 \kappa(t-\tau)} \frac{2}{\pi} (f_2(\tau) - \rho f_1(\tau)) d\tau \right] u_n(r) \\ &= \sum_{n=1}^{\infty} \left[\frac{\pi^2 \alpha_n^2 J_0^2(\alpha_n r_1) u_n(r) e^{-\alpha_n^2 \kappa t}}{2(J_0^2(\alpha_n r_1) - J_0^2(\alpha_n r_2))} \right] \\ &\quad \left[\int_{r_1}^{r_2} g(r) u_n(r) r dr + \kappa \int_0^t e^{\alpha_n^2 \kappa \tau} \frac{2}{\pi} f_2(\tau) d\tau \right] - \kappa \int_0^t e^{\alpha_n^2 \kappa \tau} \frac{2}{\pi} \frac{J_0(\alpha_n r_2)}{J_0(\alpha_n r_1)} f_1(\tau) d\tau \\ &= \pi \sum_{n=1}^{\infty} \left[\frac{\alpha_n^2 J_0(\alpha_n r_1) u_n(r) e^{-\alpha_n^2 \kappa t}}{J_0^2(\alpha_n r_1) - J_0^2(\alpha_n r_2)} \right] \\ &\quad \left[\frac{\pi}{2} J_0(\alpha_n r_1) \int_{r_1}^{r_2} g(r) u_n(r) r dr + \kappa J_0(\alpha_n r_1) \int_0^t e^{\alpha_n^2 \kappa \tau} f_2(\tau) d\tau \right. \\ &\quad \left. - \kappa J_1(\alpha_n r_2) \int_0^t e^{\alpha_n^2 \kappa \tau} f_1(\tau) d\tau \right]. \end{aligned}$$

5. HYPERBOLIC DIFFUSION

Mathematics is the most beautiful and most powerful creation of the human spirit.

Stephan Banach (1892–1945)

5.1 Introduction

In this chapter, the solution to the hyperbolic diffusion equation in cylindrical coordinates that was developed in (2.44) will be derived. The problem will be cast in terms of a limited reservoir in which there exists two initial conditions and two boundary conditions. Of the two boundary conditions, the first will be specified at the internal boundary $r = r_1$, which is the wellbore, while the second will be specified at the external boundary, $r = r_2$, which is the edge of the reservoir. The reservoir is assumed to be of purely horizontal radial flow and the effects of gravity are neglected.

Just as in Chapter 4, by derivation of different Hankel transforms, which have not been found in the literature for this particular application, we will develop solutions to the radial flow hyperbolic diffusion equation where the pressure and/or flow rates are arbitrary functions of time at the inner and outer radii and the initial condition is an arbitrary function of the reservoir radius.

To solve the following IBVPs, we will follow the procedure outlined in Chapter 4. Once all three cases are solved, we will compare the solutions of the hyperbolic diffusion IBVPs with the solutions to the parabolic diffusion IBVPs.

5.2 Solutions for Radial Flow Defined at Both Boundaries

The radial flow hyperbolic diffusion IBVP where the flow rates are arbitrary functions of time at the inner and outer radii is given by

$$\frac{1}{r} \frac{\partial}{\partial r} \left(r \frac{\partial p}{\partial r} \right) = \frac{1}{a^2} \frac{\partial^2 p}{\partial t^2} + \frac{1}{\kappa} \frac{\partial p}{\partial t}, \quad (5.1a)$$

$$p(r, 0) = g_1(r), \quad (5.1b)$$

$$\frac{\partial p}{\partial t}(r, 0) = g_2(r), \quad (5.1c)$$

$$r \frac{\partial p}{\partial r} \Big|_{r=r_1} = f_1(t), \quad (5.1d)$$

$$r \frac{\partial p}{\partial r} \Big|_{r=r_2} = f_2(t). \quad (5.1e)$$

As stated in Theorem 3.3(e) and the remark following the theorem, we can represent an arbitrary function $f \in L_w^2[a, b]$ as an infinite series given by (3.11). If zero is an eigenvalue of a Sturm-Liouville problem we will begin the infinite series in (3.11) with $n = 0$ instead of $n = 1$.

The appropriate Hankel transform for (5.1) is identical to that given in (4.7) for (4.1). Restating the Hankel transform we have for $n = 0$ ($\alpha_0 = 0$) and $n \geq 1$, respectively,

$$\mathcal{H}\{Sf\}(\alpha_n) = r_2 f'(r_2) - r_1 f'(r_1).$$

and

$$\mathcal{H}\{Sf\}(\alpha_n) = -\alpha_n^2 \mathcal{H}\{f\}(\alpha_n) + \frac{2}{\pi \alpha_n} \left(\frac{f'(r_1)}{\rho} - f'(r_2) \right),$$

where we used the definition of ρ in (4.3).

To solve the IBVP (5.1), we now apply the Hankel transform \mathcal{H} and obtain the initial value problem for $n = 0$

$$\frac{1}{a^2} \frac{d^2 P}{dt^2}(\alpha_0, t) + \frac{1}{\kappa} \frac{dP}{dt}(\alpha_0, t) = f_2(t) - f_1(t), \quad (5.2a)$$

$$P(\alpha_0, 0) = G_1(\alpha_0), \quad (5.2b)$$

$$\frac{dP}{dt}(\alpha_n, 0) = G_2(\alpha_n), \quad (5.2c)$$

and for $n \geq 1$

$$\frac{1}{a^2} \frac{d^2 P}{dt^2}(\alpha_0, t) + \frac{1}{\kappa} \frac{dP}{dt}(\alpha_n, t) + \alpha_n^2 P(\alpha_n, t) = \frac{2}{\pi \alpha_n} \left(\frac{f_1(t)}{r_1 \rho} - \frac{f_2(t)}{r_2} \right), \quad (5.3a)$$

$$P(\alpha_n, 0) = G_1(\alpha_n), \quad (5.3b)$$

$$\frac{dP}{dt}(\alpha_n, 0) = G_2(\alpha_n). \quad (5.3c)$$

We define the function $F_n(t)$ by

$$F_n(t) := \begin{cases} f_2(t) - f_1(t), & n = 0, \\ \frac{2}{\pi \alpha_n} \left(\frac{f_1(t)}{r_1 \rho} - \frac{f_2(t)}{r_2} \right), & n \geq 1. \end{cases} \quad (5.4)$$

It is easy to see that when $n = 0$ the solution to (5.2) is given by

$$\begin{aligned} P(\alpha_0, t) &= G_1(\alpha_0) + \frac{\kappa}{a^2} \left(1 - e^{-\frac{a^2 t}{\kappa}} \right) G_2(\alpha_0) \\ &\quad + 2\kappa \int_0^t F_0(\tau) e^{-\frac{a^2(t-\tau)}{2\kappa}} \sinh \left(\frac{a^2}{2\kappa} (t - \tau) \right) d\tau. \end{aligned}$$

When $n \geq 1$ the solution to (5.3) is given by

$$P(\alpha_n, t) = \begin{cases} G_1(\alpha_n) e^{-\frac{a^2 t}{2\kappa}} \left(\frac{a^2}{2\kappa \mathcal{J}(\alpha_n)} \sinh(t \mathcal{J}(\alpha_n)) + \cosh(t \mathcal{J}(\alpha_n)) \right) \\ \quad + G_2(\alpha_n) \frac{e^{-\frac{a^2 t}{2\kappa}}}{\mathcal{J}(\alpha_n)} \sinh(t \mathcal{J}(\alpha_n)) \\ \quad + \frac{a^2}{\mathcal{J}(\alpha_n)} \int_0^t F_n(\tau) e^{-\frac{a^2(t-\tau)}{2\kappa}} \sinh((t-\tau) \mathcal{J}(\alpha_n)) d\tau, & \alpha_n < \frac{a}{2\kappa}, \\ \\ \left(G_1(\alpha_n) \left(\frac{a^2 t}{2\kappa} + 1 \right) + G_2(\alpha_n) t \right. \\ \quad \left. + a^2 \int_0^t e^{\frac{a^2 \tau}{2\kappa}} F_n(\tau) (t-\tau) d\tau \right) e^{-\frac{a^2 t}{2\kappa}}, & \alpha_n = \frac{a}{2\kappa}, \\ \\ G_1(\alpha_n) e^{-\frac{a^2 t}{2\kappa}} \left(\frac{a^2}{2\kappa \mathcal{J}(\alpha_n)} \sin(t \mathcal{J}(\alpha_n)) + \cos(t \mathcal{J}(\alpha_n)) \right) \\ \quad + G_2(\alpha_n) \frac{e^{-\frac{a^2 t}{2\kappa}}}{\mathcal{J}(\alpha_n)} \sin(t \mathcal{J}(\alpha_n)) \\ \quad + \frac{a^2}{\mathcal{J}(\alpha_n)} \int_0^t F_n(\tau) e^{-\frac{a^2(t-\tau)}{2\kappa}} \sin((t-\tau) \mathcal{J}(\alpha_n)) d\tau, & \alpha_n > \frac{a}{2\kappa}, \end{cases} \quad (5.5)$$

where

$$\mathcal{J}(\alpha_n) = \begin{cases} \frac{\sqrt{a^4 - 4a^2 \kappa^2 \alpha_n^2}}{2\kappa}, & \alpha_n < \frac{a}{2\kappa}, \\ \frac{\sqrt{4a^2 \kappa^2 \alpha_n^2 - a^4}}{2\kappa}, & \alpha_n > \frac{a}{2\kappa}. \end{cases} \quad (5.6)$$

Notice that the solution for the case $\alpha_n = \frac{a}{2\kappa}$ results from taking the limit as $\alpha_n \rightarrow \frac{a}{2\kappa}$ in either of the other two cases. Keeping this in mind and recalling the relationships

$$\sinh(iz) = i \sin(z) \quad \text{and} \quad \cosh(iz) = \cos(z), \quad (5.7)$$

we can represent the function simply as

$$\begin{aligned}
P(\alpha_n, t) = & G_1(\alpha_n) e^{-\frac{a^2 t}{2\kappa}} \left(\frac{a^2}{\sqrt{a^4 - 4a^2 \kappa^2 \alpha_n^2}} \sinh \left(t \frac{\sqrt{a^4 - 4a^2 \kappa^2 \alpha_n^2}}{2\kappa} \right) \right. \\
& \left. + \cosh \left(t \frac{\sqrt{a^4 - 4a^2 \kappa^2 \alpha_n^2}}{2\kappa} \right) \right) \\
& + G_2(\alpha_n) \frac{2\kappa e^{-\frac{a^2 t}{2\kappa}}}{\sqrt{a^4 - 4a^2 \kappa^2 \alpha_n^2}} \sinh \left(t \frac{\sqrt{a^4 - 4a^2 \kappa^2 \alpha_n^2}}{2\kappa} \right) \\
& + \frac{2\kappa a^2}{\sqrt{a^4 - 4a^2 \kappa^2 \alpha_n^2}} \int_0^t F_n(\tau) e^{-\frac{a^2(t-\tau)}{2\kappa}} \sinh \left((t-\tau) \frac{\sqrt{a^4 - 4a^2 \kappa^2 \alpha_n^2}}{2\kappa} \right) d\tau,
\end{aligned} \tag{5.8}$$

letting the hyperbolic trigonometric functions switch over to regular trigonometric functions when the argument $\frac{\sqrt{a^4 - 4a^2 \kappa^2 \alpha_n^2}}{2\kappa}$ becomes imaginary (i.e., when $\alpha_n > \frac{a}{2\kappa}$). We will exercise this option below when stating the complete solution to (5.1).

Recall that, by Theorem 3.3, $p(r, t)$ can be expanded in an infinite series of the eigenfunctions $\{u_n(r)\}_{n=0}^\infty$ as in (3.11) where the $u_n(r)$ are defined by (4.2) and (4.4), and the coefficients in (3.11) are now given by (4.5) and (4.6).

Observe,

$$\begin{aligned}
p(r, t) &= \sum_{n=0}^{\infty} \frac{\langle u_n, p \rangle_w}{\langle u_n, u_n \rangle_w} u_n(r) \\
&= \sum_{n=0}^{\infty} \frac{\int_{r_1}^{r_2} p(r, t) u_n(r) r dr}{\int_{r_1}^{r_2} u_n^2(r) r dr} u_n(r) \\
&= \sum_{n=0}^{\infty} \frac{P(\alpha_n, t)}{\int_{r_1}^{r_2} u_n^2(r) r dr} u_n(r) \\
&= \frac{P(\alpha_0, t)}{\int_{r_1}^{r_2} u_0^2(r) r dr} + \sum_{n=1}^{\infty} \frac{P(\alpha_n, t)}{\int_{r_1}^{r_2} u_n^2(r) r dr} u_n(r) \\
&= \frac{2}{r_2^2 - r_1^2} \left(G_1(\alpha_0) + \frac{\kappa}{a^2} \left(1 - e^{-\frac{a^2 t}{\kappa}} \right) G_2(\alpha_0) \right. \\
&\quad \left. + 2\kappa \int_0^t F_0(\tau) e^{-\frac{a^2(t-\tau)}{2\kappa}} \sinh \left(\frac{a^2}{2\kappa} (t - \tau) \right) d\tau \right) \\
&\quad + \sum_{n=1}^{\infty} \left[\frac{\pi^2 \alpha_n^2 J_1^2(\alpha_n r_1) u_n(r)}{2(J_1^2(\alpha_n r_1) - J_1^2(\alpha_n r_2))} \right] \\
&\quad \left[G_1(\alpha_n) e^{-\frac{a^2 t}{2\kappa}} \left(\frac{a^2}{\sqrt{a^4 - 4a^2 \kappa^2 \alpha_n^2}} \sinh \left(t \frac{\sqrt{a^4 - 4a^2 \kappa^2 \alpha_n^2}}{2\kappa} \right) \right. \right. \\
&\quad \left. \left. + \cosh \left(t \frac{\sqrt{a^4 - 4a^2 \kappa^2 \alpha_n^2}}{2\kappa} \right) \right) \right. \\
&\quad \left. + G_2(\alpha_n) \frac{2\kappa e^{-\frac{a^2 t}{2\kappa}}}{\sqrt{a^4 - 4a^2 \kappa^2 \alpha_n^2}} \sinh \left(t \frac{\sqrt{a^4 - 4a^2 \kappa^2 \alpha_n^2}}{2\kappa} \right) \right. \\
&\quad \left. + \frac{2\kappa a^2}{\sqrt{a^4 - 4a^2 \kappa^2 \alpha_n^2}} \int_0^t F_n(\tau) e^{-\frac{a^2(t-\tau)}{2\kappa}} \sinh \left((t - \tau) \frac{\sqrt{a^4 - 4a^2 \kappa^2 \alpha_n^2}}{2\kappa} \right) d\tau \right]
\end{aligned}$$

$$\begin{aligned}
&= \frac{2}{r_2^2 - r_1^2} \left(\int_{r_1}^{r_2} g_1(r)r \, dr + \frac{\kappa}{a^2} \left(1 - e^{-\frac{a^2 t}{\kappa}}\right) \int_{r_1}^{r_2} g_2(r)r \, dr \right. \\
&+ 2\kappa \int_0^t (f_2(\tau) - f_1(\tau)) e^{-\frac{a^2(t-\tau)}{2\kappa}} \sinh\left(\frac{a^2}{2\kappa}(t-\tau)\right) d\tau \Big) \\
&+ \sum_{n=1}^{\infty} \left[\frac{\pi^2 \alpha_n^2 J_1^2(\alpha_n r_1) u_n(r)}{2(J_1^2(\alpha_n r_1) - J_1^2(\alpha_n r_2))} \right] \\
&\left[e^{-\frac{a^2 t}{2\kappa}} \left(\frac{a^2}{\sqrt{a^4 - 4a^2 \kappa^2 \alpha_n^2}} \sinh\left(t \frac{\sqrt{a^4 - 4a^2 \kappa^2 \alpha_n^2}}{2\kappa}\right) + \cosh\left(t \frac{\sqrt{a^4 - 4a^2 \kappa^2 \alpha_n^2}}{2\kappa}\right) \right) \right. \\
&\int_{r_1}^{r_2} g_1(r) u_n(r) r \, dr + \frac{2\kappa e^{-\frac{a^2 t}{2\kappa}}}{\sqrt{a^4 - 4a^2 \kappa^2 \alpha_n^2}} \sinh\left(t \frac{\sqrt{a^4 - 4a^2 \kappa^2 \alpha_n^2}}{2\kappa}\right) \int_{r_1}^{r_2} g_2(r) u_n(r) r \, dr \\
&+ \frac{2\kappa a^2}{\sqrt{a^4 - 4a^2 \kappa^2 \alpha_n^2}} \\
&\left. \int_0^t \frac{2}{\pi \alpha_n} \left(\frac{f_1(\tau)}{r_1 \rho} - \frac{f_2(\tau)}{r_2} \right) e^{-\frac{a^2(t-\tau)}{2\kappa}} \sinh\left((t-\tau) \frac{\sqrt{a^4 - 4a^2 \kappa^2 \alpha_n^2}}{2\kappa}\right) d\tau \right] \\
&= \frac{2}{r_2^2 - r_1^2} \left(\int_{r_1}^{r_2} g_1(r)r \, dr + \frac{\kappa}{a^2} \left(1 - e^{-\frac{a^2 t}{\kappa}}\right) \int_{r_1}^{r_2} g_2(r)r \, dr \right. \\
&+ 2\kappa \int_0^t (f_2(\tau) - f_1(\tau)) e^{-\frac{a^2(t-\tau)}{2\kappa}} \sinh\left(\frac{a^2}{2\kappa}(t-\tau)\right) d\tau \Big) \\
&+ \pi \sum_{n=1}^{\infty} \left[\frac{\alpha_n^2 J_1(\alpha_n r_1) u_n(r)}{J_1^2(\alpha_n r_1) - J_1^2(\alpha_n r_2)} \right] \\
&\left[\frac{\pi}{2} J_1(\alpha_n r_1) e^{-\frac{a^2 t}{2\kappa}} \left(\frac{a^2}{\sqrt{a^4 - 4a^2 \kappa^2 \alpha_n^2}} \sinh\left(t \frac{\sqrt{a^4 - 4a^2 \kappa^2 \alpha_n^2}}{2\kappa}\right) \right. \right. \\
&+ \left. \left. \cosh\left(t \frac{\sqrt{a^4 - 4a^2 \kappa^2 \alpha_n^2}}{2\kappa}\right) \right) \int_{r_1}^{r_2} g_1(r) u_n(r) r \, dr \right. \\
&+ \frac{\pi \kappa J_1(\alpha_n r_1) e^{-\frac{a^2 t}{2\kappa}}}{\sqrt{a^4 - 4a^2 \kappa^2 \alpha_n^2}} \sinh\left(t \frac{\sqrt{a^4 - 4a^2 \kappa^2 \alpha_n^2}}{2\kappa}\right) \int_{r_1}^{r_2} g_2(r) u_n(r) r \, dr \\
&+ J_1(\alpha_n r_2) \frac{2\kappa a^2}{\alpha_n r_1 \sqrt{a^4 - 4a^2 \kappa^2 \alpha_n^2}} \int_0^t f_1(\tau) e^{-\frac{a^2(t-\tau)}{2\kappa}} \sinh\left((t-\tau) \frac{\sqrt{a^4 - 4a^2 \kappa^2 \alpha_n^2}}{2\kappa}\right) d\tau \\
&\left. - J_1(\alpha_n r_1) \frac{2\kappa a^2}{\alpha_n r_2 \sqrt{a^4 - 4a^2 \kappa^2 \alpha_n^2}} \int_0^t f_2(\tau) e^{-\frac{a^2(t-\tau)}{2\kappa}} \sinh\left((t-\tau) \frac{\sqrt{a^4 - 4a^2 \kappa^2 \alpha_n^2}}{2\kappa}\right) d\tau \right].
\end{aligned}$$

5.3 Solutions for Pressure Defined at the Inner Boundary and Radial Flow

Defined at the Outer Boundary

The radial hyperbolic diffusion IBVP where at the internal radius the pressure is an arbitrary function of time while at the outer radius the flow rate is an arbitrary function of time is given by

$$\frac{1}{r} \frac{\partial}{\partial r} \left(r \frac{\partial p}{\partial r} \right) = \frac{1}{a^2} \frac{\partial^2 p}{\partial t^2} + \frac{1}{\kappa} \frac{\partial p}{\partial t}, \quad (5.9a)$$

$$p(r, 0) = g_1(r), \quad (5.9b)$$

$$\frac{\partial p}{\partial t}(r, 0) = g_2(r), \quad (5.9c)$$

$$p(r_1, t) = f_1(t), \quad (5.9d)$$

$$p(r_2, t) = f_2(t). \quad (5.9e)$$

The appropriate Hankel transform for (5.9) is identical that given in (4.14) which was defined for (4.10). Restating the Hankel transform we have

$$\mathcal{H}\{Sf\}(\alpha_n) = -\alpha_n^2 F(\alpha_n) + \frac{2}{\pi \alpha_n} (\alpha_n \rho f(r_1) + f'(r_2)),$$

where we used the definition of ρ in (4.11).

To solve the IBVP (5.9), we now apply the Hankel transform \mathcal{H} and obtain the initial value problem for $n \geq 1$

$$\frac{1}{a^2} \frac{d^2 P}{dt^2}(\alpha_n, t) + \frac{1}{\kappa} \frac{dP}{dt}(\alpha_n, t) + \alpha_n^2 P(\alpha_n, t) = -\frac{2}{\pi} \left(\rho f_1(t) + \frac{f_2(t)}{\alpha_n r_2} \right), \quad (5.10a)$$

$$P(\alpha_n, 0) = G_1(\alpha_n) \quad (5.10b)$$

$$\frac{dP}{dt}(\alpha_n, 0) = G_2(\alpha_n). \quad (5.10c)$$

Defining the function $F_n(t)$ by

$$F_n(t) := -\frac{2}{\pi} \left(\rho f_1(t) + \frac{f_2(t)}{\alpha_n r_2} \right), \quad n \geq 1, \quad (5.11)$$

the solution to (5.10) is given by (5.5) where the function $F_n(t)$ in (5.5) is now defined by (5.11). When stating the complete solution to (5.9), we will use the representation (5.8) with the function $F_n(t)$ in (5.8) defined by (5.11).

Recall that, by Theorem 3.3, $p(r, t)$ can be expanded in an infinite series of the eigenfunctions $\{u_n(r)\}_{n=1}^{\infty}$ as in (3.11) where the $u_n(r)$ are defined by (4.12) and the coefficients in (3.11) are now given by (4.13).

Observe,

$$\begin{aligned} p(r, t) &= \sum_{n=1}^{\infty} \frac{\langle u_n, p \rangle_w}{\langle u_n, u_n \rangle_w} u_n(r) \\ &= \sum_{n=1}^{\infty} \frac{\int_{r_1}^{r_2} p(r, t) u_n(r) r dr}{\int_{r_1}^{r_2} u_n^2(r) r dr} u_n(r) \\ &= \sum_{n=1}^{\infty} \frac{P(\alpha_n, t)}{\int_{r_1}^{r_2} u_n^2(r) r dr} u_n(r) \\ &= \sum_{n=1}^{\infty} \left[\frac{\pi^2 \alpha_n^2 J_0^2(\alpha_n r_1) u_n(r)}{2(J_0^2(\alpha_n r_1) - J_1^2(\alpha_n r_2))} \right] \\ &\quad \left[G_1(\alpha_n) e^{-\frac{a^2 t}{2\kappa}} \left(\frac{a^2}{\sqrt{a^4 - 4a^2 \kappa^2 \alpha_n^2}} \sinh \left(t \frac{\sqrt{a^4 - 4a^2 \kappa^2 \alpha_n^2}}{2\kappa} \right) \right. \right. \\ &\quad \left. \left. + \cosh \left(t \frac{\sqrt{a^4 - 4a^2 \kappa^2 \alpha_n^2}}{2\kappa} \right) \right) \right. \\ &\quad \left. + G_2(\alpha_n) \frac{2\kappa e^{-\frac{a^2 t}{2\kappa}}}{\sqrt{a^4 - 4a^2 \kappa^2 \alpha_n^2}} \sinh \left(t \frac{\sqrt{a^4 - 4a^2 \kappa^2 \alpha_n^2}}{2\kappa} \right) \right. \\ &\quad \left. + \frac{2\kappa a^2}{\sqrt{a^4 - 4a^2 \kappa^2 \alpha_n^2}} \int_0^t F_n(\tau) e^{-\frac{a^2(t-\tau)}{2\kappa}} \sinh \left((t-\tau) \frac{\sqrt{a^4 - 4a^2 \kappa^2 \alpha_n^2}}{2\kappa} \right) d\tau \right] \end{aligned}$$

$$\begin{aligned}
&= \sum_{n=1}^{\infty} \left[\frac{\pi^2 \alpha_n^2 J_0^2(\alpha_n r_1) u_n(r)}{2(J_0^2(\alpha_n r_1) - J_1^2(\alpha_n r_2))} \right] \\
&\left[e^{-\frac{a^2 t}{2\kappa}} \left(\frac{a^2}{\sqrt{a^4 - 4a^2 \kappa^2 \alpha_n^2}} \sinh \left(t \frac{\sqrt{a^4 - 4a^2 \kappa^2 \alpha_n^2}}{2\kappa} \right) + \cosh \left(t \frac{\sqrt{a^4 - 4a^2 \kappa^2 \alpha_n^2}}{2\kappa} \right) \right) \right. \\
&\int_{r_1}^{r_2} g_1(r) u_n(r) r \, dr + \frac{2\kappa e^{-\frac{a^2 t}{2\kappa}}}{\sqrt{a^4 - 4a^2 \kappa^2 \alpha_n^2}} \sinh \left(t \frac{\sqrt{a^4 - 4a^2 \kappa^2 \alpha_n^2}}{2\kappa} \right) \int_{r_1}^{r_2} g_2(r) u_n(r) r \, dr \\
&- \frac{2\kappa a^2}{\sqrt{a^4 - 4a^2 \kappa^2 \alpha_n^2}} \\
&\left. \int_0^t \frac{2}{\pi} \left(\rho f_1(t) + \frac{f_2(t)}{\alpha_n r_2} \right) e^{-\frac{a^2(t-\tau)}{2\kappa}} \sinh \left((t-\tau) \frac{\sqrt{a^4 - 4a^2 \kappa^2 \alpha_n^2}}{2\kappa} \right) d\tau \right] \\
&= \pi \sum_{n=1}^{\infty} \left[\frac{\alpha_n^2 J_0(\alpha_n r_1) u_n(r)}{J_0^2(\alpha_n r_1) - J_1^2(\alpha_n r_2)} \right] \\
&\left[\frac{\pi}{2} J_0(\alpha_n r_1) e^{-\frac{a^2 t}{2\kappa}} \left(\frac{a^2}{\sqrt{a^4 - 4a^2 \kappa^2 \alpha_n^2}} \sinh \left(t \frac{\sqrt{a^4 - 4a^2 \kappa^2 \alpha_n^2}}{2\kappa} \right) \right. \right. \\
&+ \left. \left. \cosh \left(t \frac{\sqrt{a^4 - 4a^2 \kappa^2 \alpha_n^2}}{2\kappa} \right) \right) \int_{r_1}^{r_2} g_1(r) u_n(r) r \, dr \right. \\
&+ \frac{\pi \kappa J_0(\alpha_n r_1) e^{-\frac{a^2 t}{2\kappa}}}{\sqrt{a^4 - 4a^2 \kappa^2 \alpha_n^2}} \sinh \left(t \frac{\sqrt{a^4 - 4a^2 \kappa^2 \alpha_n^2}}{2\kappa} \right) \int_{r_1}^{r_2} g_2(r) u_n(r) r \, dr \\
&- \frac{2\kappa a^2 J_1(\alpha_n r_2)}{\sqrt{a^4 - 4a^2 \kappa^2 \alpha_n^2}} \int_0^t f_1(\tau) e^{-\frac{a^2(t-\tau)}{2\kappa}} \sinh \left((t-\tau) \frac{\sqrt{a^4 - 4a^2 \kappa^2 \alpha_n^2}}{2\kappa} \right) d\tau \\
&\left. - \frac{2\kappa a^2 J_0(\alpha_n r_1)}{\sqrt{a^4 - 4a^2 \kappa^2 \alpha_n^2}} \int_0^t \frac{f_2(t)}{\alpha_n r_2} e^{-\frac{a^2(t-\tau)}{2\kappa}} \sinh \left((t-\tau) \frac{\sqrt{a^4 - 4a^2 \kappa^2 \alpha_n^2}}{2\kappa} \right) d\tau \right].
\end{aligned}$$

5.4 Solutions for Pressure Defined at Both Boundaries

The radial parabolic diffusion IBVP where the pressures are arbitrary functions of time at the inner and outer radii is given by

$$\frac{1}{r} \frac{\partial}{\partial r} \left(r \frac{\partial p}{\partial r} \right) = \frac{1}{a^2} \frac{\partial^2 p}{\partial t^2} + \frac{1}{\kappa} \frac{\partial p}{\partial t}, \quad (5.12a)$$

$$p(r, 0) = g_1(r), \quad (5.12b)$$

$$\frac{\partial p}{\partial t}(r, 0) = g_2(r), \quad (5.12c)$$

$$p(r_1, t) = f_1(t), \quad (5.12d)$$

$$p(r_2, t) = f_2(t). \quad (5.12e)$$

The appropriate Hankel transform for (5.12) is identical that given in (4.20) which was defined for (4.16). Restating the Hankel transform we have

$$\mathcal{H}\{Sf\}(\alpha_n) = -\alpha_n^2 F(\alpha_n) + \frac{2}{\pi} (f(r_2) - \rho f(r_1)),$$

where we used the definition of ρ in (4.17).

To solve the IBVP (5.12), we now apply the Hankel transform \mathcal{H} and obtain the initial value problem for $n \geq 1$

$$\frac{1}{a^2} \frac{d^2 P}{dt^2}(\alpha_n, t) + \frac{1}{\kappa} \frac{dP}{dt}(\alpha_n, t) + \alpha_n^2 P(\alpha_n, t) = \frac{2}{\pi} (f_2(t) - \rho f_1(t)), \quad (5.13a)$$

$$P(\alpha_n, 0) = G_1(\alpha_n) \quad (5.13b)$$

$$\frac{dP}{dt}(\alpha_n, 0) = G_2(\alpha_n). \quad (5.13c)$$

Defining the function $F_n(t)$ by

$$F_n(t) := \frac{2}{\pi} (f_2(t) - \rho f_1(t)), \quad n \geq 1, \quad (5.14)$$

the solution to (5.13) is given by (5.5) where the function $F_n(t)$ in (5.5) is now defined by (5.14). When stating the complete solution to (5.12), we will use the representation (5.8) with the function $F_n(t)$ in (5.8) defined by (5.14).

Recall that, by Theorem 3.3, $p(r, t)$ can be expanded in an infinite series of the eigenfunctions $\{u_n(r)\}_{n=1}^{\infty}$ as in (3.11) where the $u_n(r)$ are defined by (4.18) and the coefficients in (3.11) are now given by (4.19).

Observe,

$$\begin{aligned} p(r, t) &= \sum_{n=1}^{\infty} \frac{\langle u_n, p \rangle_w}{\langle u_n, u_n \rangle_w} u_n(r) \\ &= \sum_{n=1}^{\infty} \frac{\int_{r_1}^{r_2} p(r, t) u_n(r) r dr}{\int_{r_1}^{r_2} u_n^2(r) r dr} u_n(r) \\ &= \sum_{n=1}^{\infty} \frac{P(\alpha_n, t)}{\int_{r_1}^{r_2} u_n^2(r) r dr} u_n(r) \\ &= \sum_{n=1}^{\infty} \left[\frac{\pi^2 \alpha_n^2 J_0^2(\alpha_n r_1) u_n(r)}{2(J_0^2(\alpha_n r_1) - J_0^2(\alpha_n r_2))} \right] \\ &\quad \left[G_1(\alpha_n) e^{-\frac{a^2 t}{2\kappa}} \left(\frac{a^2}{\sqrt{a^4 - 4a^2 \kappa^2 \alpha_n^2}} \sinh \left(t \frac{\sqrt{a^4 - 4a^2 \kappa^2 \alpha_n^2}}{2\kappa} \right) \right. \right. \\ &\quad \left. \left. + \cosh \left(t \frac{\sqrt{a^4 - 4a^2 \kappa^2 \alpha_n^2}}{2\kappa} \right) \right) \right. \\ &\quad \left. + G_2(\alpha_n) \frac{2\kappa e^{-\frac{a^2 t}{2\kappa}}}{\sqrt{a^4 - 4a^2 \kappa^2 \alpha_n^2}} \sinh \left(t \frac{\sqrt{a^4 - 4a^2 \kappa^2 \alpha_n^2}}{2\kappa} \right) \right. \\ &\quad \left. + \frac{2\kappa a^2}{\sqrt{a^4 - 4a^2 \kappa^2 \alpha_n^2}} \int_0^t F_n(\tau) e^{-\frac{a^2(t-\tau)}{2\kappa}} \sinh \left((t-\tau) \frac{\sqrt{a^4 - 4a^2 \kappa^2 \alpha_n^2}}{2\kappa} \right) d\tau \right] \end{aligned}$$

$$\begin{aligned}
&= \sum_{n=1}^{\infty} \left[\frac{\pi^2 \alpha_n^2 J_0^2(\alpha_n r_1) u_n(r)}{2(J_0^2(\alpha_n r_1) - J_1^2(\alpha_n r_2))} \right] \\
&\left[e^{-\frac{a^2 t}{2\kappa}} \left(\frac{a^2}{\sqrt{a^4 - 4a^2 \kappa^2 \alpha_n^2}} \sinh \left(t \frac{\sqrt{a^4 - 4a^2 \kappa^2 \alpha_n^2}}{2\kappa} \right) + \cosh \left(t \frac{\sqrt{a^4 - 4a^2 \kappa^2 \alpha_n^2}}{2\kappa} \right) \right) \right. \\
&\int_{r_1}^{r_2} g_1(r) u_n(r) r \, dr + \frac{2\kappa e^{-\frac{a^2 t}{2\kappa}}}{\sqrt{a^4 - 4a^2 \kappa^2 \alpha_n^2}} \sinh \left(t \frac{\sqrt{a^4 - 4a^2 \kappa^2 \alpha_n^2}}{2\kappa} \right) \int_{r_1}^{r_2} g_2(r) u_n(r) r \, dr \\
&\left. + \frac{2\kappa a^2}{\sqrt{a^4 - 4a^2 \kappa^2 \alpha_n^2}} \int_0^t \frac{2}{\pi} (f_2(t) - \rho f_1(t)) e^{-\frac{a^2(t-\tau)}{2\kappa}} \sinh \left((t-\tau) \frac{\sqrt{a^4 - 4a^2 \kappa^2 \alpha_n^2}}{2\kappa} \right) d\tau \right] \\
&= \pi \sum_{n=1}^{\infty} \left[\frac{\alpha_n^2 J_0(\alpha_n r_1) u_n(r)}{J_0^2(\alpha_n r_1) - J_0^2(\alpha_n r_2)} \right] \\
&\left[\frac{\pi}{2} J_0(\alpha_n r_1) e^{-\frac{a^2 t}{2\kappa}} \left(\frac{a^2}{\sqrt{a^4 - 4a^2 \kappa^2 \alpha_n^2}} \sinh \left(t \frac{\sqrt{a^4 - 4a^2 \kappa^2 \alpha_n^2}}{2\kappa} \right) \right. \right. \\
&+ \left. \left. \cosh \left(t \frac{\sqrt{a^4 - 4a^2 \kappa^2 \alpha_n^2}}{2\kappa} \right) \right) \int_{r_1}^{r_2} g_1(r) u_n(r) r \, dr \right. \\
&+ \frac{\pi \kappa J_0(\alpha_n r_1) e^{-\frac{a^2 t}{2\kappa}}}{\sqrt{a^4 - 4a^2 \kappa^2 \alpha_n^2}} \sinh \left(t \frac{\sqrt{a^4 - 4a^2 \kappa^2 \alpha_n^2}}{2\kappa} \right) \int_{r_1}^{r_2} g_2(r) u_n(r) r \, dr \\
&- \frac{2\kappa a^2 J_0(\alpha_n r_2)}{\sqrt{a^4 - 4a^2 \kappa^2 \alpha_n^2}} \int_0^t f_1(\tau) e^{-\frac{a^2(t-\tau)}{2\kappa}} \sinh \left((t-\tau) \frac{\sqrt{a^4 - 4a^2 \kappa^2 \alpha_n^2}}{2\kappa} \right) d\tau \\
&\left. + \frac{2\kappa a^2 J_0(\alpha_n r_1)}{\sqrt{a^4 - 4a^2 \kappa^2 \alpha_n^2}} \int_0^t f_2(t) e^{-\frac{a^2(t-\tau)}{2\kappa}} \sinh \left((t-\tau) \frac{\sqrt{a^4 - 4a^2 \kappa^2 \alpha_n^2}}{2\kappa} \right) d\tau \right].
\end{aligned}$$

5.5 Comparison of the Solutions to the Hyperbolic and Parabolic Diffusion Equations

In this section we will compare and contrast the solutions to the hyperbolic the IBVP (5.1) and the corresponding parabolic IBVP (4.1). Via a dimensionless analog, we will show that as $a \rightarrow \infty$ in (5.1), its solution tends to the solution to (4.1). We will also compare the pseudo-steady state solutions the IBVPs both analytically and

graphically.

5.5.1 Solution to the dimensionless hyperbolic diffusion initial boundary value problem

We can represent the hyperbolic diffusion equation (5.1a) in dimensionless form by defining the following dimensionless variables

$$\begin{aligned}
 p_D &:= \frac{2\pi kh(p_i - p)}{q\mu}, \\
 r_D &:= \frac{r}{r_1}, \\
 R &:= \frac{r_2}{r_1}, \\
 t_D &:= \frac{\kappa t}{r_1^2}, \\
 \tau &:= \frac{\kappa}{ar_1},
 \end{aligned}$$

where p_i is the initial reservoir pressure. We set the initial conditions (5.1b) and (5.1c) to

$$\begin{aligned}
 g_1(r) &= p_i \\
 g_2(r) &= 0,
 \end{aligned}$$

respectively. The boundary conditions (5.1d) and (5.1e) are set to

$$f_1(t) = \frac{q\mu}{2\pi kh} \quad \text{and} \quad f_2(t) = 0,$$

respectively. This translates to a constant terminal rate at the wellbore and a no-flow outer boundary.

We can now write the IBVP (5.1) in dimensionless form by

$$\frac{1}{r_D} \frac{\partial}{\partial r_D} \left(r_D \frac{\partial p_D}{\partial r_D} \right) = \tau^2 \frac{\partial^2 p_D}{\partial t_D^2} + \frac{\partial p_D}{\partial t_D}, \quad (5.15a)$$

$$p(r, 0) = 0, \quad (5.15b)$$

$$\frac{\partial p}{\partial t}(r, 0) = 0, \quad (5.15c)$$

$$r_D \frac{\partial p_D}{\partial r_D} \Big|_{r_D=1} = -1, \quad (5.15d)$$

$$r_D \frac{\partial p_D}{\partial r_D} \Big|_{r_D=R} = 0. \quad (5.15e)$$

From the solution methods presented in this chapter as well as Chapter 3, we see that there are three approaches we can take. We choose to use the method of Laplace transforms to solve (5.15). The reason for this choice is that the solution that will be obtained from the Laplace transform does not require a priori knowledge of three separate fundamental solutions as in the method of separation of variables. Also, if we chose to use the Hankel transform method outlined in Section (5.2), the form of the pseudosteady state portion of the equation would not be evident.

The Laplace transform of $p_D(r_D, t_D)$ with respect to t_D is given by (3.23) as

$$P(r_D, s) = \mathcal{L}\{p(r_D, t_D)\}(s) = \int_0^\infty e^{-st_D} p(r_D, t_D) dt.$$

Implementing Theorem 3.9 and Theorem 3.10, we also have

$$\begin{aligned} \frac{\partial p_D}{\partial t_D}(r_D, t_D) &= sP(r_D, s) - p(r_D, 0) = sP(r_D, s), \\ \tau^2 \frac{\partial^2 p_D}{\partial t_D^2}(r_D, t_D) &= \tau^2 \left(s^2 P(r_D, s) - sp(r_D, 0) - \frac{\partial p_D}{\partial t_D}(r_D, 0) \right) = \tau^2 s^2 P(r_D, s), \end{aligned}$$

and

$$\frac{\partial p_D}{\partial r_D}(r_D, t_D) = \frac{\partial P}{\partial r_D}(r_D, t_D).$$

Thus, the Laplace transformation of the IBVP (5.1) is now a second order BVP

$$\frac{1}{r_D} \frac{\partial}{\partial r_D} \left(r_D \frac{\partial P}{\partial r_D} \right) - (\tau^2 s^2 + s) P(r_D, s) = 0, \quad 1 < r_D < R, \quad (5.16a)$$

$$r_D \frac{\partial P}{\partial r_D} \Big|_{r_D=1} = -\frac{1}{s}, \quad (5.16b)$$

$$r_D \frac{\partial P}{\partial r_D} \Big|_{r_D=R} = 0. \quad (5.16c)$$

Note that (5.16a) is a form of the modified Bessel equation of order zero. Thus, the general solution to (5.16a) is given by

$$P(r_D, s) = A(s)I_0(r_D\sqrt{\tau^2 s^2 + s}) + B(s)K_0(r_D\sqrt{\tau^2 s^2 + s}), \quad (5.17)$$

where $A(s)$ and $B(s)$ are to be determined by implementing the boundary conditions (5.16b) and (5.16c). In doing so we obtain the particular solution to (5.16a)

$$P(r_D, s) = \frac{K_1(R\sqrt{\tau^2 s^2 + s}) I_0(r_D\sqrt{\tau^2 s^2 + s}) + I_1(R\sqrt{\tau^2 s^2 + s}) K_0(r_D\sqrt{\tau^2 s^2 + s})}{s\sqrt{\tau^2 s^2 + s} (I_1(R\sqrt{\tau^2 s^2 + s}) K_1(\sqrt{\tau^2 s^2 + s}) - K_1(R\sqrt{\tau^2 s^2 + s}) I_1(\sqrt{\tau^2 s^2 + s}))}. \quad (5.18)$$

The inverse Laplace transform can be found by evaluating the following contour integral

$$p(r_D, t_D) = \mathcal{L}^{-1}\{P(r_D, s)\}(t_D) = \frac{1}{2\pi i} \oint_{s_n} e^{st_D} P(r_D, s) ds, \quad n = 0, 1, 2, \dots$$

By inspection, we can identify the isolated singular points of (5.18) and then

implement Theorem 3.11. First observe that there is a second order pole at $s = 0$ and a first order pole at $s = -\frac{1}{\tau^2}$. We find our residue $\rho_0(r, t)$ of $e^{st}P(r, s)$ at $s_0 = 0$ by

$$\begin{aligned}\rho_0(r_D, t_D) &= \lim_{s \rightarrow 0} \left[\frac{d^2}{ds^2} (s^2 e^{st_D} P(r_D, s)) \right] \\ &= \lim_{s \rightarrow 0} \left[\frac{d^2}{ds^2} \cdot \right. \\ &\quad \left. \left(\frac{se^{st_D} (K_1(R\sqrt{\tau^2 s^2 + s})I_0(r_D\sqrt{\tau^2 s^2 + s}) + I_1(R\sqrt{\tau^2 s^2 + s})K_0(r_D\sqrt{\tau^2 s^2 + s}))}{\sqrt{\tau^2 s^2 + s} (I_1(R\sqrt{\tau^2 s^2 + s})K_1(\sqrt{\tau^2 s^2 + s}) - K_1(R\sqrt{\tau^2 s^2 + s})I_1(\sqrt{\tau^2 s^2 + s}))} \right) \right] \\ &= \frac{r_D^2 + 4(t_D - \tau^2)}{2(R^2 - 1)} - \frac{R^2 \ln(r_D)}{R^2 - 1} - \frac{3R^4 - 4R^4 \ln(R) - 2R^2 - 1}{4(R^2 - 1)^2}. \quad (5.19)\end{aligned}$$

To confirm this solution we can check it against the terms before the summation in the solutions in [35, pg. 656, Eq. 5] and [36, pg. 86, Eq. 72], with $r_1 = 1$, $r_2 = R$ and appropriate sign changes in (5.19), since the inner boundary condition at $r = r_1$ in [35, 36] was $+1$ instead of -1 here in (5.15d). Similarly, we can confirm the above solution (5.19) exactly with [51, pg. 321, Eq.VII-13]. Likewise, we find our residue $\rho_1(r, t)$ of $e^{st}P(r, s)$ at $s_1 = -\frac{1}{\tau^2}$ by

$$\begin{aligned}\rho_1(r_D, t_D) &= \lim_{s \rightarrow -\frac{1}{\tau^2}} \left[\left(s + \frac{1}{\tau^2} \right) e^{st_D} P(r_D, s) \right] \\ &= \frac{2\tau^2 e^{-\frac{t_D}{\tau^2}}}{R^2 - 1}.\end{aligned} \quad (5.20)$$

To conclude, we must find the remaining singularities of $P(r_D, s)$. By inspection of denominator of (5.18), we can easily see that there are no zeros for $\tau^2 s^2 + s > 0$, but there are countably infinitely many isolated zeros for $\tau^2 s^2 + s < 0$.

Since all poles are negative, we can perform a change of variables

$$\tau^2 s^2 + s \rightarrow -u^2, \quad \text{which implies} \quad s = \frac{-1 \pm \sqrt{1 - 4\tau^2 u^2}}{2\tau^2}$$

and

$$ds = \mp \frac{2u}{\sqrt{1 - 4\tau^2 u^2}} du.$$

From these results we find that the remaining singularities can be found by evaluating

$$\begin{aligned} & -\frac{1}{2\pi i} \oint_{\alpha_n} \frac{2u}{\sqrt{1 - 4\tau^2 u^2}} e^{\frac{-1 + \sqrt{1 - 4\tau^2 u^2}}{2\tau^2} t_D} P_+(r_D, -u^2) du \\ & + \frac{1}{2\pi i} \oint_{\alpha_n} \frac{2u}{\sqrt{1 - 4\tau^2 u^2}} e^{\frac{-1 - \sqrt{1 - 4\tau^2 u^2}}{2\tau^2} t_D} P_-(r_D, -u^2) du, \end{aligned} \quad (5.21)$$

for $n = 2, 3, \dots$, where

$$\begin{aligned} P_{\pm}(r_D, -u^2) &= \frac{2\tau^2 (K_1(Riu)I_0(r_D iu) + I_1(Riu)K_0(r_D iu))}{iu(-1 \pm \sqrt{1 - 4\tau^2 u^2}) (I_1(Riu)K_1(iu) - K_1(Riu)I_1(iu))} \\ &= \pm \frac{2\tau^2 (J_1(Ru)Y_0(r_D u) - Y_1(Ru)J_0(r_D u))}{u(\mp 1 + \sqrt{1 - 4\tau^2 u^2}) (J_1(Ru)Y_1(u) - Y_1(Ru)J_1(u))}. \end{aligned} \quad (5.22)$$

We now add the two contour integrals in (5.21) by substituting in (5.22) to obtain

$$\begin{aligned} & -\frac{1}{2\pi i} \oint_{\alpha_n} \frac{e^{-\frac{t_D}{2\tau^2}(1 + \sqrt{1 - 4\tau^2 u^2})} M(t, \tau, u) U_n(r_D)}{u^2 (J_1(Ru)Y_1(u) - Y_1(Ru)J_1(u))} du \\ & = -\frac{1}{2\pi i} \oint_{\alpha_n} \frac{2e^{-\frac{t_D}{2\tau^2}} H(t, \tau, u) U_n(r_D)}{u^2 (J_1(Ru)Y_1(u) - Y_1(Ru)J_1(u))} du, \end{aligned} \quad (5.23)$$

where

$$M(t_D, \tau, u) = 1 + \sqrt{1 - 4\tau^2 u^2} + e^{\frac{t_D}{\tau^2} \sqrt{1 - 4\tau^2 u^2}} \left(1 + \sqrt{1 - 4\tau^2 u^2} \right),$$

$$U_n(r_D) = Y_1(Ru)J_0(r_D u) - J_1(Ru)Y_0(r_D u),$$

and

$$H(t_D, \tau, u) = \cosh\left(\frac{t_D}{2\tau^2}\sqrt{1-4\tau^2 u^2}\right) + \frac{1}{\sqrt{1-4\tau^2 u^2}} \sinh\left(\frac{t_D}{2\tau^2}\sqrt{1-4\tau^2 u^2}\right).$$

The task of evaluating (5.23) is simplified by the fact that the remaining countably infinitely many poles are isolated. Because of this fact, we can again employ Theorem 3.11. Using the Wronskian, the definition of ρ in (4.3), relationships between $I_\nu, K_\nu, J_\nu,$ and $Y_\nu,$ and a significant amount of algebra, we continue evaluating (5.23) by applying the limit as $u \rightarrow \alpha_n$ to obtain

$$\begin{aligned} & -\frac{1}{2\pi i} \oint_{\alpha_n} \frac{2e^{-\frac{t_D}{2\tau^2}} H(t, \tau, u) U_n(r_D)}{u^2 (J_1(Ru)Y_1(u) - Y_1(Ru)J_1(u))} du \\ &= -\sum_{n=2}^{\infty} \frac{2e^{-\frac{t_D}{2\tau^2}} H(t, \tau, \alpha_n) U_n(r_D)}{\alpha_n^2 \lim_{u \rightarrow \alpha_n} \left(\frac{d}{du} (J_1(Ru)Y_1(u) - Y_1(Ru)J_1(u)) \right)} \\ &= \sum_{n=2}^{\infty} \frac{2\pi J_1^2(\alpha_n) \alpha_n e^{-\frac{t_D}{2\tau^2}} H(t, \tau, \alpha_n) U_n(r_D)}{2\alpha_n^2 (J_1^2(\alpha_n) - J_1^2(\alpha_n R))} \\ &= \pi \sum_{n=2}^{\infty} \frac{J_1^2(\alpha_n) e^{-\frac{t_D}{2\tau^2}} H(t, \tau, \alpha_n) U_n(r_D)}{\alpha_n (J_1^2(\alpha_n) - J_1^2(\alpha_n R))}. \end{aligned} \quad (5.24)$$

Thus, combining (5.19), (5.20), and (5.24), we have that the solution to (5.15) is

$$\begin{aligned} p_D(r_D, t_D) &= \frac{r_D^2 + 4 \left(t_D + \tau^2 \left(e^{-\frac{t_D}{\tau^2}} - 1 \right) \right)}{2(R^2 - 1)} \\ &\quad - \frac{R^2 \ln(r_D)}{R^2 - 1} - \frac{3R^4 - 4R^4 \ln(R) - 2R^2 - 1}{4(R^2 - 1)^2} \\ &\quad + \pi \sum_{n=2}^{\infty} \frac{J_1^2(\alpha_n) e^{-\frac{t_D}{2\tau^2}} H(t_D, \tau, \alpha_n) U_n(r_D)}{\alpha_n (J_1^2(\alpha_n) - J_1^2(\alpha_n R))}. \end{aligned} \quad (5.25)$$

5.5.2 Analytic comparison of solutions

We note that through a straightforward limit calculation, we can easily show that, as $\tau \rightarrow 0$ ($a \rightarrow \infty$), the solution (5.25) to (5.15) converges to the solution to the associated dimensionless parabolic diffusion IBVP given by

$$\frac{1}{r_D} \frac{\partial}{\partial r_D} \left(r_D \frac{\partial p_D}{\partial r_D} \right) = \frac{\partial p_D}{\partial t_D}, \quad (5.26a)$$

$$p(r, 0) = 0, \quad (5.26b)$$

$$r_D \frac{\partial p_D}{\partial r_D} \Big|_{r_D=1} = -1, \quad (5.26c)$$

$$r_D \frac{\partial p_D}{\partial r_D} \Big|_{r_D=R} = 0. \quad (5.26d)$$

Notice that the second initial condition (5.15c) that was present in (5.15) is no longer necessary to obtain a unique solution to (5.26).

From the solution (5.25), observe

$$\begin{aligned} & \lim_{\tau \rightarrow 0} \frac{r_D^2 + 4 \left(t_D + \tau^2 \left(e^{-\frac{t_D}{\tau^2}} - 1 \right) \right)}{2(R^2 - 1)} - \frac{R^2 \ln(r_D)}{R^2 - 1} - \frac{3R^4 - 4R^4 \ln(R) - 2R^2 - 1}{4(R^2 - 1)^2} \\ &= \frac{r_D^2 + 4t_D}{2(R^2 - 1)} - \frac{R^2 \ln(r_D)}{R^2 - 1} - \frac{3R^4 - 4R^4 \ln(R) - 2R^2 - 1}{4(R^2 - 1)^2}. \end{aligned} \quad (5.27)$$

In the summation from the solution (5.25), we must also evaluate the behavior of

$e^{-\frac{t}{2\tau^2}} H(t, \tau, \alpha_n)$ as $\tau \rightarrow 0$. Observe,

$$\begin{aligned}
& \lim_{\tau \rightarrow 0} e^{-\frac{t_D}{2\tau^2}} H(t, \tau, \alpha_n) \\
&= \lim_{\tau \rightarrow 0} e^{-\frac{t_D}{2\tau^2}} \left(\cosh \left(\frac{t_D}{2\tau^2} \sqrt{1 - 4\tau^2 \alpha_n^2} \right) + \frac{1}{\sqrt{1 - 4\tau^2 \alpha_n^2}} \sinh \left(\frac{t_D}{2\tau^2} \sqrt{1 - 4\tau^2 \alpha_n^2} \right) \right) \\
&= \lim_{\tau \rightarrow 0} \frac{e^{-\frac{t_D}{2\tau^2}}}{2} \left(e^{\frac{t_D}{2\tau^2} \sqrt{1 - 4\tau^2 \alpha_n^2}} + e^{-\frac{t_D}{2\tau^2} \sqrt{1 - 4\tau^2 \alpha_n^2}} + \frac{e^{\frac{t_D}{2\tau^2} \sqrt{1 - 4\tau^2 \alpha_n^2}} - e^{-\frac{t_D}{2\tau^2} \sqrt{1 - 4\tau^2 \alpha_n^2}}}{\sqrt{1 - 4\tau^2 \alpha_n^2}} \right) \\
&= \lim_{\tau \rightarrow 0} \frac{1}{2} \left(e^{\frac{t_D}{2\tau^2} (-1 + \sqrt{1 - 4\tau^2 \alpha_n^2})} + \frac{e^{\frac{t_D}{2\tau^2} (-1 + \sqrt{1 - 4\tau^2 \alpha_n^2})}}{\sqrt{1 - 4\tau^2 \alpha_n^2}} \right) \\
&= \frac{1}{2} \left(e^{-t_D \alpha_n^2} + e^{-t_D \alpha_n^2} \right) \\
&= e^{-t_D \alpha_n^2}. \tag{5.28}
\end{aligned}$$

Thus, applying the results of (5.27) and (5.28), we see that the solution (5.25) to (5.15) becomes

$$\begin{aligned}
p_D(r_D, t_D) &= \frac{r_D^2 + 4t_D}{2(R^2 - 1)} - \frac{R^2 \ln(r_D)}{R^2 - 1} - \frac{3R^4 - 4R^4 \ln(R) - 2R^2 - 1}{4(R^2 - 1)^2} \\
&\quad + \pi \sum_{n=2}^{\infty} \frac{J_1^2(\alpha_n) e^{-t_D \alpha_n^2} U_n(r_D)}{\alpha_n (J_1^2(\alpha_n) - J_1^2(\alpha_n R))}, \tag{5.29}
\end{aligned}$$

which is the solution to the dimensionless parabolic diffusion IBVP (5.26).

5.5.3 Graphical comparison of the solutions

In order to best observe the behavior of the solution to the dimensionless hyperbolic diffusion IBVP and the dimensionless parabolic diffusion equation, we illustrate the behavior of the solutions via a multi-precision numerical Laplace inversion scheme [1, 49, 50] and plot the results. The algorithm employs the GWR function [48], which computes the numerical value of the inverse Laplace transform of a function at a given value.

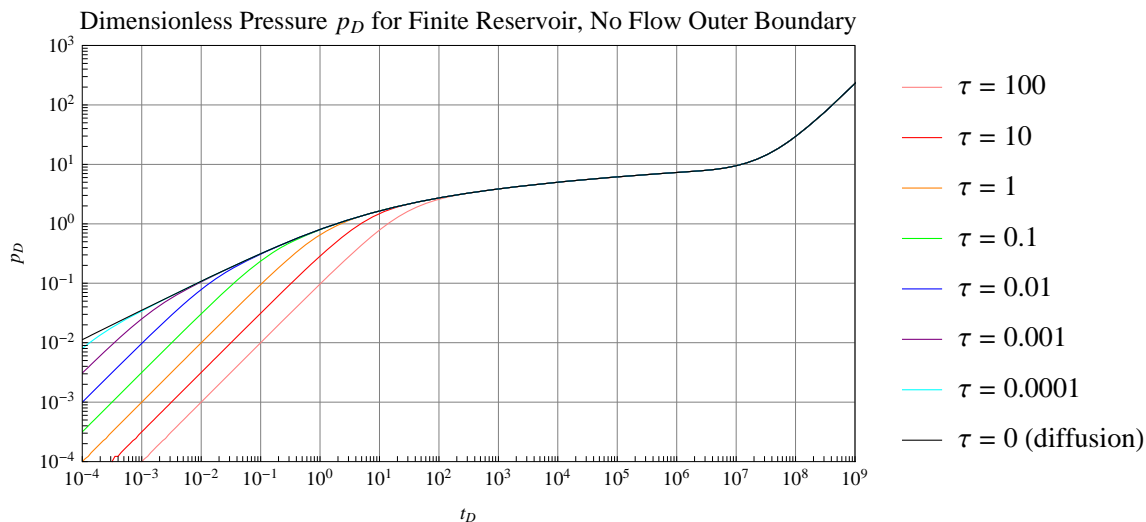


Figure 5.1: Plot of dimensionless pressure vs. dimensionless time with different values for the parameter τ .

Implementing the GWR multi-precision Laplace inversion method, we set $R = 3000$ and compute the inverse of (5.18) with

$$\tau = 0 \text{ (diffusion), } 0.0001, 0.001, 0.01, 0.1, 1, 10.$$

Of course, when $\tau = 0$ this implies that the pressure wave propagation speed is infinite. In this case we have pure diffusion. By inspecting Figure 5.1, we see that the slower the pressure wave propagation speed, the longer it takes in dimensionless time for the diffusion process to dominate. This is evident by noting that the diffusion process dominates when the plot of the dimensionless hyperbolic solution converges to the plot of the diffusion curve for a given value of τ . Further, the larger values of dimensionless time t_D , dimensionless hyperbolic pressure p_D takes longer to converge to the dimensionless pressure trace of diffusion as the value of τ increases. This delay is similar to wellbore storage, which is also illustrated in Figure 5.2.

We now illustrate the relationship between dimensionless pressure p_D and its

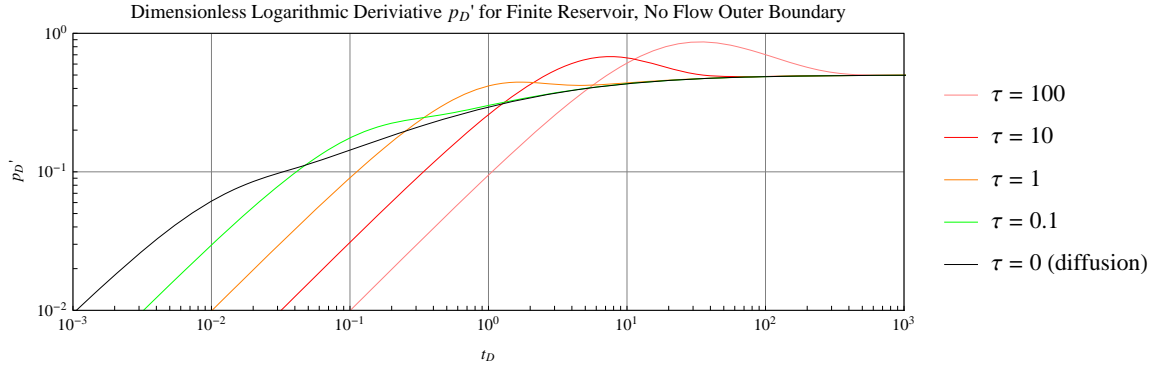


Figure 5.2: Plot of dimensionless logarithmic pressure derivative vs. dimensionless time with different values for the parameter τ .

associated logarithmic derivative p'_D , which is the pressure derivative with respect to logarithmic time. The logarithmic derivative is defined by

$$p'_D(r_D, t_D) := \frac{dp_D(r_D, t_D)}{d \ln(t_D)} = t_D \frac{dp_D(r_D, t_D)}{dt_D} = t_D \mathcal{L}^{-1}\{sP(r_D, s)\}(t_D).$$

In Figures 5.4– 5.10, $p_D := p_D(1, t_D)$ and $p'_D := p'_D(1, t_D)$, which are the dimensionless pressure and the dimensionless logarithmic derivative at the wellbore $r_D = 1$.

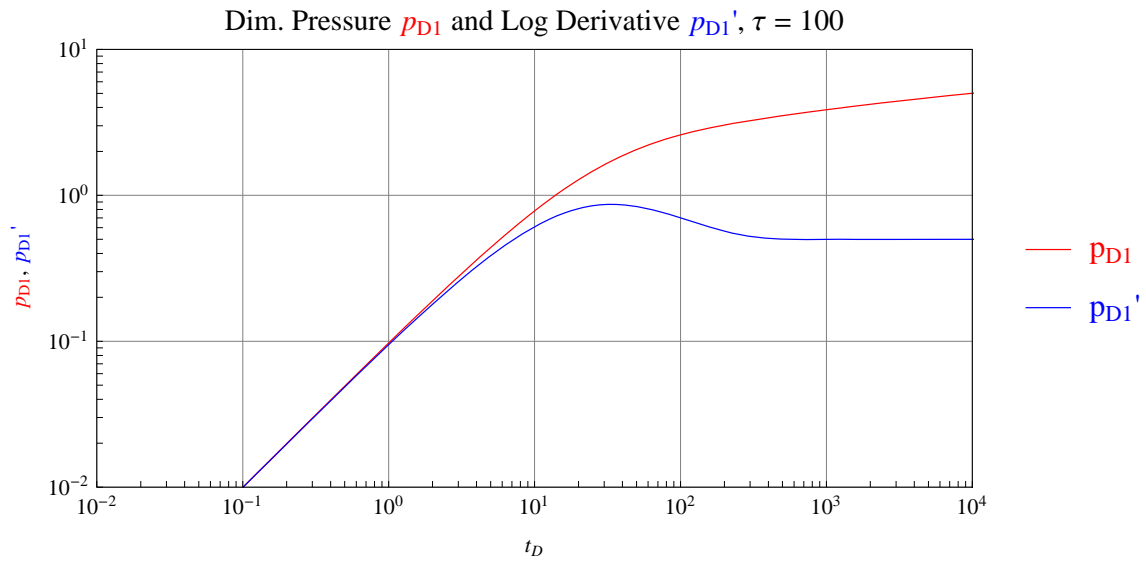


Figure 5.3: Plot of dimensionless pressure and dimensionless logarithmic derivative vs. dimensionless time with $\tau = 100$.

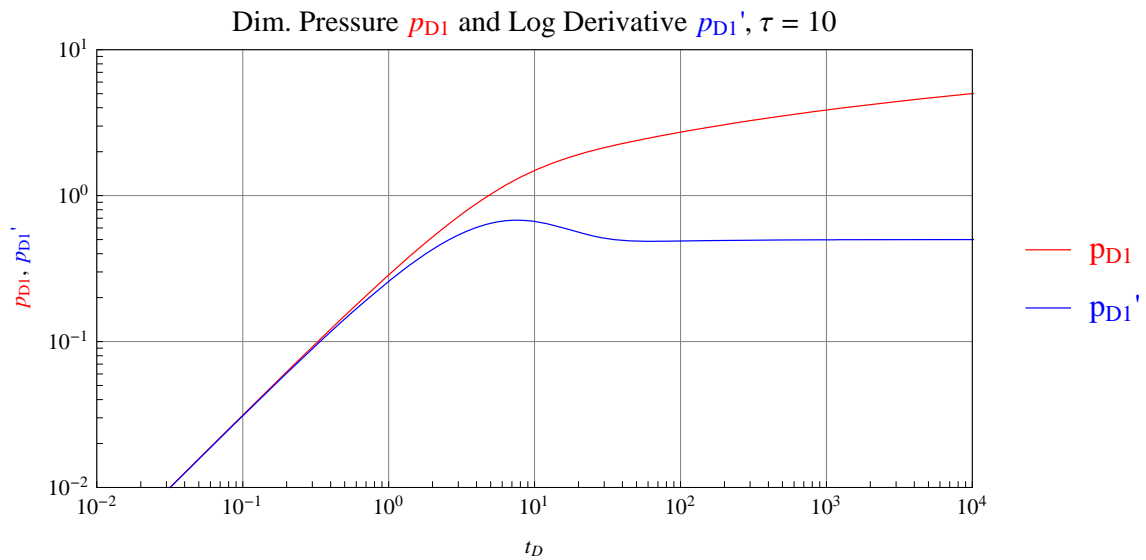


Figure 5.4: Plot of dimensionless pressure and dimensionless logarithmic derivative vs. dimensionless time with $\tau = 10$.

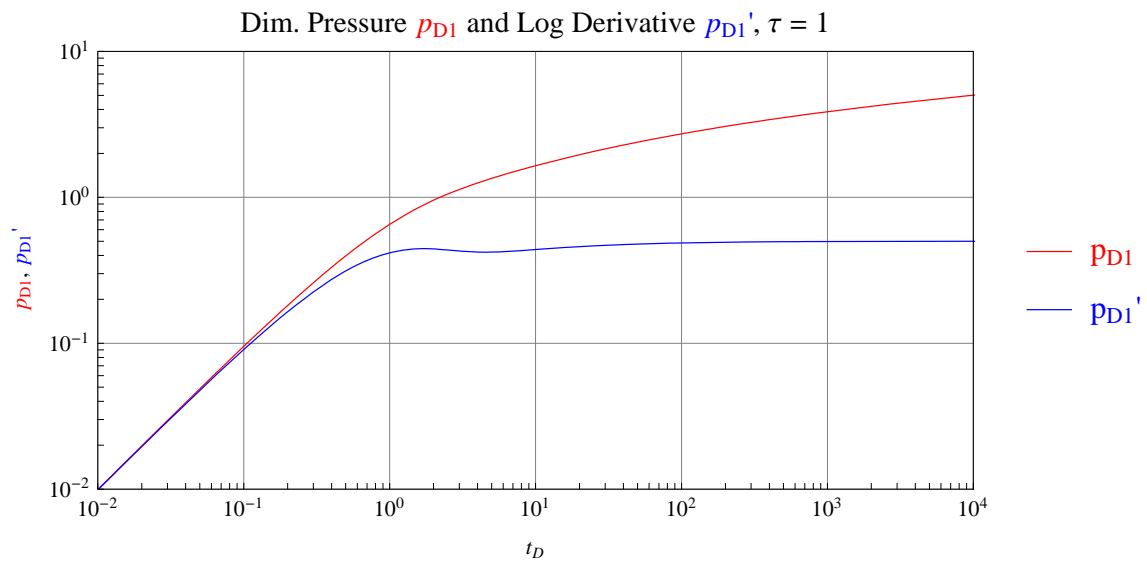


Figure 5.5: Plot of dimensionless pressure and dimensionless logarithmic derivative vs. dimensionless time with $\tau = 1$.

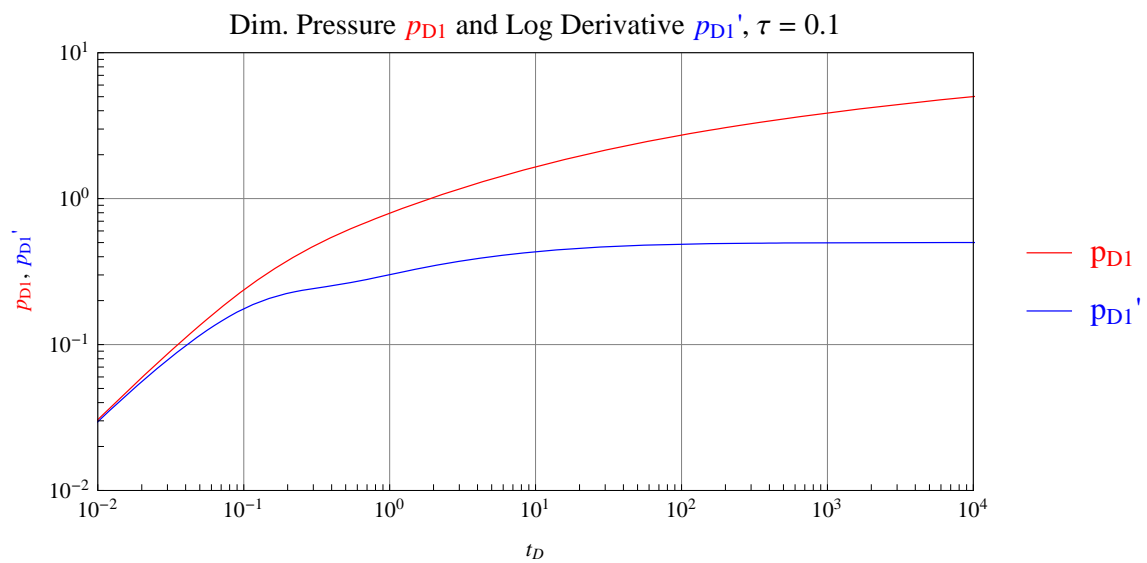


Figure 5.6: Plot of dimensionless pressure and dimensionless logarithmic derivative vs. dimensionless time with $\tau = 0.1$.

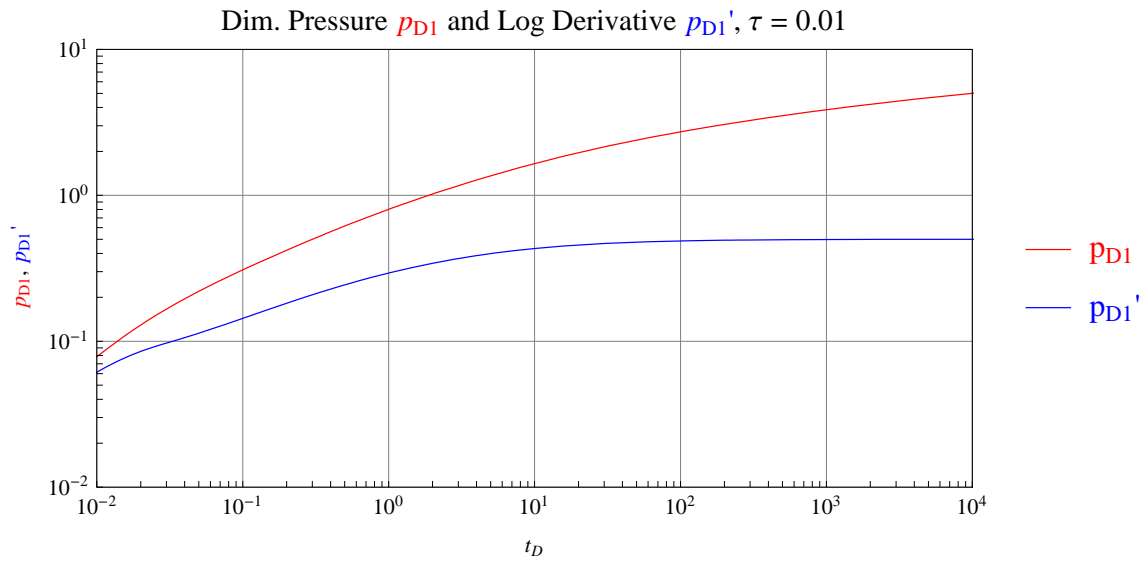


Figure 5.7: Plot of dimensionless pressure and dimensionless logarithmic derivative vs. dimensionless time with $\tau = 0.01$.

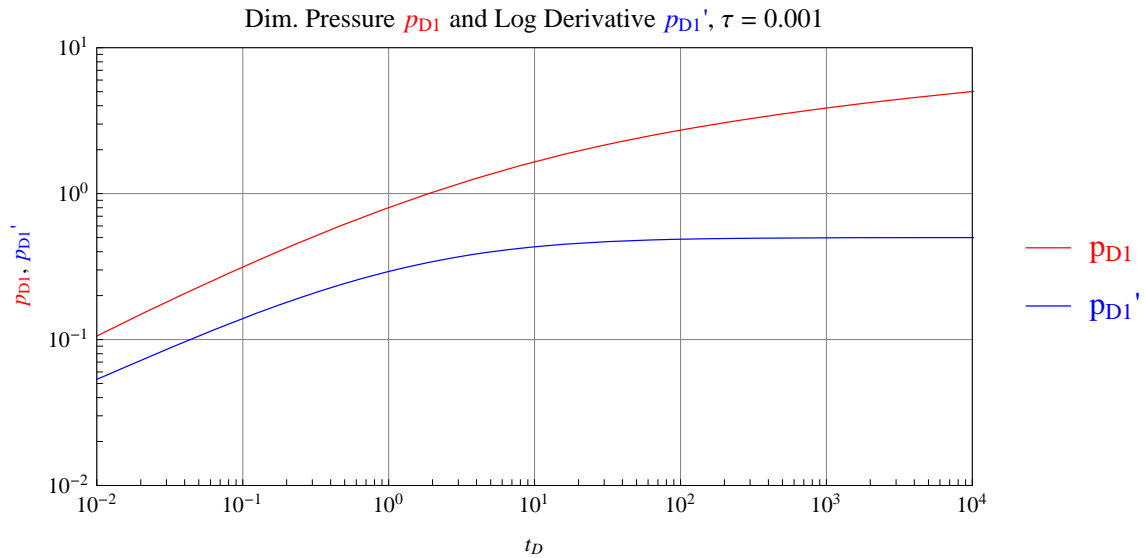


Figure 5.8: Plot of dimensionless pressure and dimensionless logarithmic derivative vs. dimensionless time with $\tau = 0.001$.

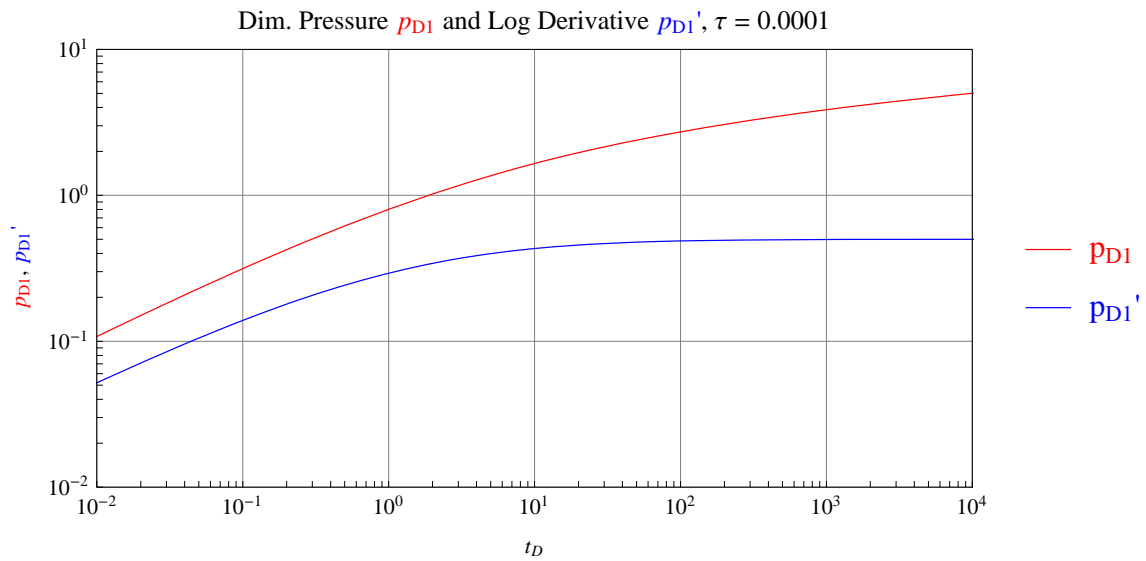


Figure 5.9: Plot of dimensionless pressure and dimensionless logarithmic derivative vs. dimensionless time with $\tau = 0.0001$.

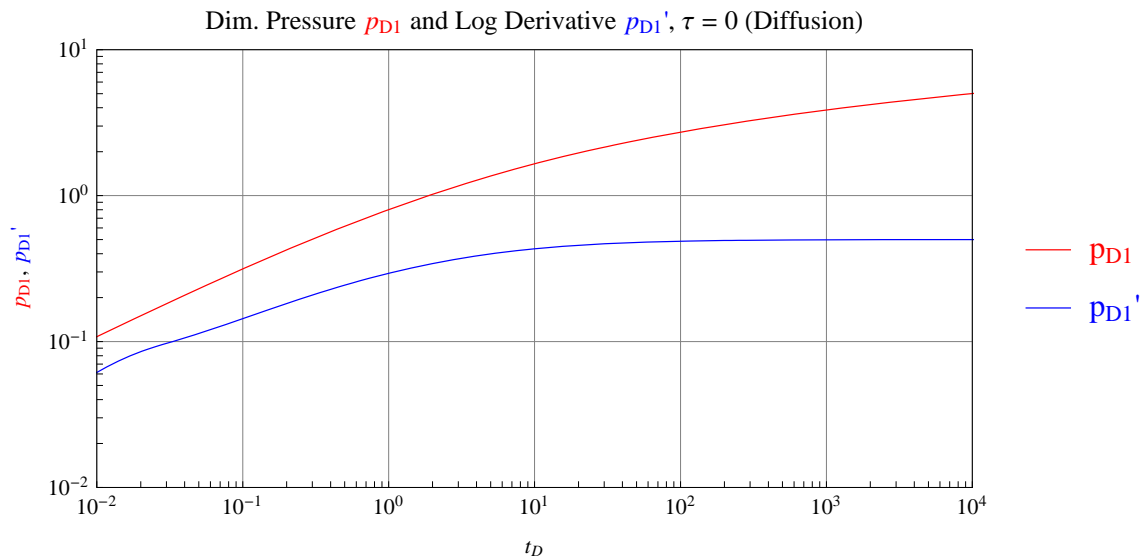


Figure 5.10: Plot of dimensionless pressure and dimensionless logarithmic derivative vs. dimensionless time with $\tau = 0$ (diffusion).

6. PRESSURE PULSE DECAY METHOD

If I were again beginning my studies, I would follow the advice of Plato and start with mathematics.

Galileo Galilei (1564–1642)

6.1 Introduction

We begin our analysis of the pressure pulse decay method with a development of the continuity equation in Cartesian coordinates. The continuity equations will be used to derive the pressure squared (p^2) diffusion equation in the Cartesian coordinate system IBVP that will be used to model the flow of gas through the core sample. We then proceed to develop the appropriate initial and boundary conditions to model the pressure pulse decay method. The solution can be used to determine permeability and porosity of a tight core sample, such as shale. The solution methods contained in [15, 23, 24] do not show the derivation of the continuity equation in Cartesian coordinates, nor do they show the detail in obtaining the solution in the Laplace domain, nor the inversion of the Laplace transform to obtain the solution in the time domain. Additionally, in the literature reviewed by the author, none of the solutions considered using the p^2 diffusion equation to model the flow of gas through a core sample. We will show the missing detail in the development of certain parts of the problem, including the development of the boundary conditions that are used as well as the solution method to obtain the infinite series in the analytic solution. To illustrate the solution, we will provide plots of the pressures versus time of both the upstream and downstream pressures that occur during the experiment. Additionally, we will show the pressure traverses that occur inside the sample during the experiment, which the author believes to be a new contribution.

6.2 Mathematical Model in the Cartesian Coordinate System

To begin, we first derive the continuity equation in the Cartesian coordinate system. Using the continuity equation that we develop, we combine it with Darcy's law, the real gas law, and some assumptions to obtain the p^2 diffusion equation in the Cartesian coordinate system. We then discuss the experimental system set-up for the pressure pulse decay method and derive the appropriate initial conditions and boundary conditions. At the conclusion of this section we will have a properly derived dimensional IBVP whose solution can be used to model the pressure decay of the gas at the end points of and passing through core the core sample during the entire duration of the test.

6.2.1 Derivation of the continuity equation in the Cartesian coordinate system

To derive the diffusion equation in Cartesian coordinates, we must first derive the continuity equation in Cartesian coordinates. The continuity equation stems from the principle of conservation of mass which states that the net rate of creation or destruction of matter is zero [27]. Considering the spatially fixed control volume in Figure 6.1, we have

$$\begin{aligned} \left[\begin{array}{l} \text{The mass flow rate into} \\ \text{the control volume } \Delta V \\ \text{during the time period } \Delta t. \end{array} \right] - \left[\begin{array}{l} \text{The mass flow rate out of} \\ \text{the control volume } \Delta V \\ \text{during the time period } \Delta t. \end{array} \right] & \quad (6.1) \\ & = \left[\begin{array}{l} \text{The rate of mass accumulation} \\ \text{in the control volume } \Delta V \\ \text{during the time period } \Delta t. \end{array} \right], \end{aligned}$$

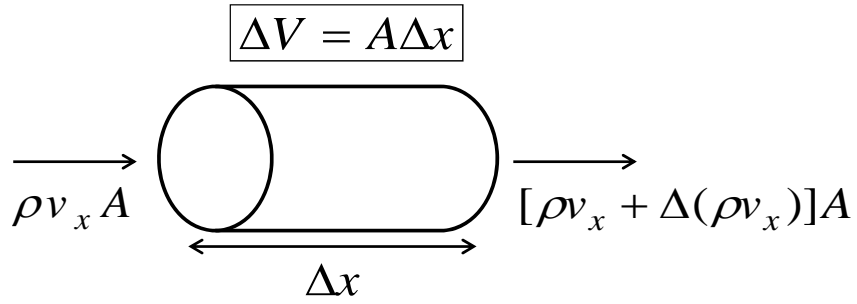


Figure 6.1: Fixed control volume ΔV for the experiment.

where we assume that there is no mass flow rate into or out of the control volume due to a source or a sink. The mass flow rate into the core is given by

$$\frac{dm_{\text{in}}}{dt} = \rho v_x A, \quad (6.2)$$

while the mass flow rate out of the core is given by

$$\frac{dm_{\text{out}}}{dt} = [\rho v_x + \Delta(\rho v_x)] A. \quad (6.3)$$

At any instance, the bulk control volume is given by

$$\Delta V_s = A\Delta x,$$

the mass control volume is given by

$$\Delta V_p = \Delta V_s \phi,$$

and thus, the mass in the control volume is given by

$$\Delta m = \rho \Delta V_p.$$

The rate of mass accumulation is the difference in mass in the control volume for the time period t to $t + \Delta t$ over the length of the time period Δt . Thus,

$$m_{\text{acc}} = \frac{|\rho A \Delta x \phi|_{t+\Delta t} - |\rho A \Delta x \phi|_t}{\Delta t}. \quad (6.4)$$

Combining (6.2), (6.3) and (6.4) and substituting into (6.1), we have

$$\frac{|\rho A \Delta x \phi|_{t+\Delta t} - |\rho A \Delta x \phi|_t}{\Delta t} = \rho v_x A - [\rho v_x + \Delta(\rho v_x)] A = -A \Delta(\rho v_x). \quad (6.5)$$

Dividing (6.5) by the bulk volume ΔV_s , we obtain

$$\frac{|\rho \phi|_{t+\Delta t} - |\rho \phi|_t}{\Delta t} = -\frac{\Delta(\rho v_x)}{\Delta x}. \quad (6.6)$$

Taking the limit of (6.6) as $\Delta x, \Delta t \rightarrow 0$, we finally obtain the continuity equation in the Cartesian coordinate system

$$\frac{\partial(\rho \phi)}{\partial t} = -\frac{\partial(\rho v_x)}{\partial x}. \quad (6.7)$$

6.2.2 Derivation of the diffusion equation in the Cartesian coordinate system

Assuming laminar flow, the form of Darcy's Law that will apply here is given by

$$v_x = -\frac{k}{\mu} \frac{\partial p}{\partial x}. \quad (6.8)$$

Substituting (6.8) into (6.7), we have

$$\frac{\partial(\rho\phi)}{\partial t} = \frac{\partial}{\partial x} \left(\rho \frac{k}{\mu} \frac{\partial p}{\partial x} \right). \quad (6.9)$$

Recall the real gas law

$$pV = znRT, \quad (6.10)$$

where $n = m/M$, m is the mass of the gas and M is the molecular weight of the gas.

We solve (6.10) for density ρ and obtain

$$\rho = \frac{m}{V} = \frac{pM}{zRT}. \quad (6.11)$$

Substituting (6.11) into (6.9), we now have

$$\frac{\partial}{\partial t} \left(\frac{pM\phi}{zRT} \right) = \frac{\partial}{\partial x} \left(\frac{kpM}{\mu zRT} \frac{\partial p}{\partial x} \right). \quad (6.12)$$

Using the fact that M and R are constant, and assuming isothermal conditions and that k is also constant, we can simplify (6.12)

$$\begin{aligned} \frac{\partial}{\partial x} \left(\frac{p}{\mu z} \frac{\partial p}{\partial x} \right) &= \frac{1}{k} \frac{\partial}{\partial t} \left(\frac{p\phi}{z} \right) \\ &= \frac{\phi}{k} \frac{\partial}{\partial t} \left(\frac{p}{z} \right) + \frac{p}{z} \frac{\partial \phi}{\partial t} \\ &= \frac{\phi}{k} \frac{\partial}{\partial p} \left(\frac{p}{z} \right) \frac{\partial p}{\partial t} + \frac{p}{z} \frac{\partial \phi}{\partial p} \frac{\partial p}{\partial t} \\ &= \frac{\phi}{k} \frac{p}{z} \frac{\partial p}{\partial t} \left(\frac{z}{p} \frac{\partial}{\partial p} \left(\frac{p}{z} \right) + \frac{1}{\phi} \frac{\partial \phi}{\partial p} \right). \end{aligned} \quad (6.13)$$

Recalling the definition of the compressibility of gas in terms of its density and implementing the real gas law (6.11) we have

$$c_g = \frac{1}{\rho} \frac{\partial \rho}{\partial p} = \frac{zRT}{pM} \frac{\partial}{\partial p} \left(\frac{pM}{zRT} \right) = \frac{z}{p} \frac{\partial}{\partial p} \left(\frac{p}{z} \right). \quad (6.14)$$

Assuming no formation compressibility, $c_f = \frac{1}{\phi} \frac{\partial \phi}{\partial p} = 0$ and substituting (6.14) into (6.13), we obtain

$$\frac{\partial}{\partial x} \left(\frac{p}{\mu z} \frac{\partial p}{\partial x} \right) = \frac{\phi c_g}{k} \frac{p}{z} \frac{\partial p}{\partial t}. \quad (6.15)$$

Recalling that

$$p \frac{\partial p}{\partial x} = \frac{1}{2} \frac{\partial p^2}{\partial x} \quad \text{and} \quad p \frac{\partial p}{\partial t} = \frac{1}{2} \frac{\partial p^2}{\partial t}, \quad (6.16)$$

we plug in (6.16) into (6.15) yielding

$$\frac{\partial}{\partial x} \left(\frac{1}{\mu z} \frac{\partial p^2}{\partial x} \right) = \frac{\phi c_g}{k} \frac{1}{z} \frac{\partial p^2}{\partial t}. \quad (6.17)$$

Assuming the term μz is constant in (6.17), we have

$$\frac{\partial^2 \psi}{\partial x^2} = \frac{\mu \phi c_g}{k} \frac{\partial \psi}{\partial t},$$

where $\psi = p^2$.

One final assumption is made. We assume that the gas compressibility is virtually constant throughout the experiment, since there is a small relative change in pressure during the decay. Thus, $c_g = 1/p \equiv \text{constant}$, which yields the final representation

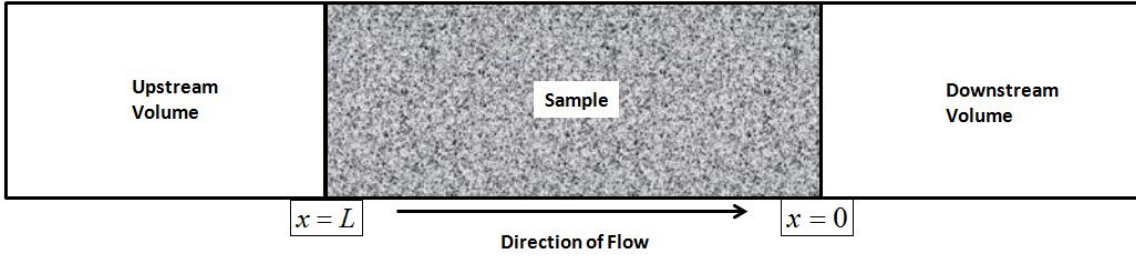


Figure 6.2: Experimental set-up of the pressure pulse permeability method on crushed cores.

of the p^2 diffusion equation as

$$\frac{\partial^2 \psi}{\partial x^2} = \frac{1}{\kappa} \frac{\partial \psi}{\partial t},$$

where $\kappa = \frac{k}{\phi \mu c_g}$.

6.3 Description of the experimental system set-up and development of the initial conditions and boundary conditions for the pressure pulse decay method

Referring to Figure 6.2, we will now describe the experimental set-up and execution of the pressure pulse decay method. The core sample is prepared by fitting it into a sleeve and placing it into a cell. The pressure in the upstream and downstream volumes, V_u and V_d , respectively, as well as the core sample is increased to the level that is required to begin the experiment. The pressures in the core as well as in the upstream and downstream volumes must be given time to equalize before the experiment begins.

A pressure pulse of less than one order of magnitude of that of the equalized pressure is put into the upstream volume. At this time, the core sample and the downstream reservoir are still isolated from the upstream volume by a valve. To begin the experiment, at time $t = 0$, a valve between the upstream volume and the

core is opened and the pressure in the upstream volume causes the gas to expand through the core sample and into the downstream volume. At the instant that the experiment begins, the upstream volume pressure will be denoted by P_{u_i} and the core sample pressure and the downstream volume pressure will be denoted by P_d , where we have that $P_{u_i} > P_d$. The pressure in the upstream volume begins to decay at the instant the valve between it and the core sample is opened. The experiment concludes when the pressure in both the upstream and downstream volumes reach an equilibrium value.

We now turn our attention to setting up the appropriate boundary conditions. The boundary condition at the face of the core, $x = L$, in contact with the upstream volume must consider the pore volume of the sample, denoted by ϕV_s , and the upstream volume, denoted by V_u . This boundary condition has to describe the conservation of mass occurring at the upstream face of the core sample as gas flows from the upstream volume into the core and eventually the downstream volume, resulting in a pressure decrease in the upstream volume. Thus, we have

$$\frac{V_u}{\kappa} \frac{\partial p^2}{\partial t} \Big|_{x=L} + \frac{\phi V_s}{L} \frac{\partial p^2}{\partial x} \Big|_{x=L} = 0, \text{ for } t > 0.$$

Given the above discussion on the boundary condition at the upstream face of the core sample, it is straightforward to define the pressure at the upstream face as a function of time by

$$p_u(t) = p(L, t) \text{ with } p_u(0) = p(L, 0) = P_{u_i},$$

where P_{u_i} denotes the initial pressure in the upstream volume at the instant the experiment begins.

Similarly, the boundary condition at the face of the core, $x = 0$, in contact with the downstream volume must also consider the pore volume of the sample, and the downstream volume, denoted by V_d . This boundary condition has to describe the conservation of mass occurring at the downstream face of the core sample as gas flows from the core sample into the downstream volume, resulting in a pressure increase in the downstream volume. Thus, we have

$$\left. \frac{V_d}{\kappa} \frac{\partial p^2}{\partial t} \right|_{x=0} - \left. \frac{\phi V_s}{L} \frac{\partial p^2}{\partial x} \right|_{x=0} = 0, \text{ for } t > 0.$$

Given the above discussion on the boundary condition at the downstream face of the core sample, it is straightforward to define the pressure at the downstream face as a function of time by

$$p_d(t) = p(0, t) \text{ with } p_d(0) = p(0, 0) = 0.$$

The complete formulation of the IBVP for modeling the pressure pulse decay method in terms of $\psi = p^2$ is thus

$$\frac{\partial^2 \psi}{\partial x^2} - \frac{1}{\kappa} \frac{\partial \psi}{\partial t} = 0, \text{ for } 0 < x < L \text{ and } t > 0, \quad (6.18a)$$

$$\psi(x, 0) = 0, \text{ for } 0 < x < L, \quad (6.18b)$$

$$\psi(0, t) = \psi_d(t) \text{ and } \psi(L, t) = \psi_u(t), \text{ for } t \geq 0,$$

$$\text{where } \psi_d(0) = 0 \text{ and } \psi_u(0) = P_{u_i}^2,$$

$$\left. \frac{LV_d}{\phi \kappa} \frac{\partial \psi}{\partial t} \right|_{x=0} - \left. V_s \frac{\partial \psi}{\partial x} \right|_{x=0} = 0, \text{ for } t > 0, \quad (6.18c)$$

$$\left. \frac{LV_u}{\phi \kappa} \frac{\partial \psi}{\partial t} \right|_{x=L} + \left. V_s \frac{\partial \psi}{\partial x} \right|_{x=L} = 0, \text{ for } t > 0. \quad (6.18d)$$

6.4 Solution to the Mathematical Model

We now proceed to solve the IBVP for modeling the pressure pulse decay method. While the dimensional IBVP (6.18) has a physical significance that is clear due to the fact that it is represented using the original physical variables and parameters, we choose to express and solve the problem using dimensionless variables. The reason is twofold. First, from a purely mathematical point of view it is more succinct and straight forward due to the algebra involved in simplifying the various forms as we progress towards the final representation. Second, numerical computations become easier to implement with dimensionless variables and one of the main uses of the solution will be to compute pressure decay profiles given a set of variables and parameters for specific cases to be modeled.

Using the dimensionless variables

$$x_D = \frac{x}{L}, \quad t_D = \frac{\kappa t}{L^2}, \quad \beta = \frac{\phi V_s}{V_u}, \quad \gamma = \frac{V_d}{V_u},$$

and

$$\psi_D(x_D, t_D) = \frac{\psi(x_D, t_D) - (p_d(0))^2}{(p_u(0))^2 - (p_d(0))^2} = \frac{\psi(x_D, t_D)}{P_{u_i}^2},$$

we represent the dimensional IBVP (6.18) in dimensionless form by

$$\frac{\partial^2 \psi_D}{\partial x_D^2} - \frac{\partial \psi_D}{\partial t_D} = 0, \text{ for } 0 < x_D < 1 \text{ and } t_D > 0, \quad (6.19a)$$

$$\psi_D(x_D, 0) = 0, \text{ for } 0 < x_D < 1, \quad (6.19b)$$

$$\psi_D(0, t_D) = \psi_{Dd}(t_D) \text{ and } \psi_D(1, t_D) = \psi_{Du}(t), \text{ for } t \geq 0,$$

$$\text{where } \psi_{Dd}(0) = 0 \text{ and } \psi_{Du}(0) = 1,$$

$$\frac{V_d}{\phi} \frac{\partial \psi_D}{\partial t_D} \Big|_{x_D=0} - V_s \frac{\partial \psi_D}{\partial x_D} \Big|_{x_D=0} = 0, \text{ for } t_D > 0, \quad (6.19c)$$

$$\frac{V_u}{\phi} \frac{\partial \psi_D}{\partial t_D} \Big|_{x_D=1} + V_s \frac{\partial \psi_D}{\partial x_D} \Big|_{x_D=1} = 0, \text{ for } t_D > 0. \quad (6.19d)$$

We proceed by taking the Laplace transform of (6.19) with respect to t_D . Defining $\Psi_D(x_D, s) := \mathcal{L}\{\psi_D(x_D, t_D)\}(s)$, we obtain

$$\frac{d^2 \Psi_D}{dx_D^2} - s \Psi_D(x_D, s) = 0, \text{ for } 0 < x_D < 1, \quad (6.20a)$$

$$s \Psi_D(0, s) - \frac{\beta}{\gamma} \frac{d \Psi_D}{dx_D} \Big|_{x_D=0} = 0, \quad (6.20b)$$

$$s \Psi_D(1, s) + \beta \frac{d \Psi_D}{dx_D} \Big|_{x_D=1} = 1. \quad (6.20c)$$

The general solution to (6.20a) is given by

$$\Psi_D(x_D, s) = A \cosh(x_D \sqrt{s}) + B \sinh(x_D \sqrt{s}), \text{ for } 0 < x_D < 1.$$

Forcing the boundary conditions we now have the particular solution to (6.20) given by

$$\Psi_D(x_D, s) = \frac{\beta \cosh(\sqrt{s} x_D) + \sqrt{s} \gamma \sinh(\sqrt{s} x_D)}{s \beta (\gamma + 1) \cosh(\sqrt{s}) + \sqrt{s} (\beta^2 + \gamma s) \sinh(\sqrt{s})} \quad (6.21)$$

In order to find the solution in the time domain, we must take the inverse Laplace

transform of $\Psi_D(x_D, s)$ in (6.21) with respect to s . We note that there are countably infinitely many poles for Ψ_D . The poles, denoted by $\{s_n\}_{n=0}^{\infty}$, are all simple poles and occur at $s_0 = 0$ and at the roots of

$$\sqrt{s}\beta(\gamma + 1) \cosh(\sqrt{s}) + (\beta^2 + \gamma s) \sinh(\sqrt{s}) = 0. \quad (6.22)$$

Since all the nonzero roots of (6.22) are along negative real axis, for each pole s_n , there exists a positive real number α_n such that $\sqrt{s_n} = i\alpha_n$, which implies $s_n = -\alpha_n^2$. Thus, we perform the change of variables $s_n \rightarrow -\alpha_n^2$ and obtain

$$f(\alpha_n) := \alpha_n\beta(\gamma + 1) \cos(\alpha_n) + (\beta^2 - \alpha_n^2\gamma) \sin(\alpha_n) = 0. \quad (6.23)$$

The countably infinitely many poles of (6.23) are all simple and are denoted by $\{\alpha_n\}_{n=0}^{\infty}$, where $0 = \alpha_0 < \alpha_1 < \alpha_2, \dots$

Implementing the appropriate residue theory, we now compute the inverse Laplace transform.

$$\begin{aligned} \psi_D(x_D, t_D) &= \mathcal{L}^{-1} \{ \Psi(r_D, s) \} (t_D) \\ &= \frac{1}{2\pi i} \oint_{\{s_n\}} e^{st_D} \Psi(r_D, s) ds \\ &= \frac{1}{2\pi i} \oint_{\{s_n\}} \frac{e^{st_D} (\beta \cosh(\sqrt{s}x_D) + \sqrt{s}\gamma \sinh(\sqrt{s}x_D))}{s\beta(\gamma + 1) \cosh(\sqrt{s}) + \sqrt{s}(\beta^2 + \gamma s) \sinh(\sqrt{s})} ds. \end{aligned}$$

Performing a u -substitution, with $s = -u^2$ and $ds = -2u du$, we obtain

$$\begin{aligned}
\psi_D(x_D, t_D) &= \frac{1}{2\pi i} \oint_{\{\alpha_n\}} \frac{2ue^{-u^2 t_D} (\beta \cos(ux_D) - u\gamma \sin(ux_D))}{u^2 \beta (\gamma + 1) \cos(u) + u(\beta^2 - \gamma u^2) \sin(u)} du \\
&= \frac{1}{2\pi i} \oint_{\{\alpha_n\}} \frac{2e^{-u^2 t_D} (\beta \cos(ux_D) - u\gamma \sin(ux_D))}{u\beta(\gamma + 1) \cos(u) + (\beta^2 - \gamma u^2) \sin(u)} du \\
&= \frac{1}{1 + \beta + \gamma} \\
&\quad + 2 \sum_{n=1}^{\infty} \frac{e^{-\alpha_n^2 t_D} (\beta \cos(\alpha_n x_D) - \alpha_n \gamma \sin(\alpha_n x_D))}{(\beta(\gamma + 1) + \beta^2 - \gamma \alpha_n^2) \cos(\alpha_n) - \alpha_n (\beta(\gamma + 1) + 2\gamma) \sin(\alpha_n)} \\
&= \frac{1}{1 + \beta + \gamma} \\
&\quad + 2 \sum_{n=1}^{\infty} \frac{e^{-\alpha_n^2 t_D} (\cos(\alpha_n x_D) - \alpha_n \gamma / \beta \sin(\alpha_n x_D))}{(1 + \gamma + \beta - \alpha_n^2 \gamma / \beta) \cos(\alpha_n) - \alpha_n (1 + \gamma + 2\gamma / \beta) \sin(\alpha_n)}.
\end{aligned}$$

Recalling that $\psi = P_{u_i}^2 \psi_D = p^2$, we have

$$\begin{aligned}
p(x_D, t_D) &= P_{u_i} \cdot \\
&\sqrt{\frac{1}{1 + \beta + \gamma} + 2 \sum_{n=1}^{\infty} \frac{e^{-\alpha_n^2 t_D} (\cos(\alpha_n x_D) - \alpha_n \gamma / \beta \sin(\alpha_n x_D))}{(1 + \gamma + \beta - \alpha_n^2 \gamma / \beta) \cos(\alpha_n) - \alpha_n (1 + \gamma + 2\gamma / \beta) \sin(\alpha_n)}}.
\end{aligned} \tag{6.24}$$

Note that in (6.24) all the terms in the summation have a decaying exponential function. Thus, after a sufficiently long time, the limiting pressure (i.e. the pressure at all points in the experimental set-up, including both upstream and downstream volume and the core sample), denoted by p_∞ , is given by

$$p_\infty := \lim_{t_D \rightarrow \infty} p(x_D, t_D) = \sqrt{\frac{P_{u_i}^2}{1 + \beta + \gamma}} = \sqrt{\frac{V_u P_{u_i}^2}{V_u + \phi V_s + V_d}}. \tag{6.25}$$

By observing the limiting pressure at the end of the experiment, we can compute

the porosity of the sample by solving (6.25) and obtaining

$$\phi = \frac{V_u P_{u_i}^2 - p_\infty^2 (V_u + V_d)}{p_\infty^2 V_s}.$$

6.5 Comparison of Results

Some preliminary results are shown in Figures 6.3–6.6. In Figure 6.3, we use $\beta = 1$ and $\gamma = \frac{1}{10}$, which simulates the pore space of the sample equal to the upstream volume, but the upstream volume is 10 times the downstream volume. The constants are switched to $\beta = \frac{1}{10}$ and $\gamma = 1$ in Figure 6.4, which simulates the pore volume of the sample is 10 times less than the downstream volume, but the upstream volume is equal to the downstream volume. In Figure 6.5, we use $\beta = \gamma = 1$, which simulates the pore volume of the sample, the upstream volume, and the downstream volume being equal. Finally, in Figure 6.6, we use $\beta = 1$ and $\gamma = 10$, which simulates the pore volume of the sample equal to the upstream volume, but the downstream volume is 10 times the upstream volume.

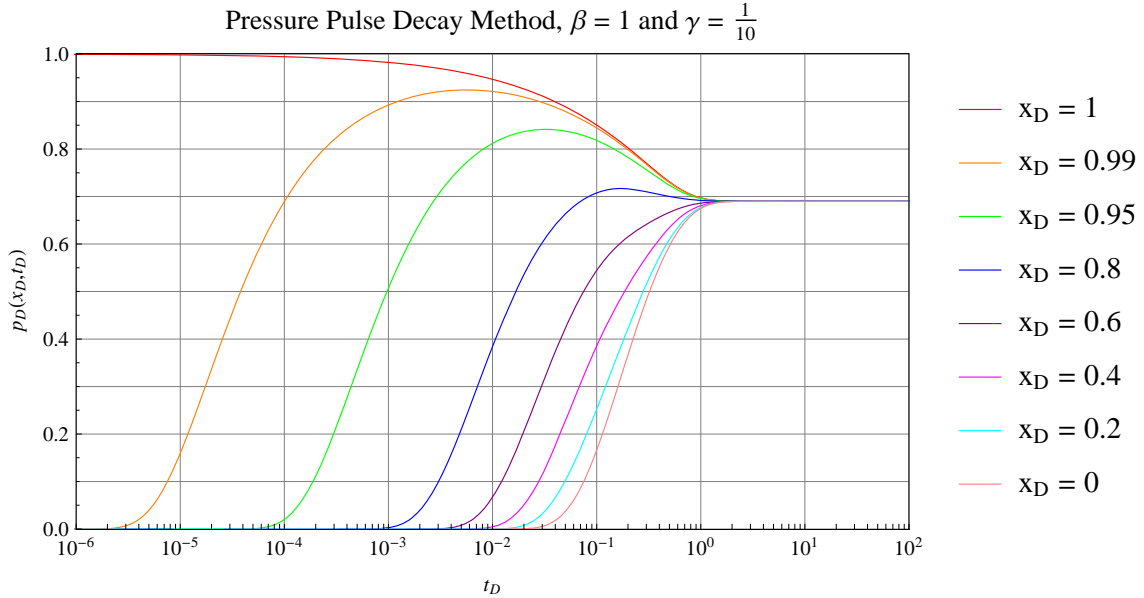


Figure 6.3: Example solution showing gas pressure in the upstream and downstream volumes as well as the pressure at different points in the sample throughout the experiment where $\beta = 1$ and $\gamma = \frac{1}{10}$.

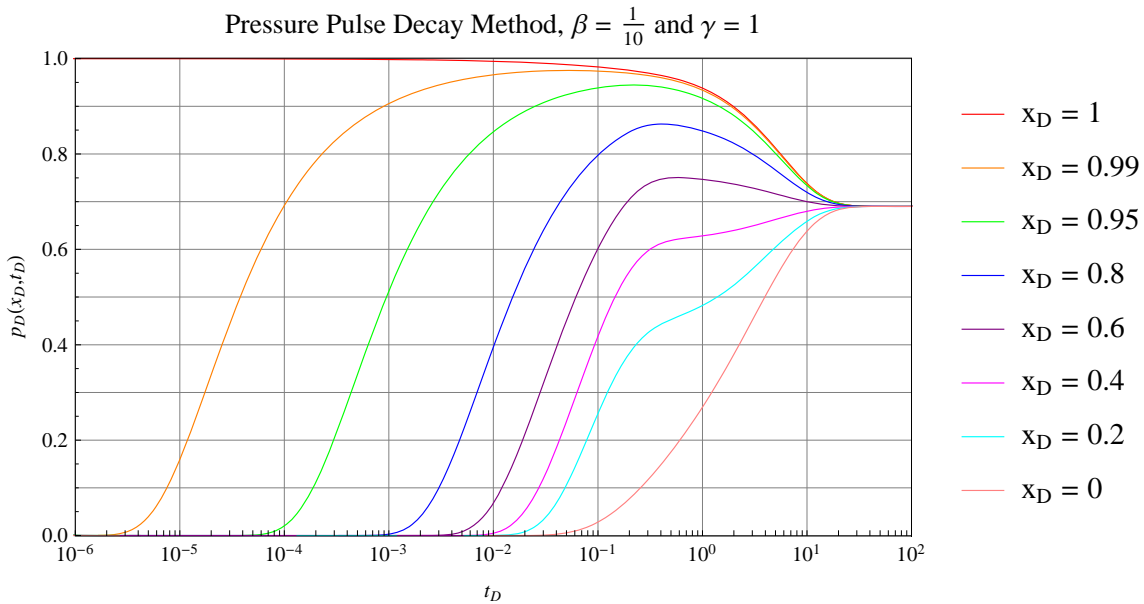


Figure 6.4: Example solution showing gas pressure in the upstream and downstream volumes as well as the pressure at different points in the sample throughout the experiment where $\beta = \frac{1}{10}$ and $\gamma = 1$.

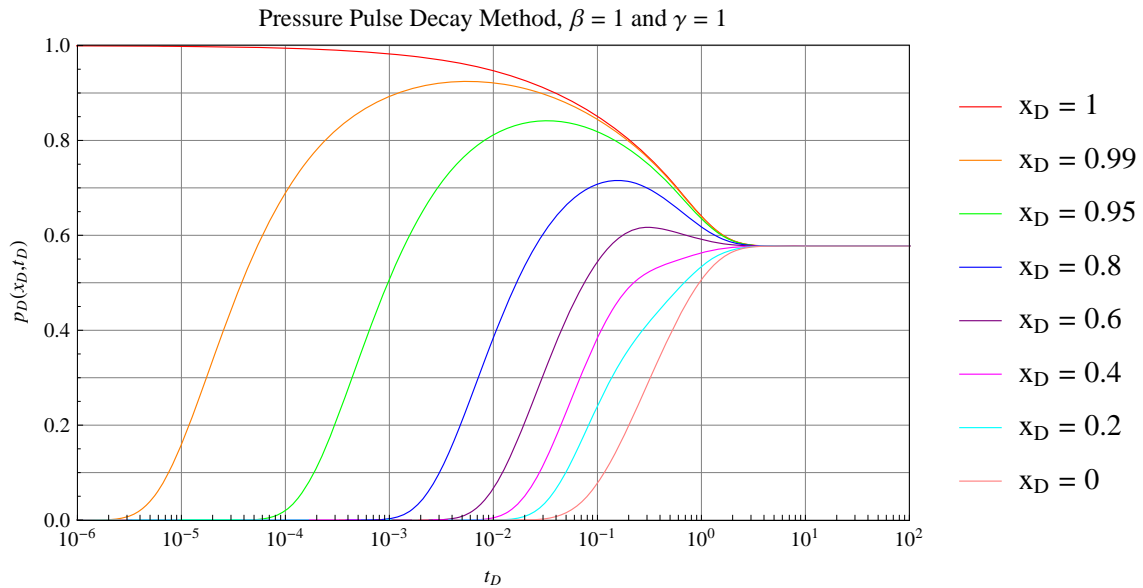


Figure 6.5: Example solution showing gas pressure in the upstream and downstream volumes as well as the pressure at different points in the sample throughout the experiment where $\beta = \gamma = 1$.

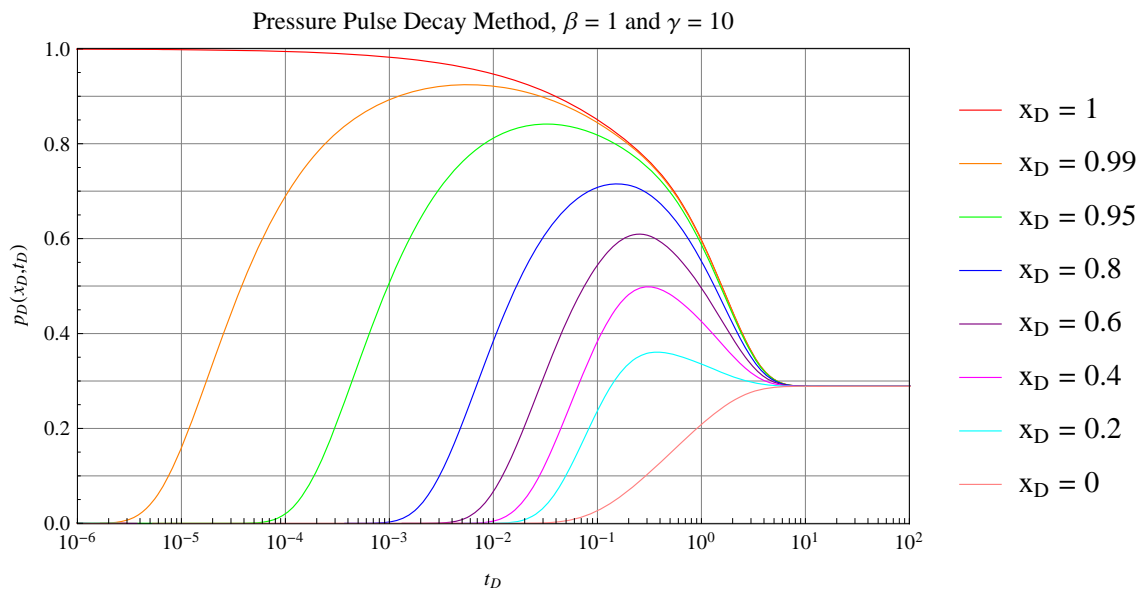


Figure 6.6: Example solution showing gas pressure in the upstream and downstream volumes as well as the pressure at different points in the sample throughout the experiment where $\beta = 1$ and $\gamma = 10$.

7. GRI CRUSHED CORE PERMEABILITY METHOD

The essence of mathematics lies in its freedom.

Georg Cantor (1845–1918)

7.1 Introduction

We begin by deriving from first principles the continuity equation and diffusion equation in the spherical coordinate system. We then derive the appropriate initial conditions and boundary conditions to model the method of pressure pulse permeability on crushed cores. Once the diffusion equation and the proper initial conditions and boundary conditions are developed, we provide a detailed step by step solution via the transform method of Pierre-Simon Laplace. We aim to preserve the spirit of solving the diffusion equation with Bessel functions in the cylindrical coordinate system [33, 51] by employing spherical Bessel functions for our solution in the spherical coordinate system.

7.2 Mathematical Model in the Spherical Coordinate System

To begin, we first derive the continuity equation in the spherical coordinate system. Using the continuity equation that we develop, we combine it with Darcy's law, the real gas law, and some assumptions to obtain the pressure squared (p^2) diffusion equation in the spherical coordinate system. We then discuss the experimental system set-up for the pressure pulse permeability method on crushed cores and derive the appropriate initial conditions and boundary conditions. At the conclusion of this section we will have a properly derived dimensional initial boundary value problem whose solution can be used to model the pressure decay of the gas surrounding the crushed core sample during the entire duration of the test, as well as other significant

results such as the logarithmic derivative of the pressure decay.

7.2.1 Derivation of the continuity equation in the spherical coordinate system

To derive the diffusion equation in spherical coordinates, we must first derive the continuity equation in spherical coordinates. The continuity equation stems from the principle of conservation of mass which states that the net rate of creation or destruction of matter is zero [27]. Considering the spatially fixed control volume in Figure 7.1, we have

$$\begin{aligned} \left[\begin{array}{l} \text{The mass flow rate into} \\ \text{the control volume } \Delta V \\ \text{during the time period } \Delta t. \end{array} \right] & - \left[\begin{array}{l} \text{The mass flow rate out of} \\ \text{the control volume } \Delta V \\ \text{during the time period } \Delta t. \end{array} \right] & (7.1) \\ & = \left[\begin{array}{l} \text{The rate of mass accumulation} \\ \text{in the control volume } \Delta V \\ \text{during the time period } \Delta t. \end{array} \right], \end{aligned}$$

where we assume that there is no mass flow rate into or out of the control volume due to a source or a sink. The mass flow rate into the sphere is given by

$$\frac{dm_{\text{in}}}{dt} = -\rho v_r A_{\text{in}} = -\rho v_r (r + \Delta r)^2 \sin(\theta) \Delta \gamma \Delta \theta, \quad (7.2)$$

while the mass flow rate out of the sphere is given by

$$\frac{dm_{\text{out}}}{dt} = -\rho v_r A_{\text{out}} = -[\rho v_r - \Delta(\rho v_r)] r^2 \sin(\theta) \Delta \gamma \Delta \theta, \quad (7.3)$$

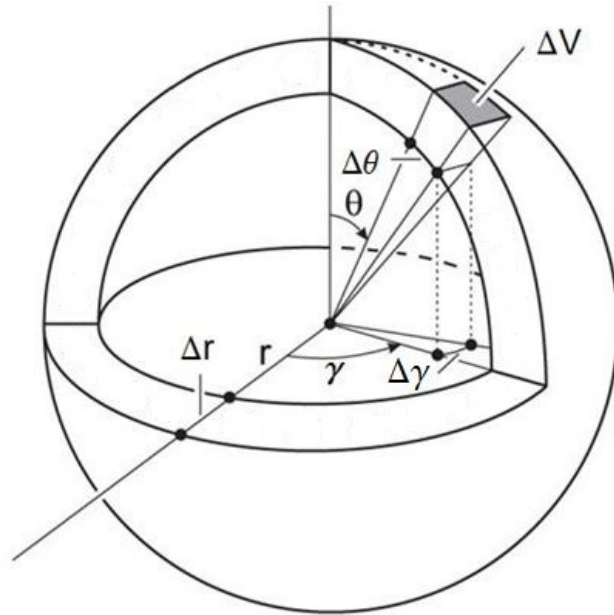


Figure 7.1: Model of spherical crushed core sample showing the spatially fixed control volume ΔV .

where the term $\Delta(\rho v_r)$ is the change in mass flux occurring inside the control volume.

At any instance, the bulk control volume is given by

$$\Delta V = r^2 \sin(\theta) \Delta\gamma \Delta r \Delta\theta, \quad (7.4)$$

the mass control volume is given by

$$\Delta V_p = \Delta V \phi, \quad (7.5)$$

and thus, the mass in the control volume is given by

$$m = \rho \Delta V_p. \quad (7.6)$$

The rate of mass accumulation is the difference in mass in the control volume for the time period t to $t + \Delta t$ over the length of the time period Δt . Thus,

$$m_{\text{acc}} = \frac{|\rho r^2 \sin(\theta) \Delta \gamma \Delta r \Delta \theta \phi|_{t+\Delta t} - |\rho r^2 \sin(\theta) \Delta \gamma \Delta r \Delta \theta \phi|_t}{\Delta t}. \quad (7.7)$$

Combining (7.2), (7.3) and (7.7) and substituting into (7.1), we have

$$\begin{aligned} & \frac{|\rho r^2 \sin(\theta) \Delta \gamma \Delta r \Delta \theta \phi|_{t+\Delta t} - |\rho r^2 \sin(\theta) \Delta \gamma \Delta r \Delta \theta \phi|_t}{\Delta t} \\ &= ((-\rho v_r (2r \Delta r + (\Delta r)^2)) - (\Delta(\rho v_r) r^2)) \sin(\theta) \Delta \gamma \Delta \theta. \end{aligned} \quad (7.8)$$

Dividing (7.8) by the bulk volume ΔV , we obtain

$$\frac{|\rho \phi|_{t+\Delta t} - |\rho \phi|_t}{\Delta t} = -\rho v_r \left(\frac{2}{r} + \frac{\Delta r}{r^2} \right) - \frac{\Delta(\rho v_r)}{\Delta r}. \quad (7.9)$$

Taking the limit of (7.9) as $\Delta r, \Delta t \rightarrow 0$, we finally obtain the continuity equation in the spherical coordinate system

$$-\frac{\partial(\rho \phi)}{\partial t} = \frac{2}{r} \rho v_r + \frac{\partial(\rho v_r)}{\partial r} = \frac{1}{r^2} \left(\frac{\partial}{\partial r} r^2 (\rho v_r) \right). \quad (7.10)$$

7.2.2 Derivation of the diffusion equation in the spherical coordinate system

The form of Darcy's Law that will apply here is given by

$$v_r = -\frac{k}{\mu} \frac{\partial p}{\partial r}. \quad (7.11)$$

Substituting (7.11) into (7.10), we have

$$\frac{\partial(\rho\phi)}{\partial t} = \frac{1}{r^2} \frac{\partial}{\partial r} \left(r^2 \rho \frac{k}{\mu} \frac{\partial p}{\partial r} \right). \quad (7.12)$$

Recall the real gas law

$$pV = znRT, \quad (7.13)$$

where $n = m/M$, m is the mass of the gas and M is the molecular weight of the gas.

We solve (7.13) for density ρ and obtain

$$\rho = \frac{m}{V} = \frac{pM}{zRT}. \quad (7.14)$$

Substituting (7.14) into (7.12), we now have

$$\frac{\partial}{\partial t} \left(\frac{pM\phi}{zRT} \right) = \frac{1}{r^2} \frac{\partial}{\partial r} \left(r^2 \frac{kpM}{\mu zRT} \frac{\partial p}{\partial r} \right). \quad (7.15)$$

Using the fact that M and R are constant and assuming k and T are also constant, we can simplify (7.15) into

$$\begin{aligned} \frac{1}{r^2} \frac{\partial}{\partial r} \left(r^2 \frac{p}{\mu z} \frac{\partial p}{\partial r} \right) &= \frac{1}{k} \frac{\partial}{\partial t} \left(\frac{p\phi}{z} \right) \\ &= \frac{\phi}{k} \frac{\partial}{\partial t} \left(\frac{p}{z} \right) + \frac{p}{z} \frac{\partial \phi}{\partial t} \\ &= \frac{\phi}{k} \frac{\partial}{\partial p} \left(\frac{p}{z} \right) \frac{\partial p}{\partial t} + \frac{p}{z} \frac{\partial \phi}{\partial p} \frac{\partial p}{\partial t} \\ &= \frac{\phi p}{k z} \frac{\partial p}{\partial t} \left(\frac{z}{p} \frac{\partial}{\partial p} \left(\frac{p}{z} \right) + \frac{1}{\phi} \frac{\partial \phi}{\partial p} \right). \end{aligned} \quad (7.16)$$

Recalling the definition of the compressibility of gas in terms of its density and implementing the real gas law (7.14) we have

$$c_g = \frac{1}{\rho} \frac{\partial \rho}{\partial p} = \frac{zRT}{pM} \frac{\partial}{\partial p} \left(\frac{pM}{zRT} \right) = \frac{z}{p} \frac{\partial}{\partial p} \left(\frac{p}{z} \right). \quad (7.17)$$

Assuming no formation (crushed core) compressibility, $c_f = \frac{1}{\phi} \frac{\partial \phi}{\partial p} = 0$ and substituting (7.17) into (7.16), we obtain

$$\frac{1}{r^2} \frac{\partial}{\partial r} \left(r^2 \frac{p}{\mu z} \frac{\partial p}{\partial r} \right) = \frac{\phi c_g}{k} \frac{p}{z} \frac{\partial p}{\partial t}. \quad (7.18)$$

Noting that

$$p \frac{\partial p}{\partial r} = \frac{1}{2} \frac{\partial p^2}{\partial r} \quad \text{and} \quad p \frac{\partial p}{\partial t} = \frac{1}{2} \frac{\partial p^2}{\partial t},$$

we get

$$\frac{1}{r^2} \frac{\partial}{\partial r} \left(r^2 \frac{1}{\mu z} \frac{\partial p^2}{\partial r} \right) = \frac{\phi c_g}{k} \frac{1}{z} \frac{\partial p^2}{\partial t}. \quad (7.19)$$

Assuming the term μz is constant in (7.19), we have

$$\frac{1}{r^2} \frac{\partial}{\partial r} \left(r^2 \frac{\partial \psi}{\partial r} \right) = \frac{\mu \phi c_g}{k} \frac{\partial \psi}{\partial t},$$

where $\psi = p^2$.

One final assumption is made. We assume that the gas compressibility is virtually constant throughout the experiment, since there is such a small overall change in pressure during the decay. Thus, $c_g = 1/p \equiv \text{const}$, which yields the final repre-

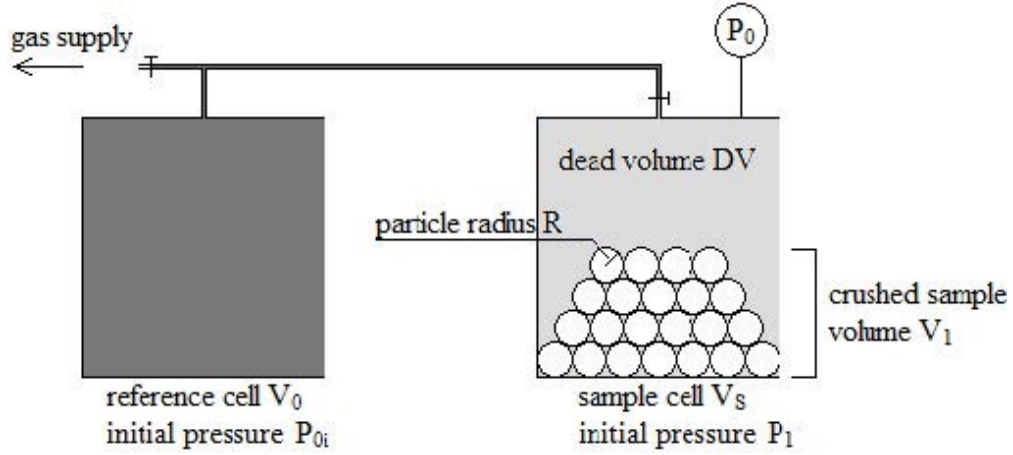


Figure 7.2: Experimental set-up of the pressure pulse permeability method on crushed cores [41].

sentation of the pressure squared diffusion equation as

$$\frac{1}{r^2} \frac{\partial}{\partial r} \left(r^2 \frac{\partial \psi}{\partial r} \right) = \frac{1}{\kappa} \frac{\partial \psi}{\partial t},$$

where $\kappa = \frac{k}{\phi \mu c_g}$.

7.3 Description of the experimental system set-up and development of the initial conditions and boundary conditions for the crushed core permeability method

Referring to Figure 7.2, we will now describe the experimental set-up and execution of the pressure pulse permeability method on crushed cores. The reference cell with volume V_0 contains gas at an initial pressure P_{0i} that is higher than the initial pressure P_1 sample cell of volume V_s . The volume of the sample cell is the sum of the dead volume V_d (denoted by DV in Figure 7.2) and the volume of the particles V_1 . The particles are assumed to be spherical in shape, with radius R . The number

of spherical particles n in the sample cell is calculated by

$$n = \frac{3V_1}{4\pi R^3}.$$

At the beginning of the experiment the valve located just above the sample cell is opened and instantaneously the pressures in the reference cell and the sample cell equalize to the pressure P_0 , indicated by the pressure gauge attached to the sample cell in Figure 7.2. The value of P_0 is computed using a Boyle-Mariotte pressure-volume assumption to obtain

$$P_0 = \frac{P_{0i}V_0 + P_1V_d}{V_0 + V_d}.$$

Thus, the initial pressure condition at time $t = 0$ for each of the n spheres in the sample cell is P_1 , for any distance $0 \leq r < R$ inside the sphere, while the initial pressure condition at time $t = 0$ for each of the n spheres in the sample cell is P_0 , on the exterior of the sphere $r = R$ is P_0 . We note that the pressure on the exterior of the spheres for all time $t \geq 0$ is also the pressure that is recorded by the pressure gauge and is used to indicate the pressure decay as time goes on.

We now turn our attention to setting up the appropriate boundary conditions on each of the n spheres in the sample cell. The interior boundary condition at $r = 0$ is for each sphere is a no-flow boundary condition

$$r^2 \frac{d\psi}{dr} = 0$$

which is relatively easy to derive because at the center of the sphere there will simply be no flow. The exterior boundary condition requires a little more work.

Consulting [10] and making the appropriate changes to a pressure diffusion equa-

tion instead of a heat diffusion equation, we have that the incremental change in pressure δp in the incremental time δt is given by

$$Q\delta t - H(p - p_0)\delta t - K\delta t \int \int \frac{dp}{dn} dS = S_t \delta p,$$

which implies

$$H(p - p_0) + 4\pi R^2 K \frac{dp}{dr} + S_t \frac{dp}{dt} - Q = 0.$$

Above Q is an external source of volume per unit time, H is a volumetric rate per unit pressure, $K = \frac{k}{\mu}$ is the conductivity of the sample, and $K \int \int \frac{dp}{dn} dS = 4\pi R^2 K \frac{dp}{dr}$ is the rate of flow of pressure over the surface area of a sphere of radius R , with units of volume per unit time. The parameter $S_t := V_t c_g$ is the compressive storage, with units of volume per unit pressure, of the total open space volume $V_t := V_0 + V_d$, and $\frac{dp}{dt}$ is the rate of change of pressure per unit time. Since we do not lose any pressure to an outside source via radiation and we do not have an external pressure source during the experiment, both H and Q are zero, respectively. We do, however, have a rate of flow of pressure over the surface area of a sphere of radius R which is equal to the loss of volume pressure per unit time. Thus, the exterior boundary condition at $r = R$ is

$$4\pi R^2 K \frac{dp}{dr} + S_t \frac{dp}{dt} = 0,$$

which, in terms of $\psi = p^2$, is equivalent to

$$4\pi R^2 \frac{k}{\mu} \frac{d\psi}{dr} + V_t c_g \frac{d\psi}{dt} = 0.$$

Further simplifying, we can now write the exterior boundary condition as

$$4\pi R^2 \kappa \frac{d\psi}{dr} + \frac{1}{\phi} V_t \frac{d\psi}{dt} = 0.$$

The complete formulation of the initial boundary value problem for modeling the pressure pulse permeability method on crushed cores is thus

$$\frac{1}{r^2} \frac{\partial}{\partial r} \left(r^2 \frac{\partial \psi}{\partial r} \right) = \frac{1}{\kappa} \frac{\partial \psi}{\partial t} \quad (7.20a)$$

$$\psi(r, 0) = P_1^2, \quad 0 \leq r < R, \quad (7.20b)$$

$$\psi(r, 0) = P_0^2, \quad r = R, \quad (7.20c)$$

$$r^2 \frac{\partial \psi}{\partial r} \Big|_{r=0} = 0, \quad 4\pi r^2 \kappa \frac{\partial \psi}{\partial r} \Big|_{r=R} + \frac{1}{\phi} V_t \frac{\partial \psi}{\partial t} \Big|_{r=R} = 0. \quad (7.20d)$$

7.4 Solution to the Mathematical Model

We now proceed to solve the initial boundary value problem for modeling the pressure pulse permeability method on crushed cores. While the dimensional initial boundary value problem (7.20) has a physical significance that is clear due to the fact that it is represented using the original physical variables and parameters, we choose to express and solve the problem using dimensionless variables. The reason is twofold. First, from a purely mathematical point of view it is more succinct and straight forward due to the algebra involved in simplifying the various forms as we progress towards the final representation. Second, numerical computations become easier to implement with dimensionless variables and one of the main uses of the solution will be to compute pressure decay profiles given a set of variables and parameters for specific cases to be modeled.

Using the dimensionless variables

$$r_D = \frac{r}{R}, \quad t_D = \frac{\kappa t}{R^2}, \quad \text{and} \quad \psi_D(r_D, t_D) = \frac{\psi(r_D, t_D) - P_1^2}{P_0^2 - P_1^2},$$

we represent the dimensional initial boundary value problem (7.20) in dimensionless form by

$$\frac{1}{r_D^2} \frac{\partial}{\partial r_D} \left(r_D^2 \frac{\partial \psi_D}{\partial r_D} \right) = \frac{\partial \psi_D}{\partial t_D} \quad (7.21a)$$

$$\psi_D(r_D, 0) = 0, \quad 0 \leq r_D < 1 \quad (7.21b)$$

$$\psi_D(r_D, 0) = 1, \quad r_D = 1, \quad (7.21c)$$

$$r_D^2 \frac{\partial \psi_D}{\partial r_D} \Big|_{r_D=0} = 0, \quad (7.21d)$$

$$r_D^2 \frac{\partial \psi_D}{\partial r_D} \Big|_{r_D=1} + \frac{C_D}{\phi} \frac{\partial \psi_D}{\partial t_D} \Big|_{r_D=1} = 0, \quad (7.21e)$$

where we define the dimensionless volume ratio by

$$C_D := \frac{V_t}{3V_1} \quad (7.22)$$

We proceed by taking the Laplace transform of (7.21) with respect to t_D . Defining $\Psi_D(r_D, s) := \mathcal{L}\{\psi_D(r_D, t_D)\}(s)$, we obtain

$$\frac{1}{r_D^2} \frac{d}{dr_D} \left(r_D^2 \frac{d\Psi_D}{dr_D} \right) = (s\Psi_D(r_D, s) - \psi_D(r_D, 0)) \quad (7.23a)$$

$$r_D^2 \frac{d\Psi_D}{dr_D} \Big|_{r_D=0} = 0, \quad (7.23b)$$

$$r_D^2 \frac{d\Psi_D}{dr_D} \Big|_{r_D=1} + \frac{C_D}{\phi} (s\Psi_D(r_D, s) - \psi_D(r_D, 0)) \Big|_{r_D=1} = 0. \quad (7.23c)$$

The general solution to (7.23a) is given by

$$\Psi(r, s) = A i_0(r_D \sqrt{s}) + B k_0(r_D \sqrt{s}),$$

where i_0 and k_0 are the modified spherical Bessel functions of order zero the first and second kind, respectively. Forcing the interior boundary condition we see that $B = 0$ to avoid the singularity at $r_D = 0$ and thus

$$\Psi(r_D, s) = A i_0(r_D \sqrt{s}).$$

Forcing the exterior boundary condition we see that the particular solution to (7.23) is given by

$$\Psi(r_D, s) = \frac{i_0(r_D \sqrt{s}) C_D}{\phi \sqrt{s} i_1(\sqrt{s}) + s i_0(\sqrt{s}) C_D}$$

In order to find the solution in the time domain, we must take the inverse Laplace transform of $\Psi_D(r_D, s)$ in (7.23) with respect to s . We note that there are countably infinitely many poles for Ψ_D . The poles, denoted by $\{s_n\}_{n=0}^{\infty}$, are all simple poles and occur at $s_0 = 0$ and at the roots of

$$\phi i_1(\sqrt{s}) + \sqrt{s} i_0(\sqrt{s}) C_D \tag{7.24}$$

Since all the nonzero poles of (7.24) are along the negative axis, for each pole s_n , $0 < n < \infty$, there exists a positive real number α_n such that $\sqrt{s_n} = i\alpha_n$, which implies $s_n = -\alpha_n^2$. Thus, we perform the change of variables $s_n \rightarrow -\alpha_n^2$ and obtain

$$\phi j_1(\alpha) + \alpha j_0(\alpha) C_D, \tag{7.25}$$

where j_0 and j_1 are the spherical Bessel functions of the first kind of order zero and

one, respectively. The countably infinitely many poles of (7.25) are all simple and are denoted by $\{\alpha_n\}_{n=0}^{\infty}$, where $0 = \alpha_0 < \alpha_1 < \alpha_2, \dots$

Implementing the appropriate residue theory, we now compute the inverse Laplace transform.

$$\begin{aligned}\psi_D(r_D, t_D) &= \mathcal{L}^{-1} \{ \Psi(r_D, s) \} (t_D) \\ &= \frac{1}{2\pi i} \oint_{\{s_n\}} e^{st_D} \Psi(r_D, s) ds \\ &= \frac{1}{2\pi i} \oint_{\{s_n\}} \frac{e^{st_D} i_0(r_D \sqrt{s}) C_D}{\phi \sqrt{s} i_1(\sqrt{s}) + s i_0(\sqrt{s}) C_D} ds.\end{aligned}$$

Performing a u -substitution, with $s = -u^2$ and $ds = -2u du$, we obtain

$$\begin{aligned}\psi_D(r_D, t_D) &= \frac{1}{2\pi i} \oint_{\{\alpha_n\}} \frac{-2ue^{-u^2 t_D} i_0(r_D \sqrt{-u^2}) C_D}{\phi \sqrt{-u^2} i_1(\sqrt{-u^2}) + -u^2 i_0(\sqrt{-u^2}) C_D} du \\ &= \frac{1}{2\pi i} \oint_{\{\alpha_n\}} \frac{-2ue^{-u^2 t_D} i_0(ir_D u) C_D}{\phi iu i_1(iu) - u^2 i_0(iu) C_D} du \\ &= \frac{1}{2\pi i} \oint_{\{\alpha_n\}} \frac{2ue^{-u^2 t_D} j_0(r_D u) C_D}{\phi u j_1(u) + u^2 j_0(u) C_D} du \\ &= \sum_{n=0}^{\infty} \text{Res} \left[2ue^{-u^2 t_D} \Psi(r_D, -u^2), \alpha_n \right] \\ &= \frac{3C_D}{\phi + 3C_D} + 2 \sum_{n=1}^{\infty} \frac{e^{-\alpha_n^2 t_D} j_0(r_D \alpha_n) C_D}{(3C_D + \phi) j_0(\alpha_n) - \alpha_n C_D j_1(\alpha_n)}.\end{aligned}$$

Thus, we may now define dimensionless pressure by

$$p_D(r_D, t_D) := \sqrt{\psi_D(r_D, t_D)}. \quad (7.26)$$

Recalling the definition of C_D in (7.22) and that $\psi(r_D, t_D) = P_1^2 + (P_0^2 - P_1^2) \psi_D(r_D, t_D)$,

Table 7.1: Parameters used to model the pressure decay in the GRI Topical Report 93/0297 [29].

Parameter	Value	Units
bulk density	2.54	g/cc
sample mass	30	g
V_1	11.811	cc
k	1×10^{-7}	md
ϕ	0.0214	—
R	0.335	mm
V_d	11.339	cc
P_1	101008	Pa
P_{0i}	1479960	Pa
P_0	695474	Pa
V_0	8.592	cc
μ	1.863×10^{-6}	cp
c_g	1.4379×10^{-8}	Pa^{-1}
n	75000.6	—

we have the solution

$$\psi(r_D, t_D) = P_1^2 + \frac{V_t(P_0^2 - P_1^2)}{\phi V_1 + V_t} + 2 \sum_{n=1}^{\infty} \frac{e^{-\alpha_n^2 t_D} j_0(r_D \alpha_n) V_t (P_0^2 - P_1^2)}{(V_t + 3V_1 \phi) j_0(\alpha_n) - \alpha_n V_t j_1(\alpha_n)}.$$

Finally, recalling $r_D = \frac{r}{R}$ and $t_D = \frac{\kappa t}{R^2}$, we have

$$\psi(r, t) = P_1^2 + \frac{V_t(P_0^2 - P_1^2)}{\phi V_1 + V_t} + 2 \sum_{n=1}^{\infty} \frac{e^{-\alpha_n^2 \frac{\kappa t}{R^2}} j_0(\frac{r}{R} \alpha_n) V_t (P_0^2 - P_1^2)}{(V_t + 3V_1 \phi) j_0(\alpha_n) - \alpha_n V_t j_1(\alpha_n)},$$

which implies that the definition of the dimensional pressure is

$$p(r, t) := \sqrt{\psi(r, t)}. \quad (7.27)$$

Table 7.2: Parameters used to model the pressure decay in Profice [41].

Parameter	Value	Units
V_1	75×10^{-6}	m^3
k	1×10^{-18}	md
ϕ	0.1	—
R	10	mm
V_d	26.5×10^{-6}	m^3
P_1	1×10^5	Pa
P_{0i}	1×10^6	Pa
P_0	487097	Pa
V_0	20×10^{-6}	m^3
μ	1.863×10^{-6}	cp
c_g	2.12658×10^{-6}	Pa^{-1}
n	18	—

7.5 Comparison of Results

Since actual pressure versus time data was not available, the solution plots of pressure versus time in [29,41] were digitized as accurately and precisely as possible. The digitized values were then used as a comparison for our results.

To begin, we refer to Figure 7.3. The data that is available in the literature is sparse, so certain parameters had to be estimated with a swag. The values for the necessary parameters are given by Table 7.1. By inspection, there is a very good agreement between the estimated [7] GRI model and the GRI observed data when compared with the model developed in this paper.

We now turn our attention to Figure 7.4. All the required data for this experiment was provided in [41]. The values for the necessary parameters are restated in Table 7.2. There is excellent agreement between the solution derived in this paper when compared to the digitized data set [7] that was estimated from [41].

Figure 7.5 demonstrates an interesting plot of dimensionless pressure versus di-

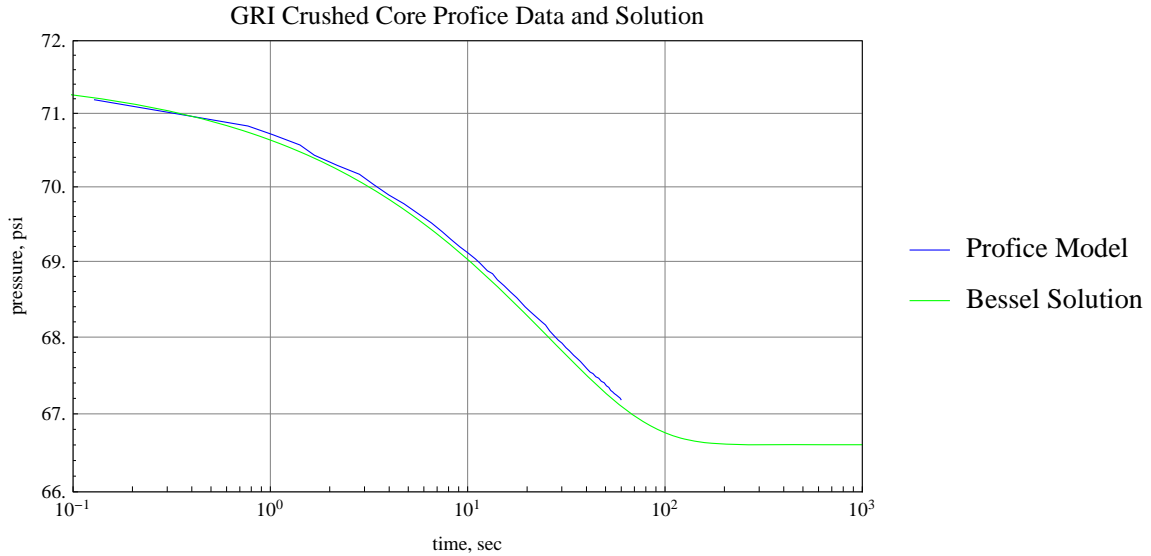


Figure 7.3: Comparison of digitized GRI Model [29] and digitized GRI data [29], and the dimensional solution (7.27).

mensionless time behavior of the sphere at different radii. It is interesting to note that at shallower depths into the sphere the pressure increases sharply to a value that is greater than the limiting pressure of $p_\infty := \sqrt{\frac{3C_D}{\phi+3C_D}}$, then decays to the limit as time progresses, while at deeper depths into the sphere the pressure is always increasing towards the limiting pressure.

To complete the analysis of the GRI crushed core permeability method, type curves will be generated and shown below in Figures 7.6–7.15. In Figures 7.16–7.23 below, we examine the behavior of the ratio of dimensionless pressure to the limiting pressure p_D/p_∞ versus dimensionless time t_D . The following curves show the sensitivity of the method to changes in permeability, porosity, and C_D . The range of C_D is $\frac{1}{256} \leq C_D \leq 2$ and the range of porosity is $0.005 \leq \phi \leq 0.05$.

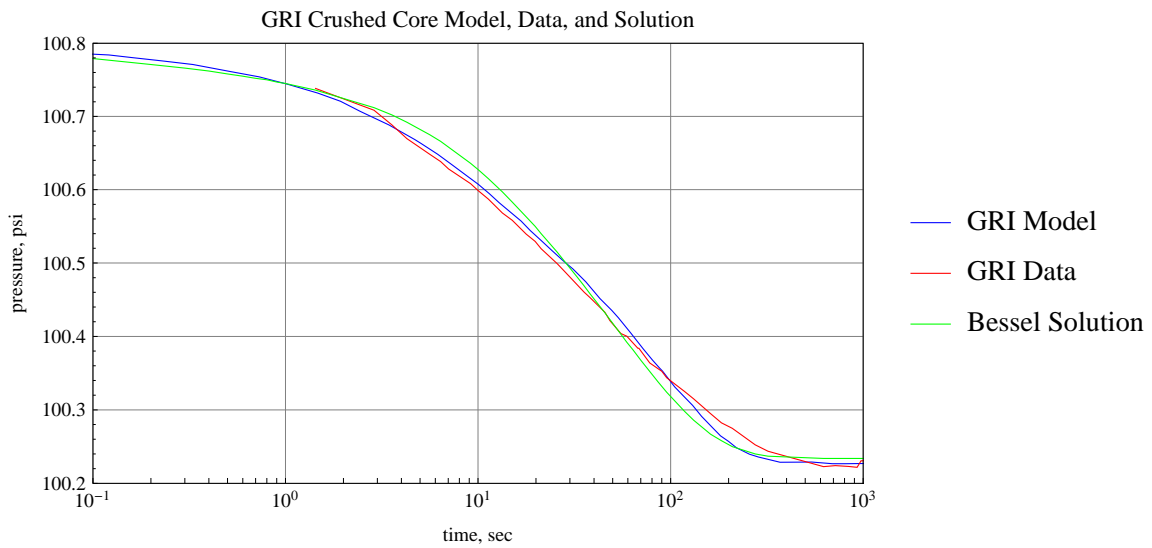


Figure 7.4: Comparison of digitized data [41] and the dimensional solution (7.27).

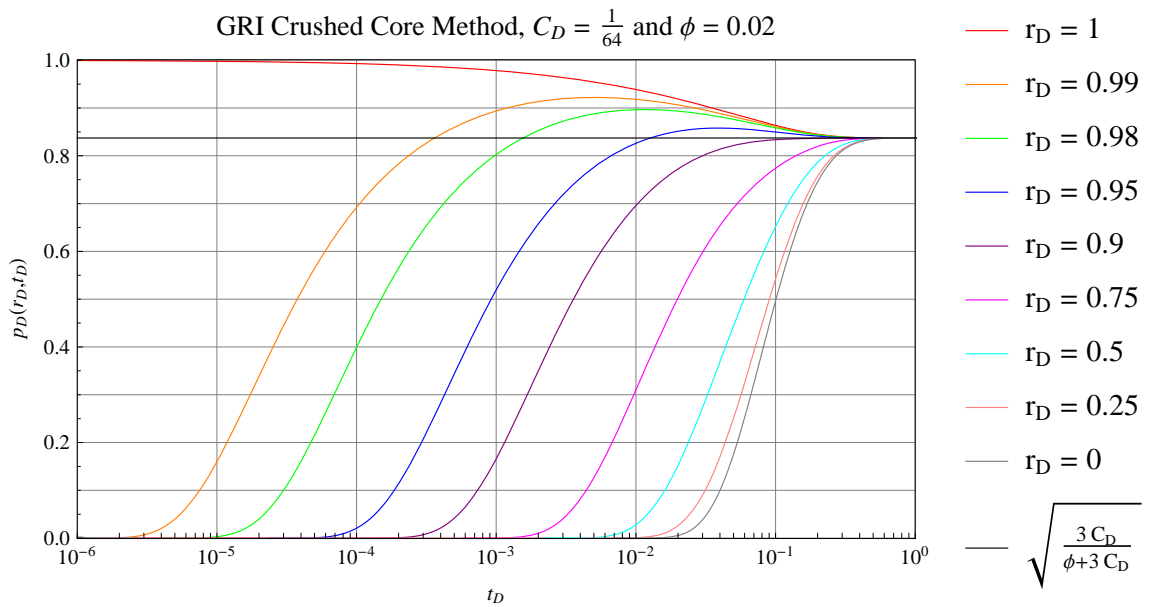


Figure 7.5: Interesting pressure v. time behavior at multiple radii using the dimensionless solution (7.26).

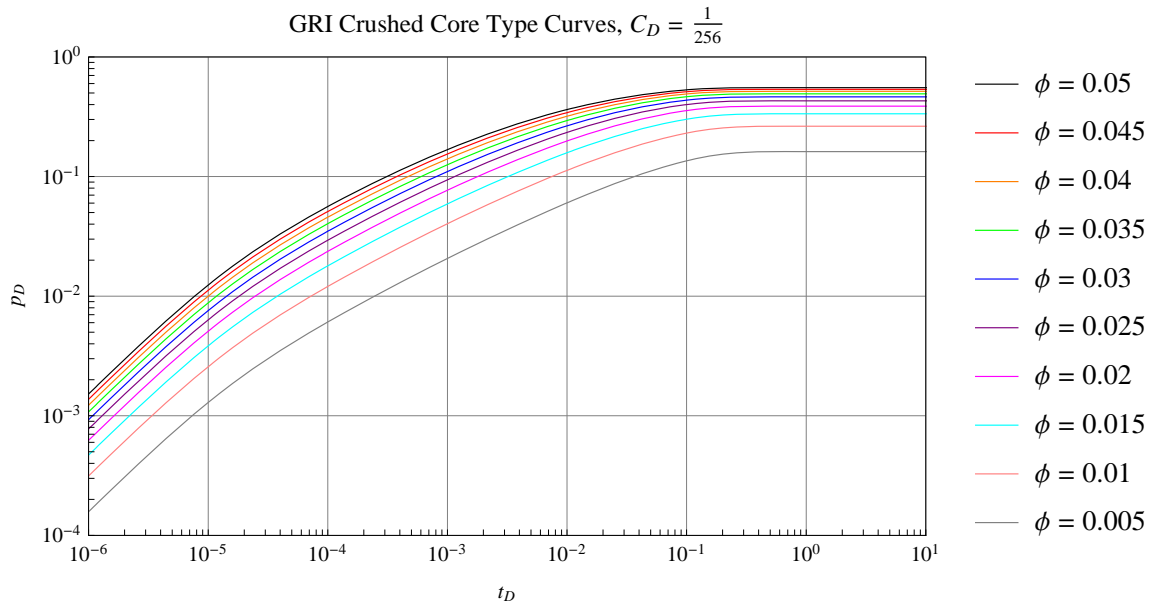


Figure 7.6: GRI method type curve for the dimensionless volume ratio $C_D = \frac{1}{256}$.

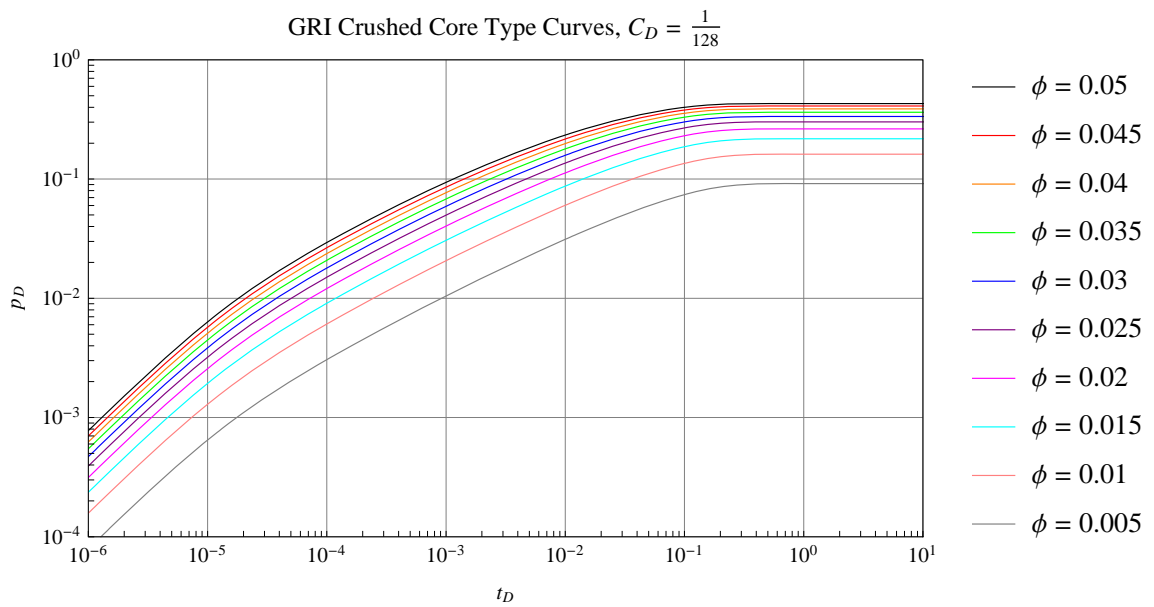


Figure 7.7: GRI method type curve for the dimensionless volume ratio $C_D = \frac{1}{128}$.

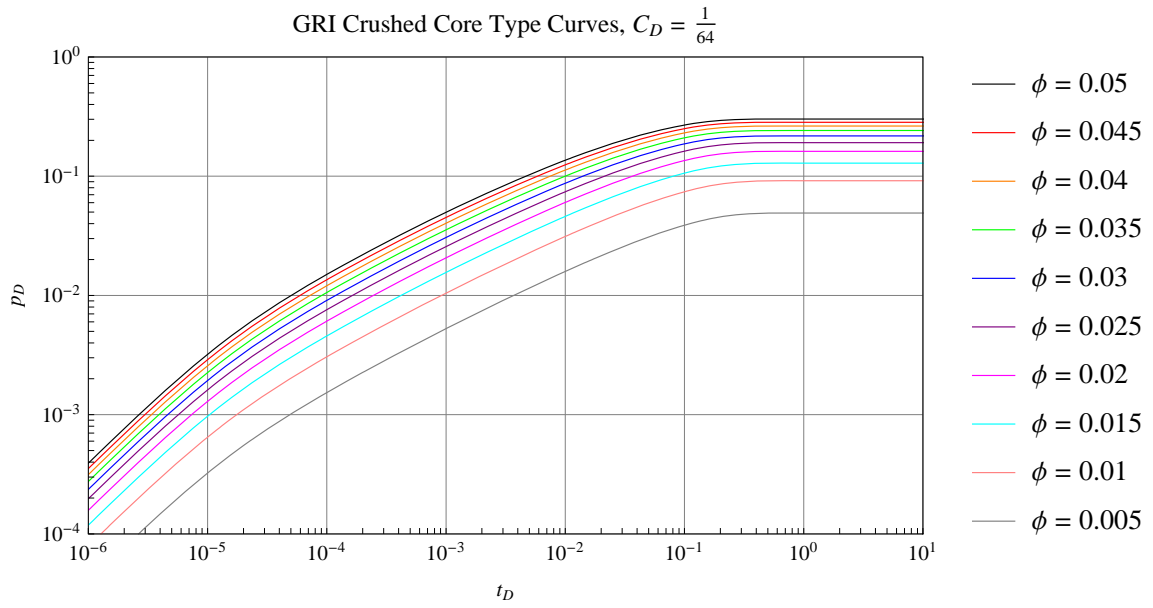


Figure 7.8: GRI method type curve for the dimensionless volume ratio $C_D = \frac{1}{64}$.

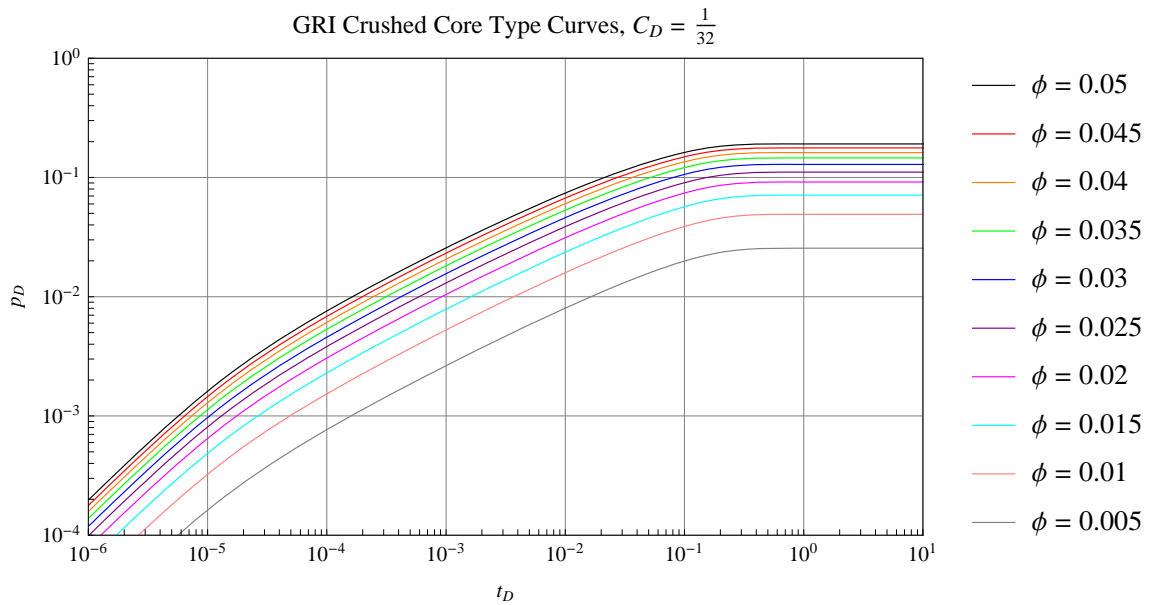


Figure 7.9: GRI method type curve for the dimensionless volume ratio $C_D = \frac{1}{32}$.

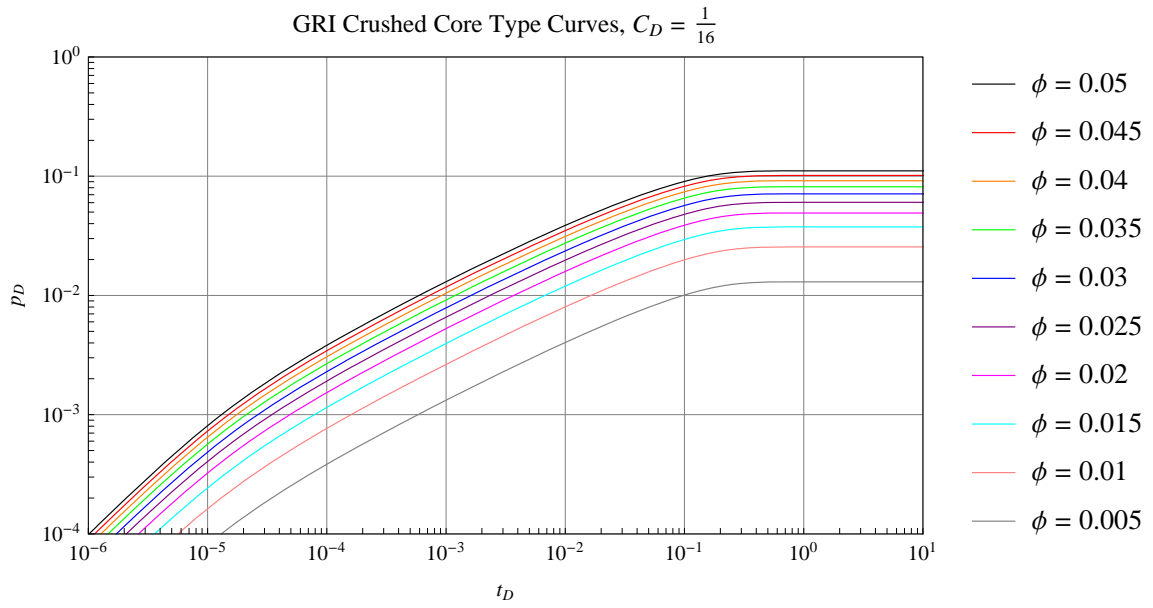


Figure 7.10: GRI method type curve for the dimensionless volume ratio $C_D = \frac{1}{16}$.

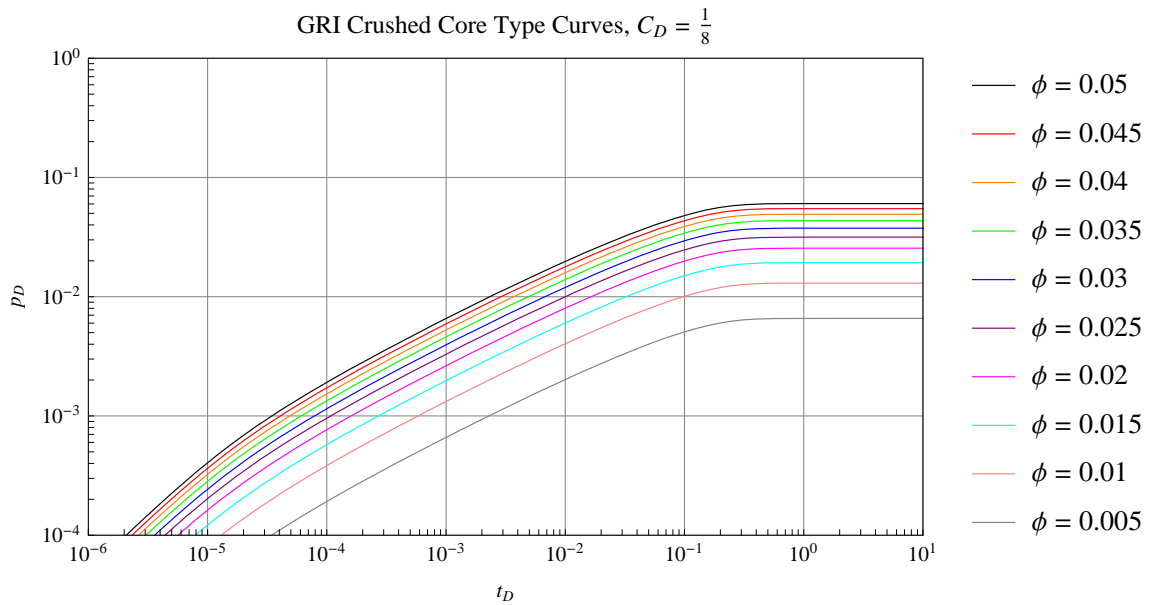


Figure 7.11: GRI method type curve for the dimensionless volume ratio $C_D = \frac{1}{8}$.

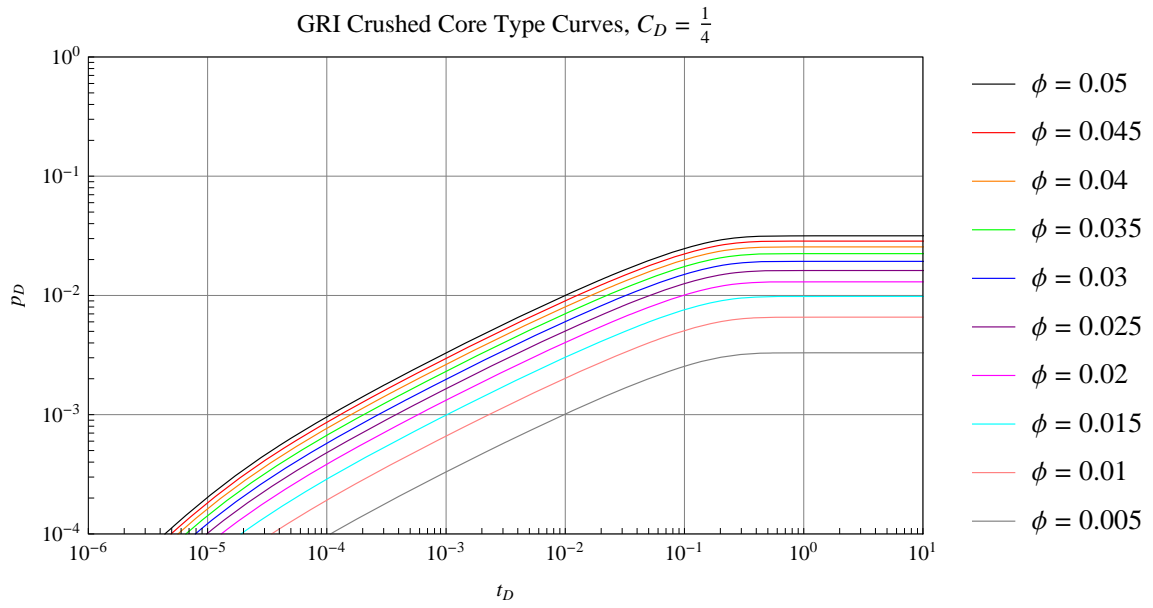


Figure 7.12: GRI method type curve for the dimensionless volume ratio $C_D = \frac{1}{4}$.

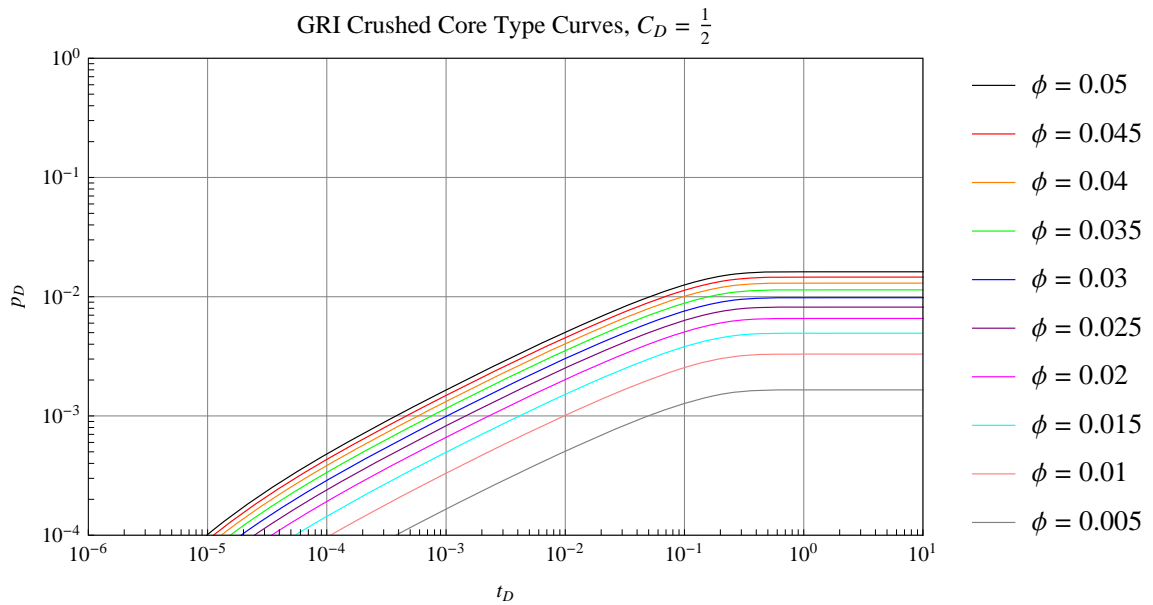


Figure 7.13: GRI method type curve for the dimensionless volume ratio $C_D = \frac{1}{2}$.

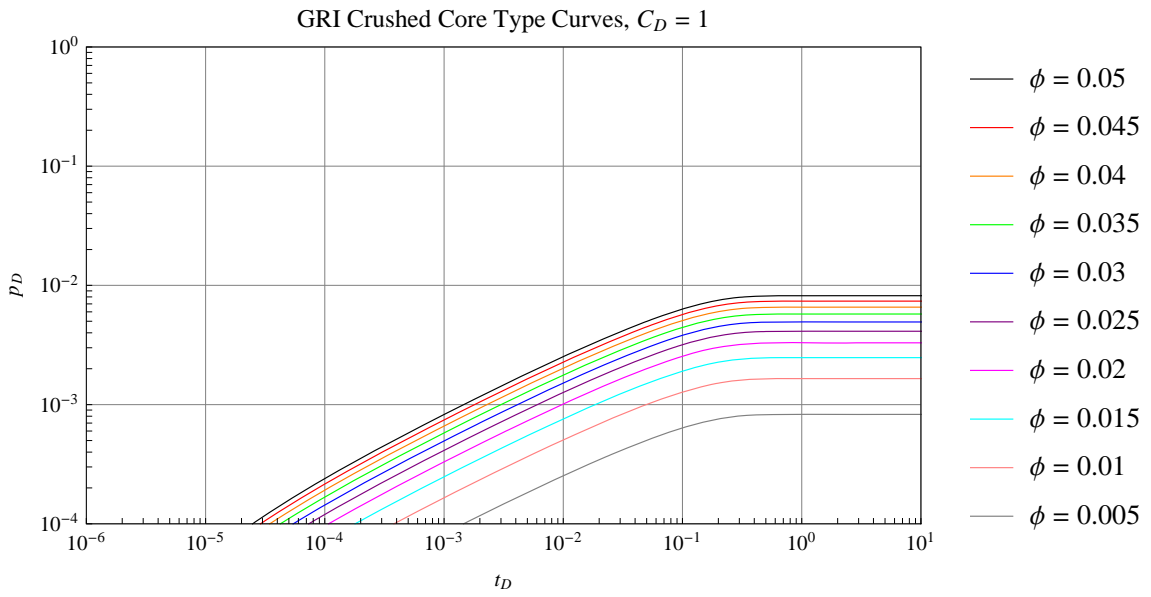


Figure 7.14: GRI method type curve for the dimensionless volume ratio $C_D = 1$.

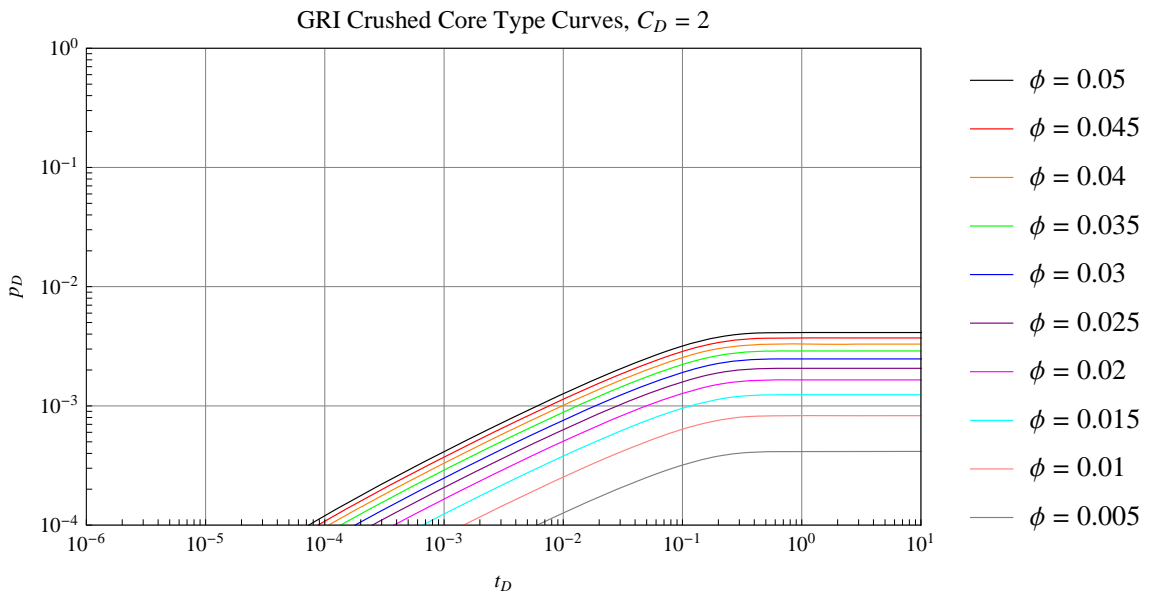


Figure 7.15: GRI method type curve for the dimensionless volume ratio $C_D = 2$.

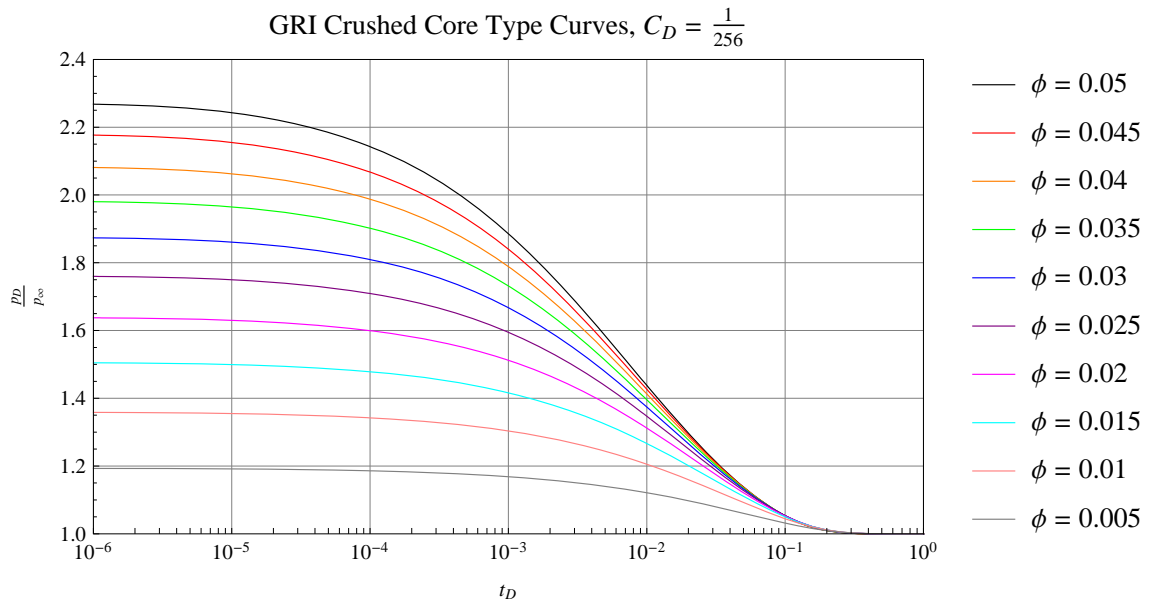


Figure 7.16: GRI method type curve using $\frac{pD}{p_\infty}$ for the dimensionless volume ratio $C_D = \frac{1}{256}$.

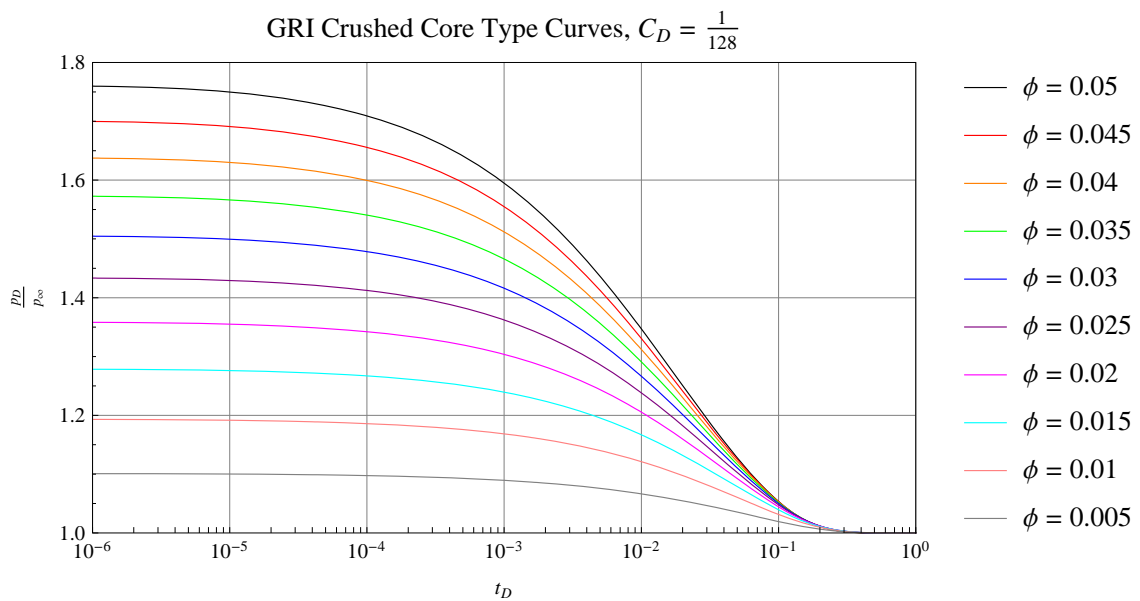


Figure 7.17: GRI method type curve using $\frac{pD}{p_\infty}$ for the dimensionless volume ratio $C_D = \frac{1}{128}$.

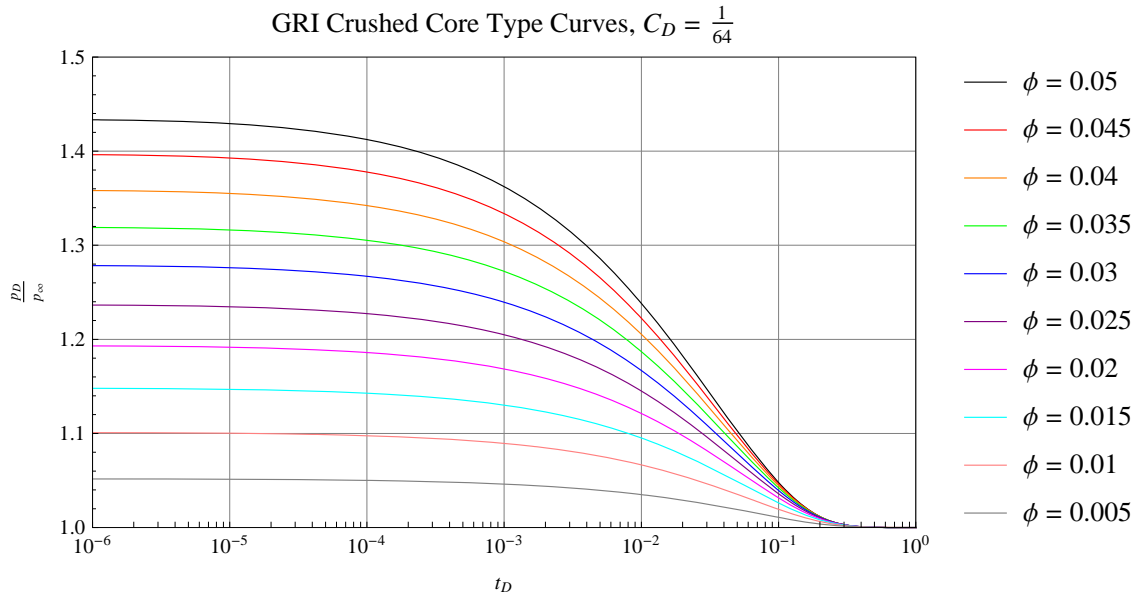


Figure 7.18: GRI method type curve using $\frac{p_D}{p_\infty}$ for the dimensionless volume ratio $C_D = \frac{1}{64}$.

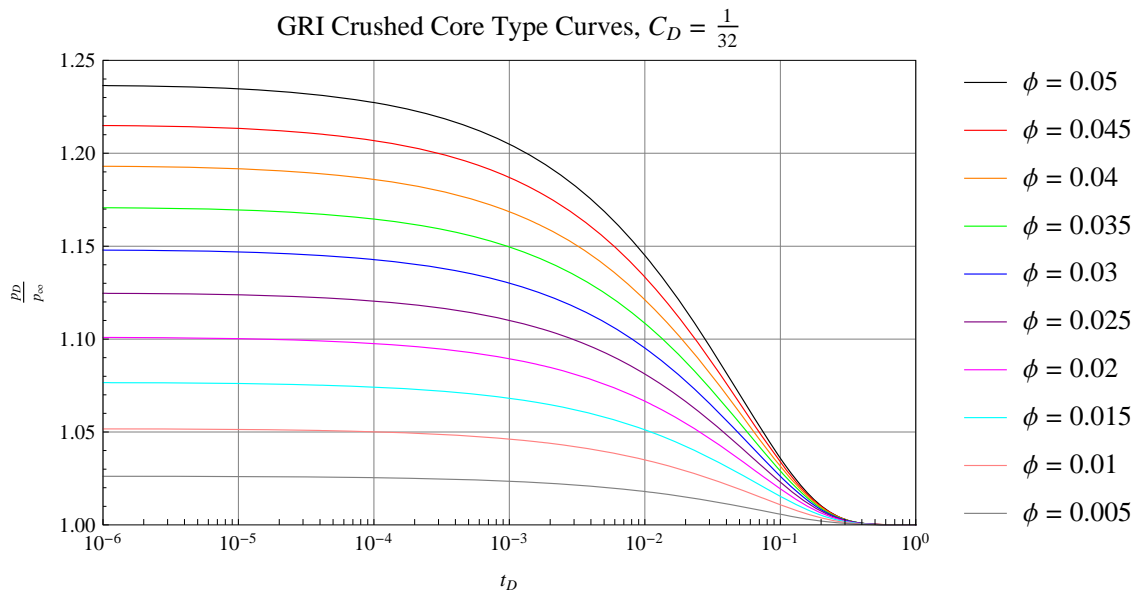


Figure 7.19: GRI method type curve using $\frac{p_D}{p_\infty}$ for the dimensionless volume ratio $C_D = \frac{1}{32}$.

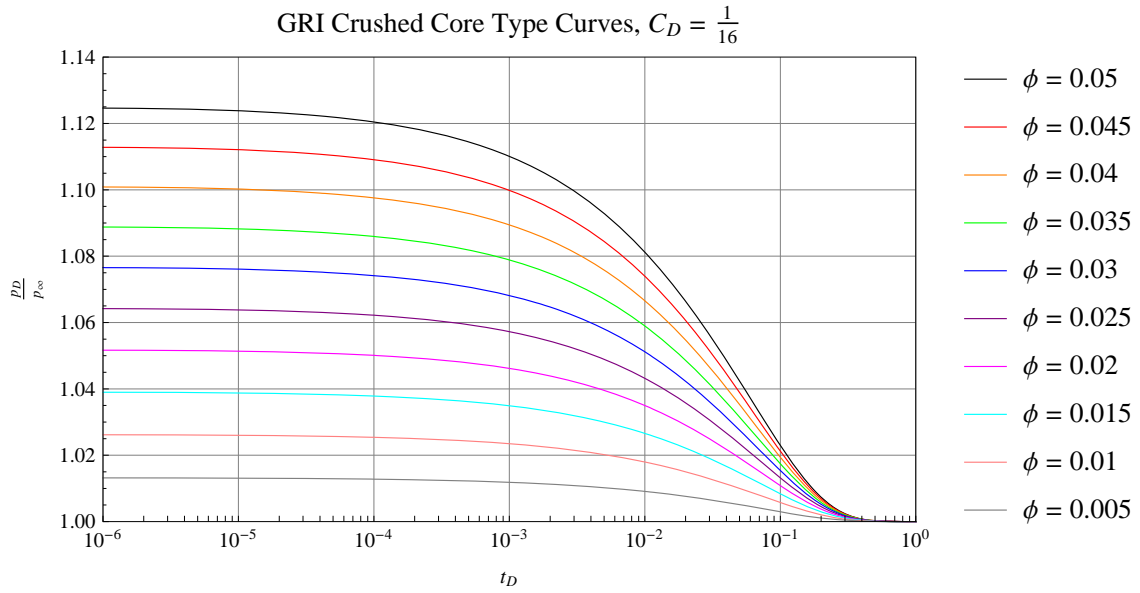


Figure 7.20: GRI method type curve using $\frac{p_D}{p_\infty}$ for the dimensionless volume ratio $C_D = \frac{1}{16}$.

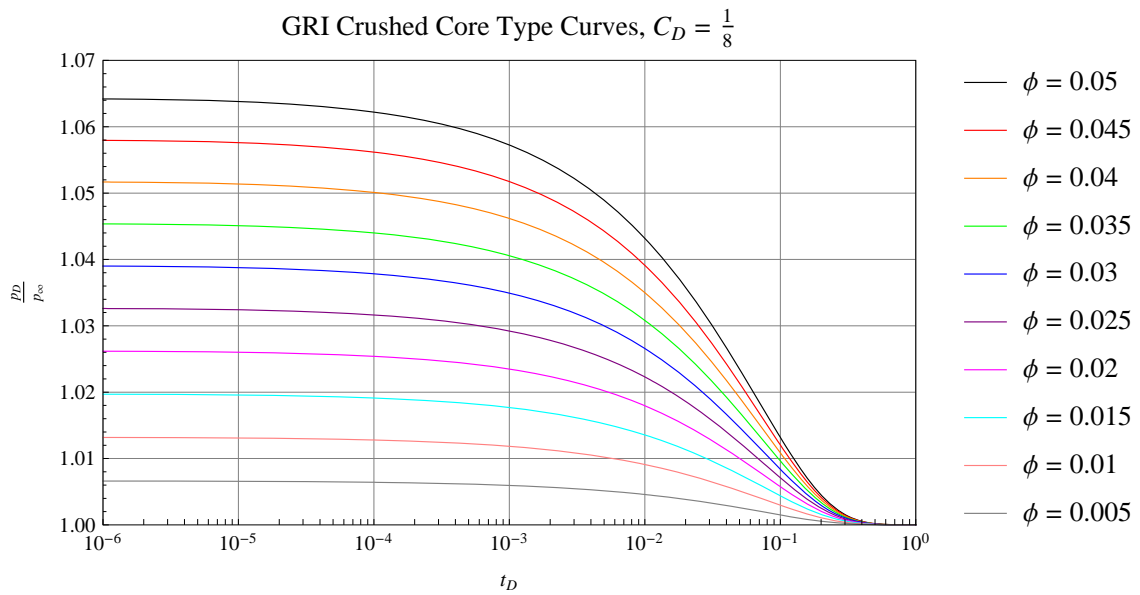


Figure 7.21: GRI method type curve using $\frac{p_D}{p_\infty}$ for the dimensionless volume ratio $C_D = \frac{1}{8}$.

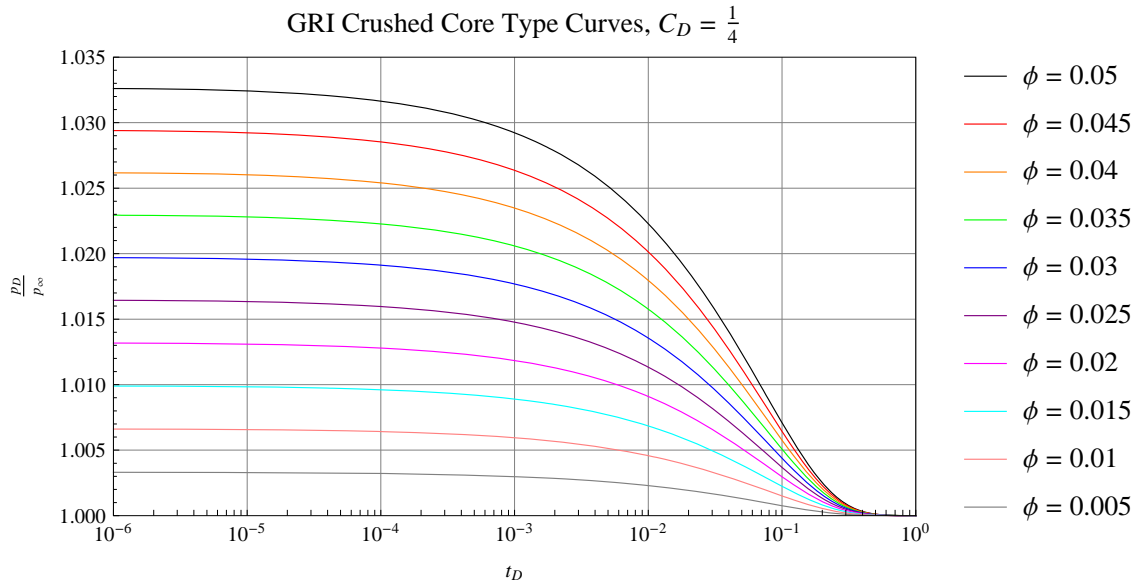


Figure 7.22: GRI method type curve using $\frac{p_D}{p_\infty}$ for the dimensionless volume ratio $C_D = \frac{1}{4}$.

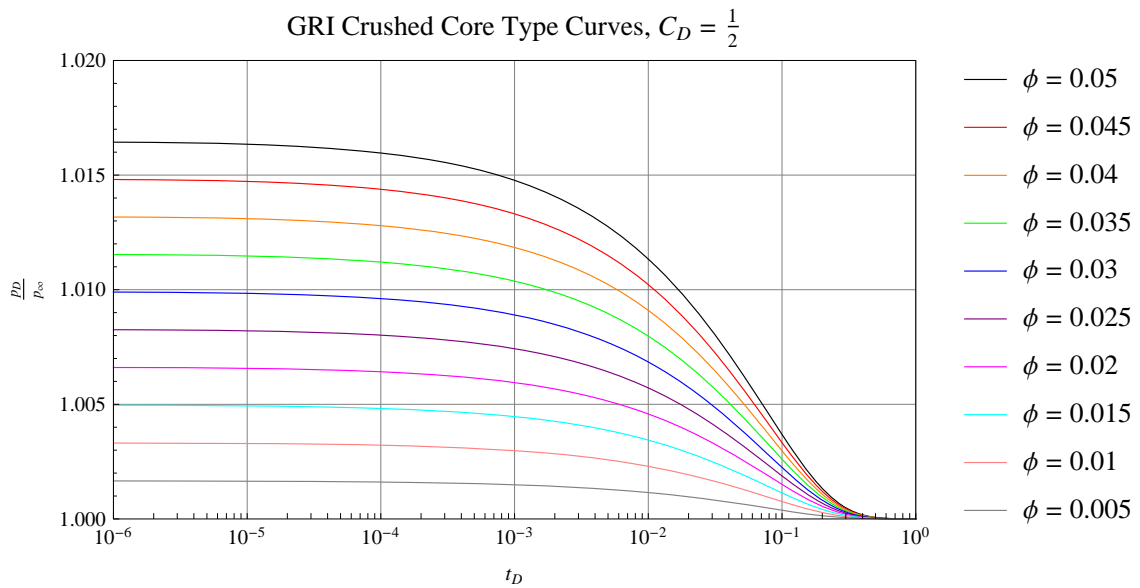


Figure 7.23: GRI method type curve using $\frac{p_D}{p_\infty}$ for the dimensionless volume ratio $C_D = \frac{1}{2}$.

8. SUMMARY AND CONCLUSIONS

The fundamental laws necessary for the mathematical treatment of a large part of physics and the whole of chemistry are thus completely known, and the difficulty lies only in the fact that application of these laws leads to equations that are too complex to be solved.

Paul Dirac (1902–1984)

8.1 Summary

In this thesis, we studied the existing solution methods and results of the parabolic diffusion equation and provided a generalization of the parabolic diffusion equation that takes into account a finite propagation speed for pressure propagation in the fluid. This generalization is the hyperbolic wave equation, which was referred to as the hyperbolic diffusion equation herein. The hyperbolic diffusion equation results from deriving the hydrodynamic equations for the flow of fluids in porous media. In particular, we began with a generalization of Darcy's law which included the effects of fluid inertia. This generalization led us to the hyperbolic diffusion equation. It was noted that when the effects of fluid inertia were ignored as in Darcy's law, the usual parabolic diffusion equation results.

We continued by developing the theoretical background of the different mathematical methods that are used to solve the two aforementioned diffusion equations with various boundary conditions. The methods are Sturm-Liouville theory, eigenfunction expansions, and Laplace transformations. Further, we introduced the application of a nonsingular Hankel transform method for finding the solution to the two diffusion equations with nonzero and nonconstant initial and boundary conditions. It was shown that the Hankel transform method developed herein proved to be a more straight forward and less time consuming computation than those found in the

literature.

Once the solutions to the parabolic and hyperbolic diffusion equations were developed, we then investigated the solutions to the parabolic diffusion equation and the hyperbolic diffusion equation. We showed that, as expected, the solution to the hyperbolic diffusion equation converges in the limit to the diffusion equation, as the propagation speed in the hyperbolic model approached infinity. We then illustrated the comparison by plotting dimensionless pressure versus dimensionless time with different propagation speeds in the hyperbolic diffusion equation against the dimensionless pressure solution to the parabolic diffusion equation. The convergence of the hyperbolic model to the parabolic model was evident. Similar results were found when examining the logarithmic derivatives as well.

To show the application of the parabolic diffusion equation, we derived the solutions to the pressure pulse decay method as well as the well-known GRI crushed core permeability method. After the derivations of the solutions, it was shown that the results obtained have excellent agreement with the data that can be found from sources for the pressure pulse decay method and the actual crushed core experiments from the GRI. To provide further insight, we investigated the pressure behavior inside the crushed core samples and core samples as the pressure response moves from transient to steady-state. This type of analysis has not been discussed in existing literature until now.

8.2 Conclusions

From the work in this thesis, we conclude the following:

1. The well-known parabolic diffusion equation for modeling the flow of fluids through porous media can be generalized, in terms of pressure propagation speed, by the hyperbolic diffusion equation, which is a direct result from gen-

eralizing Darcy's law to include the effects of fluid inertia.

2. The associated IBVPs with functions as boundary conditions (instead of constants as found in the literature) can be solved by implementing the different nonsingular Hankel transforms that were derived in this thesis. This solution method is more straightforward and in some cases can yield the solution in less time than the existing methods.
3. Using the Laplace transform theory developed herein, the solutions to the pressure pulse decay method and the GRI crushed core method can be found. Further investigation of these solutions graphically provided new insight with respect to the transient pressure response inside the samples.

8.3 Recommendations for Future Work

The author recommends the two following topics for future work.

8.3.1 Hyperbolic diffusion equation to model the pressure pulse decay method and the GRI method

An interesting topic would be to cast the pressure pulse decay method and the GRI crushed core permeability method as hyperbolic diffusion IBVPs. The solutions should be compared and contrasted against the solutions found when using the parabolic diffusion equation in this thesis. The reason that this type of work may be fruitful is that the information regarding the properties of the rock are found from modeling the transient behavior of the pressure response. It may be that the assumption of an infinite pressure propagation speed in the gas is not acceptable for these methods.

8.3.2 *Solution of the Hyperbolic Diffusion Equation with Boundary Conditions Specified at the Wellbore*

Implementation of the diffusion equations on reservoirs with finite dimension provide models to describe the density and pressure distributions in the reservoir. To solve this problem analytically, one must have knowledge of the diffusion coefficient κ , the speed of sound a in the fluid, as well as the wellbore and reservoir radii, r_1 and r_2 , respectively. Obtaining a representative values of a and κ can be accomplished by measurements taken on a core sample and assuming constant reservoir properties throughout. The parameter that may not be initially measured before the production of a well commences is the exterior radius r_2 .

A second topic for future work would be to investigate the hyperbolic diffusion equation where the two required spatial boundary conditions are defined at the interior radius of the reservoir. This type of solution does not require a priori knowledge of the radius of the reservoir. If the pressure and the flow rate can be measured from the reservoir beginning at the instant that the well begins production, at which time we call $t = 0$, then *embedded in the two boundary conditions that are at the interior radius of the reservoir (the pressure and flow rate) will be the information (the characteristics of the reservoir) necessary to compute the external radius of the reservoir.* This has been investigated some in the literature as an ill-posed heat equation, but the details for its application in flow of fluids in porous media do not seem to exist. The author has found only a limited numbers of papers [9, 26] that investigate the solution to the parabolic diffusion equation with both boundary conditions defined at one boundary for the parabolic diffusion equation in cylindrical coordinates. A method that is used to solve this problem is to cast it as a hyperbolic diffusion equation with a small coefficient of the second derivative with respect to time. In both

papers [9, 26], the convergence of the solution to the parabolic diffusion equation is questionable since the solutions are assumed to have the form of a power series.

The author's idea for future work in this area stems first from the observation that there does not seem to be any research in the flow of fluids through porous media which contemplates the problem of solving the hyperbolic diffusion equation in cylindrical with the two required boundary conditions both being defined at one boundary, in this case, at the interior (wellbore) radius r_1 . Second, the author believes that along with sound, pressure propagates as waves with a finite speed, as opposed to an infinite propagation speed as implied by the parabolic diffusion equations.

We now attempt to begin the solution to this problem. In doing so, we recall the old saying by Danish poet and mathematician Piet Hein (1905–1996), *Problems worthy of attack prove their worth by hitting back*. This claim by Hein will be proven shortly.

We consider the BVP

$$\frac{\partial^2 p}{\partial r^2} + \frac{1}{r} \frac{\partial p}{\partial r} = \frac{1}{a^2} \frac{\partial^2 p}{\partial t^2} + \frac{1}{\kappa} \frac{\partial p}{\partial t}, \quad (8.1a)$$

$$p(r_1, t) = f(t), \quad (8.1b)$$

$$r \frac{\partial p}{\partial r} \Big|_{r=r_1} = F(t). \quad (8.1c)$$

where $f(t)$ and $F(t)$ are functions representing the terminal pressure and terminal rate, both at the wellbore $r = r_1$.

We seek solutions that are harmonic in time. In this case, we see that particular solutions to (8.1) have the form

$$(A(\omega)J_0(\xi r) + B(\omega)Y_0(\xi r)) e^{-i\omega t}, \quad (8.2)$$

where

$$\xi = \frac{1}{a} \sqrt{\omega^2 + i \frac{a^2 \omega}{\kappa}}.$$

The complete solution over the entire continuous spectrum is given by

$$p(r, t) = \int_{-\infty}^{\infty} (A(\omega)J_0(\xi r) + B(\omega)Y_0(\xi r)) e^{-i\omega t} d\omega. \quad (8.3)$$

The character of the function $p(r, t)$ is such that the infinite integral in (8.3) converges uniformly. A result of this uniform convergence is that we may take the partial derivative of $p(r, t)$ with respect to both r and t .

In order to determine $A(\omega)$ and $B(\omega)$, we enforce the boundary conditions (8.1b) and (8.1c) on (8.3) obtaining

$$\begin{aligned} p(r_1, t) = f(t) &= \int_{-\infty}^{\infty} (A(\omega)J_0(\xi r_1) + B(\omega)Y_0(\xi r_1)) e^{-i\omega t} d\omega \\ r \frac{\partial p}{\partial r} \Big|_{r=r_1} = F(t) &= r_1 \int_{-\infty}^{\infty} -\xi (A(\omega)J_1(\xi r_1) + B(\omega)Y_1(\xi r_1)) e^{-i\omega t} d\omega. \end{aligned}$$

The coefficients of $e^{-i\omega t}$ may be interpreted as the Fourier transforms of $f(t)$ and $F(t)$, respectively. Thus we have

$$\begin{aligned} A(\omega)J_0(\xi r_1) + B(\omega)Y_0(\xi r_1) &= \frac{1}{2\pi} \int_{-\infty}^{\infty} f(\alpha) e^{i\omega \alpha} d\alpha \\ A(\omega)J_1(\xi r_1) + B(\omega)Y_1(\xi r_1) &= -\frac{1}{2\pi r_1 \xi} \int_{-\infty}^{\infty} F(\alpha) e^{i\omega \alpha} d\alpha. \end{aligned}$$

Solving for $A(\omega)$ and $B(\omega)$, we substitute into (8.3) obtaining an exact solution

to (8.1) given by

$$\begin{aligned}
 p(r, t) = \frac{1}{4} \int_{-\infty}^{\infty} \int_{-\infty}^{\infty} & \left((J_1(\xi r_1) Y_0(\xi r) - Y_1(\xi r_1) J_0(\xi r)) \xi r_1 f(\alpha) \right. \\
 & \left. + (J_0(\xi r_1) Y_0(\xi r) - Y_0(\xi r_1) J_0(\xi r)) F(\alpha) \right) e^{i\omega(\alpha-t)} d\omega d\alpha. \quad (8.4)
 \end{aligned}$$

There is great difficulty in further evaluating (8.4) due to the complexity of ξ in the argument of the Bessel functions. If one can find the transformation that removes ξ from the argument of the Bessel functions in (8.4), then the author conjectures that a tractable solution could then be constructed.

REFERENCES

- [1] J. Abate and P.P. Valkó, Multi-precision Laplace transform inversion, *International Journal for Numerical Methods in Engineering* **60** No. 5–7 (2004), 979–993.
- [2] M. Abramowitz and I. Stegun, *Handbook of Mathematical Functions*, Dover Publications, Mineola, New York, 1970.
- [3] J.O Amaefule, K. Wolfe, J.D. Walls, A.O. Ajufu, and E. Peterson, Laboratory determination of effective liquid permeability in low-quality reservoir rocks by the pulse decay technique, SPE 15149, Society of Petroleum Engineers, 1986.
- [4] W.E. Aryton and J. Perry, Experiments on the heat-conductivity of stone, based on Fourier’s ‘théorie de la chaleur’, *The London, Edinburgh, and Dublin Philosophical Magazine and Journal of Science, Fifth Series* **5** No. 31 (April 1878), 241–267.
- [5] K.J. Baumeister and T.D. Hamill, Hyperbolic heat-conduction equation—A solution for the semi-inifinite body problem, *Journal of Heat Transfer* **91** No. 4 (1969), 543–548.
- [6] T.A. Blasingame, Derivation of the diffusivity equation for single-phase liquid flow (in any flow geometry), Petroleum Engineering 620 Course Notes, 1997.
- [7] T.A. Blasingame, Private correspondences, May–July 2013.
- [8] W.F. Brace, J.B. Walsh, and W.T. Frangos, Permeability of granite under high pressure, *Journal of Geophysical Research* **73** No. 6 (1968), 2225–2236.
- [9] O.R. Burggraf, An exact solution of the inverse problem of heat conduction, *Journal of Heat Transfer* **86C** (1964), 373–382.
- [10] H. Carslaw and J. Jaeger, *Conduction of Heat in Solids*, 2nd. Ed., University Press, Oxford, 1978.
- [11] C.R. Cattaneo, Sur une de l’équation de la chaleur eliminant le paradoxe d’une propagation instantanée, *Comptes Rendus Académie Des Sciences* **247** No. 4 (1958), 431–433.
- [12] R.V. Churchill, *Operational Mathematics*, 3rd. Ed., McGraw-Hill, New York, 1972.
- [13] X. Cui, A.M. Bustin, and R.M. Bustin, Measurements of gas permeability and diffusivity of tight reservoir rocks: different approaches and their applications, *Geofluids* **9** (2009), 208–223.

- [14] J.M. Davis, *Introduction to Applied Partial Differential Equations*, W.H. Freeman and Company, New York, 2013.
- [15] A.I. Dicker and R.M. Smits, A practical approach for determining permeability from laboratory pressure-pulse decay measurements, SPE 17578, Society of Petroleum Engineers, 1988.
- [16] D.G. Duffy, *Transform Methods for Solving Partial Differential Equations*, 2nd. Ed., Chapman and Hall/CRC, Boca Raton, Florida, 2004.
- [17] P. Egermann, N. Doerler, M. Fleury, J. Behot, F. Deflandre, and R. Lenormand, Petrophysical measurements from drill cuttings: An added value for the reservoir characterization process, SPE 88684, *Society of Petroleum Engineers Reservoir Evaluation & Engineering Journal* **9** No. 4 (2006), 302–307.
- [18] P. Egermann, R. Lenormand, and D. Longeron, A fast and direct method of permeability measurements on drill cuttings, SPE 77563, *Society of Petroleum Engineers Reservoir Evaluation & Engineering Journal* **8** No. 4 (2005), 269–275.
- [19] W.R. Foster, J.M. McMillen, and A.S. Odeh, The equations of motion of fluids in porous media: I. Propagation velocity of pressure pulses, SPE 1762, *Society of Petroleum Engineers Journal* **7** No. 4 (1967), 333–341.
- [20] W.R. Foster, J.M. McMillen, and G.C. Wallick, The equations of motion of fluids in porous media: II. Shape of pressure pulses, SPE 2322, Society of Petroleum Engineers, 1968.
- [21] I. Gradshteyn and I. Ryzhik, *Table of Integrals, Series, and Products*, 6th. Ed., Academic Press, San Diego, California, 2000.
- [22] D.A. Handwerger, R. Suarez-Rivera, K.I. Vaughn, and J.F. Keller, Improved petrophysical core measurements on tight shale reservoirs using retort and crushed samples, SPE 147456, Society of Petroleum Engineers, 2011.
- [23] S.E. Haskett, G.M. Narahara, S.A. Holditch, A method for simultaneous determination of permeability and porosity in low-permeability cores, SPE 15379, *Society of Petroleum Engineers Formation Evaluation Journal* **3** No. 3 (1988), 651–658.
- [24] P.A. Hsieh, J.V. Tracy, C.E. Neuzil, J.D. Bredehoeft, and S.E. Silliman, A transient laboratory method for determining the hydraulic properties of ‘tight’ rocks—I. Theory, *International Journal of Rock Mechanics and Mining Sciences & Geomechanics Abstracts* **18** (1981), 245–252.

- [25] J. Kamath, R.E. Boyer, F.M. Nakagawa, Characterization of core scale heterogeneities using laboratory pressure transients, *Society of Petroleum Engineers Formation Evaluation Journal* **7** No. 3 (1992), 219–227.
- [26] Langford, D., New analytic solutions of the one-dimensional heat equation for temperature and heat flow rate both prescribed at the same fixed boundary (with applications to the phase change problem), *Quarterly of Applied Mathematics* **24** (1967), 315–322.
- [27] J. Lee, J.B. Rollins, and J.P. Spivey, *Pressure Transient Testing*, SPE Textbook Series **9**, Society of Petroleum Engineers, Richardson, Texas, 2003.
- [28] T. Löfqvist and G. Rehbinder, Transient flow towards a well in an aquifer including the effect of fluid inertia, *Applied Scientific Research* **51** (1993), 611–623.
- [29] D.L. Luffel, Advances in shale core analyses, GRI Topical Report, GRI-93/0297, Gas Research Institute, June 1993.
- [30] D.L. Luffel and F.K. Guidry, New core analysis methods for measuring reservoir rock properties of Devonian shale, SPE 20571, *Journal of Petroleum Technology* **44** No. 11 (1992), 1184–1190.
- [31] D.L. Luffel, C.W. Hopkins, and P.D. Schettler Jr., Matrix permeability measurement of gas productive shales, SPE 26633, Society of Petroleum Engineers, 1993.
- [32] K. Lund and H.S. Fogler, The prediction of the movement of acid and permeability fronts in sandstone, *Chemical Engineering Science* **31** No. 31 (1976), 381–392.
- [33] C. Matthews and D. Russell, *Pressure Buildup and Flow Tests in Wells*, Society of Petroleum Engineers of the AIME, Monograph Series **1**, Dallas, (TX 1967).
- [34] P.M Morse, H. Feshbach, *Methods of Theoretical Physics*, Vol. I, Feshbach Publishing, LLC, Minneapolis, Minnesota, 1981.
- [35] M. Muskat, *Flow of Homogeneous Fluids Through Porous Media*, 1st Ed., 2nd. Printing, J.W. Edwards, Inc., Ann Arbor, Michigan, 1946.
- [36] M. Muskat, The flow of compressible fluids through porous media and some problems in heat conduction, *Physics* **5** No. 71 (1934), 71–94.
- [37] C.E. Neuzil, C. Cooley, S.E. Silliman, J.D. Bredehoeft, and P.A. Hsieh, A transient laboratory method for determining the hydraulic properties of ‘tight’ rocks–II. Application, *International Journal of Rock Mechanics and Mining Sciences & Geomechanics Abstracts* **18** (1981), 253–258.

- [38] T. Oroveanu and H. Pascal, On the propagation of pressure waves in a liquid flowing through a porous medium, *Revue de Mécanique Appliquée* **4** (1959), 445–448.
- [39] M.N. Özisik and D.Y. Tzou, On the wave theory in heat conduction, *Transactions of the ASME* **116** No. 3 (1994), 526–535.
- [40] H. Pascal, Pressure wave propagation in a fluid flowing through a porous medium and problems related to interpretation of Stoneley’s wave attenuation in acoustical well logging, *International Journal of Engineering Science* **24** No. 9 (1986), 1553–1570.
- [41] S. Profice, D. Lasseux, Y. Jannot, N. Jebara, and G. Hamon, Permeability, porosity and Klinkenberg coefficient determination on crushed porous media, SCA 2011-32, Society of Core Analysts, 2011.
- [42] R. Raghavan, *Well Test Analysis*, Prentice Hall, Englewood Cliffs, New Jersey, 1993.
- [43] M. Renardy and R.C. Rogers, *An Introduction to Partial Differential Equations*, Texts in Applied Mathematics **13**, Springer, New York, 1993.
- [44] J.A. Rushing, K.E. Newsham, P.M. Laswell, J.C. Cox, and T.A. Blasingame, Klinkenberg-corrected permeability measurements in tight gas sands: steady-state versus unsteady-state techniques, SPE 89867, Society of Petroleum Engineers, 2004.
- [45] D. Russell, Private correspondences, December 2012–February 2013.
- [46] S. Sinha, E.M Braun, Q.R. Passey, S.A. Leonardi, A.C. Wood III, T. Zirkle, J.A. Boros, and R.A. Kudva, Advances in measurement standards and flow properties measurements for tight rocks such as shales, SPE 152257, Society of Petroleum Engineers, 2012.
- [47] M. Spiegel, *Shaum’s Outline of Advanced Mathematics for Engineers and Scientists*, McGraw Hill, New York, 1971.
- [48] P.P. Valkó, Numerical Laplace inversion (GWR function), <http://library.wolfram.com/infocenter/MathSource/4738/>, accessed on 5 May 2014.
- [49] P.P. Valkó and J. Abate, Comparison of sequence accelerators for the Gaver method of numerical Laplace transform inversion, *Computers and Mathematics with Application* **48** No. 3–40 (2004), 629–636.

- [50] P.P. Valkó and S. Vajda, Inversion of noise-free Laplace transforms: towards a standardized set of test problems, *Inverse Problems in Engineering* **10** No.5 (2002), 467–483.
- [51] A. van Everdingen and W. Hurst, The application of the Laplace transformation to flow problems in reservoirs, *Transactions of the AIME* **186** (1949), 305–324.
- [52] P. Vernotte, Les paradoxes de la theorie continue de l'équation de la chaleur, *Comptes Rendus Académie Des Sciences* **246** No. 22 (1958), 3154.